NOTTINGHAM
TRENT UNIVERSITY

High Bandwidth Angular Instrumentation System for the Measurement and Analysis of Stepper Motor Drives

Christopher J Cain

August 2004

A thesis submitted to The Nottingham Trent University
in partial fulfilment of the requirements for the degree
of Master of Philosophy

The Nottingham Trent University
in collaboration with
SmartDrive Ltd

SmartDrive

Abstract

Modern automatic control systems often rely on the facility to accurately move a tool or simply a payload to a precise position. The requirements of efficiency may demand that the movement is accomplished in the minimum possible time. To achieve this objective the acceleration and deceleration profile must be both smooth and rapid, but at the end of the move the settlement at the position of rest must free from oscillations. Stepper motors are very often used in such applications because they will move a precise number of fixed angle steps in response to a fixed number of digital pulses sent to the motor. This is the basis of numerical control.

The motor is to achieve precise placement without oscillation at the end of the move. The path of the motor must be smooth in transition throughout the entire velocity profile (including phases of acceleration, steady speed and deceleration). However stepper motors are susceptible to slipping out of step with the pulses supplied to the motor. This is most likely to occur during acceleration or deceleration if the motor cannot produce sufficient torque to match the load being moved by the motor. The motor can also suffer from oscillation if the frequency of the steps matches the natural frequency (or a sub-multiple of the natural frequency) of the motor and its load. If these oscillations are large enough, the effect will be cumulative in successive steps and will cause the motor to fall out of step.

The technique of micro-stepping (an electronic means of generating a set number of points of equilibrium between natural steps of the motor) provides a means of more accurate position control. Micro-stepping also reduces (but does not eliminate) resonance due to running at speeds related to the natural frequency of the motor. In order to reduce oscillations, techniques are applied using measurements of disturbances in the electric current in the motor to trace its path of motion and to regulate acceleration to a rate that ensures the motor does not slip out of step. Because this technique tracks the motion of the motor without the use of external transducers, it is known as sensorless feedback.

An instrumentation system has been developed to better understand the efficiency of control systems to facilitate improved algorithms for sensorless feedback. The instrumentation system is able to reconstruct the magnetic flux waveform of the motor. The current and voltage waveforms (the data used for sensorless feedback) have been compared with the PWM pulses, the magnetic flux waveform and with position monitoring from a high bandwidth digital shaft encoder. A test bed was developed to investigate the control performance of a micro-step motor driver supplied by the industrial partner. Some causes of oscillations at low speeds of the motor have been determined and solutions have been proposed. A research platform that integrates the functions of the micro-step driver and the instrumentation onto a common digital signal processor (DSP) has been developed. This increases the bandwidth of the instrumentation and reduces the possibility of quantisation errors in capturing the signals from the motor controller. Alternative methods of analysing the effects of motor motion on the phase current and voltage waveforms have been proposed.

The work described in this Thesis is the Author's own, unless otherwise stated, and it is as far as he is aware, original.

Acknowledgements

I wish to thank Dr Paul Orton, my first supervisor' for the privilege of his wise counsel throughout the duration of this project has been an inspiration to me. However busy he has been, he has always made time to listen and offer timely response.

A special thank you to Dr Janet Poliakoff, my second supervisor; her advice I have always done well to heed and her encouragement has always been uplifting.

It is also very apt to extend my thanks to other members of staff, especially Mr Mark Howson and to my fellow research students who have helped me so much throughout the duration of my time on this project and helped to make my time in the Intelligent Machines research group enjoyable as well as profitable.

Most important of all a heart felt thank you to my wife Jacqueline; her patience and support has been unstinting.

Table of Contents

Glossary of Terms*

Bandwidth	A measure of system response. It is the frequency range that a control system can follow.
Back EMF	The voltage produced across a winding of a motor due to the winding turns being cut by a magnetic field while the motor is operating. This voltage is directly proportional to rotor velocity and is opposite in polarity to the applied voltage. Also referred to as Motional Voltage in stepper motors.
Commutation	The switching sequence of drive voltage into motor phase windings necessary to assure continuous motor rotation.
Closed Loop	A broadly applied term relating to any system where the output is measured and compared to the input. The output is then adjusted to reach the desired condition.
Damping	An indication of the rate of decay of a signal to its steady state value. Related to settling time.
Dead Band	A range of input signals for which there is no system response.
Detent Torque	The minimal torque present in an un-energized motor. The detent torque of a step motor is typically about 1% of its static energized torque.
Duty Cycle	For a repetitive cycle, the ratio of on time to total cycle time.
Electrical Time Constant	The ratio of armature inductance to armature resistance.
Encoder	A device that translates mechanical motion into electronic signals used for monitoring position or velocity.
Holding Torque	Sometimes called static torque, it specifies the maximum external force or torque that can be applied to a stopped, energized motor without causing the rotor to rotate continuously.
Incremental Motion	A motion control term that describes a device that produces one step of motion for each step command (usually a pulse) received.
Inertia	A measure of an object's resistance to a change in velocity. The larger an object's inertia, the larger the torque that is required to accelerate or decelerate it. Inertia is a function of an object's mass and its shape.
Mid-Range Instability	Designates the condition resulting from energizing a motor at a multiple of its natural frequency (usually the third orders condition). Torque loss and oscillation can occur in under-damped open-loop systems.
Micro-stepping	An electronic control technique that proportions the current in a step motor's windings to provide additional intermediate positions between poles. Produces smooth rotation over a wide speed range and high positional resolution.
Motional Voltage	See Back EMF.
Open Loop	Refers to a control system where no external sensors are used to provide correction signals.
Phase Angle	The angle at which the steady state input signal to a system leads the output signal.
Pulse Rate	The frequency of the step pulses applied to a motor driver. The pulse rate multiplied by the resolution of the motor/ drive combination (in steps per revolution) yields the rotational speed in revolutions per second.
PWM	Pulse Width Modulation. A method of controlling the average current or voltage in a power converter by varying the on-time (duty cycle) of transistor switches.
Rated Torque	The torque producing capacity of a motor at a given sped. This is the maximum torque the motor can deliver to a load and is usually specified with a torque/speed curve.
Resolution	The smallest (positioning) increment that can be achieved. Frequently defined as the number of steps required for a motor's shaft to rotate one complete revolution.
Resonance	Designates the condition resulting from energizing a motor at a frequency at or close to the motor's natural frequency. Lower resolution, open-loop systems will exhibit large oscillations from minimal put.

* Most of the entries in this glossary are from Parker Motion and Control. They have however, been adapted for Motion Control usage.

Rotor	The rotating part in a motor. In a stepper motor the rotor has no windings.
Servo	A system consisting of several devices which continuously monitor actual information (position, velocity), compares those values to desired outcome and makes necessary corrections to minimize that difference.
Static Torque	The maximum torque available at zero speed.
Stator	The stationary part of an electric motor. In a stepper motor the phase windings are on the stator.
Step Angle	The angle the shaft rotates upon receipt of a single step command.
Stiffness	The ability to resist movement induced by an applied torque. Is often specified as a torque displacement curve, indicating the amount a motor shaft will rotate upon application of a known external force when stopped.
Synchronism	A motor rotating at a speed correctly corresponding to the applied step pulse frequency is said to be in synchronism. Load torques in excess of the motor's capacity (rated torque) will cause a loss of synchronism. The condition is not damaging to a step motor.
Torque	Force tending to produce rotation.
Triggers	Inputs on a controller that initiate or "trigger" the next step in a program.

Chapter 1
Introduction

1 Introduction

At the dawn of the new millennium we increasingly take for granted machines that make our lives more efficient, more comfortable, more exciting or simply more fun. Many of these devices rely upon the physical action of being able to accurately and sometimes rapidly move some item from one position to another. This may be the familiar sight of the ten pins being picked up and gently lowered into position in a bowling alley. Perhaps it could be a robot arm in a car factory, repeatedly fixing headlamp units into position, or it may be something unseen such as the very rapid and accurate movements of the read head of a hard-disk in a PC.

Human babies are not born with the ability to place a piece of food into their mouths. But after weaning, eventually mother thinks her little baby is now a bit too old to be continually spoon fed. The developing infant quickly learns the skill of guiding a piece of food into its mouth, even if the process is a little messy to begin with. Humans are very versatile when it comes to applying the control skills needed to move things to a desired position. There is nothing that can't be done, from moving a glass of beer from the bar to the mouth or typing a text message into a mobile phone. However when it comes to very rapid and/or accurate positioning such as finding the correct sector on a hard-disk or plucking a satellite out of orbit to stow safely into the cargo bay of the space shuttle [1], the human cannot compete with the machine.

Sometimes the task undertaken by the machine must mimic the most complex feats of human dexterity. Tele-surgery trials have been undertaken to allow a surgeon to perform complex surgery at a remote location; as reported in the New York Times [2]; the surgeon was in New York, the patient was 3800 miles away in Strasbourg. The surgeon controls the remote robot hands that perform the operation at the remote location. The location could perhaps be a military field hospital or a space craft in transit. The rigour of surgical procedure demands that the mimicry of the surgeons' hands is extremely precise and the motion is extremely smooth. The application of stepper-motors to surgery performed by robotics is described by Francesco Cepolino [3].

The examples cited above show that the demands of mechanical position control can require great accuracy, smoothness of movement and often very rapid motion.

Mechanical movement and position control can be achieved with any one of a number of engines or motors which can be powered by steam, compressed air, hydraulic pressure, fuel-oil, or electricity. Of these, electric motors are the most easily controlled and often the most convenient to use.

Many types and sizes of motors are available and include ac induction motors, ac synchronous motors, dc commutator motors, dc brushless motors synchros and stepper-motors. In their basic forms, many motors are used only as a motive force and not for precise position control. For instance the motor driving an electric fan simply rotates the fan blades, it is not required to move a fan blade through a specified angle (say 32°), when the fan is switched off the fan blade stops at a random position.

Many applications of motor drive require a much greater degree of control, for example a lift in mine shaft that is under automatic control or the print head in an inkjet printer. The mine lift requires a control system that will accelerate/decelerate a load following a very specific profile and accurately position the lift at the end of the wind. The load in this case has a very considerable mass which can vary substantially from one winding cycle of the lift to the next. The print head in the inkjet printer is of a small and consistent mass and must be accelerated as quickly as possible to a required position and pause at this position. Such movements can result in the print head overshooting the required position and after some amount of oscillation eventually settle at the correct position. It is essential that the overshoot is as small as possible and that the settling time is as brief as possible.

1.1 General Aspects of Stepper Motors

The stepper motor (also referred to as a step motor or a stepping motor) is one of a group of electrical machines used for precise positioning of a mechanical payload. This group of devices also includes a type of drive called a servomotor. The term servomotor is slightly misleading as more than one type of motor can be combined with other components into a control system and become a servomotor. However the majority of servomotor systems use either commutator or brushless dc motors. The servomotor is a system that depends on some information regarding the position and/or velocity of the item being moved being sent back to the servomotor controller. Such a system is said to use closed loop control. A stepper motor is a machine that moves an object to a pre-destined destination and often at a predetermined velocity and normally uses open loop control. Another type of motor used for open loop control is the selsyn or synchro. This is an analogue device which consists of a three phase generator (master) and a matched three phase motor (slave).

A human analogy of open loop and closed loop control systems is given by the following two tasks:

- Locating the gear shift lever while driving, the driver is looking at the road not the gear shift lever. The message from the brain guides the hand to the gear lever without any visual guidance. This is open loop control.
- Steering a car, the driver is steering the car with the steering wheel while looking ahead at the road observing the changing direction of the car. If the car overshoots the intended direction this information is sent from the eyes to the brain, the brain instructs the hands to make a correction to the position of the steering wheel. This process of feedback and correction is closed loop control.

Sometimes open loop and closed loop control systems are combined; as described above, the brain directs the hand to the gear lever in open loop control. When the hand has located the gear lever, the hand must now push the gear lever to the required position. If the hand pushes the gear lever too far across there is tactile feedback through the hand to the brain. The brain will send a correction signal to the hand to reposition the gear lever. Thus the complete action of changing gear has used a combination of open loop and closed loop control.

The concept of open loop and closed loop control is applied to motor control.

- Firstly, open loop control and stepper-motors are considered.

The stepper motor's rotor is rotated one step at a time. The motor is driven to the required angle by switching a specific sequence of electrical connections or steps to the motor. The detail of how this is done is explained in section 2.2.1. After the specified number of steps, the switching sequence stops but power is still applied to the last connection of the sequence which holds the motor at this static position. The force that is holding the motor in this static position is called the holding torque. The motor has been driven to a specified position (assuming no steps have been skipped) by the controlling device without any feedback and is therefore operating in open loop control.

The stepper motor is commonly used in computer numerical control (CNC) applications, as the stepper is a "digital" motion device; that is it is controlled in discrete steps rather than in continuous motion. To drive the motor to a specific position, a sequence of the correct number of pulses is originated by the CNC program, which controls the power electronics that commutate the supply to the stepper motor windings.

The angle moved at each step of a stepper motor is dependent upon the physical construction of the motor, that is the number of stator and rotor poles (see section 2.1.3). In order to achieve a higher resolution and also to improve other performance factors, it is possible to drive the motor to angles that are divisions of a motor step (discussed in the next chapter) called micro-steps.

- Closed loop control and servomotors are now briefly considered.

A servomotor system usually consists of a dc motor, either with a commutator (a rotary switch consisting of rotating copper segments on the rotor shaft and carbon brushes on the stator) or brushless. The system comprises the motor, a motor controller and a transducer that feeds back information about the motor position. The controller uses the first and second derivatives of the position to work out the velocity and acceleration respectively. A reference signal, possibly from a computer, is connected to the controller. The controller power section controls the velocity and direction of the motor, whereas the position transducer (usually a shaft encoder) feeds-back the current position of the motor shaft angle to the controller. The controller subtracts the encoder position data from the reference data, the difference and the sign (+/-) giving the error and the direction of the error. Thus the reference to the controller is modified and the controller will speed up or slow down the motor to reduce the error.

It has been explained that the stepper motor is suited to open loop control and that high degrees of positional accuracy can be achieved, however, the stepper motor may be less suitable than a servomotor for particular applications. Principally, if the mechanical load on the shaft of the stepper motor exceeds the torque that the motor can supply (called the pull out torque) the motor will slip one or more steps. In these circumstances, the control system has no feedback to produce an error signal, thus the control looses track of the position of the motor. In similar circumstances, a servomotor will merely slow down until the torque demand of the load is less than the torque produced by the motor and because of the feedback signal the control system still knows the correct position of the motor.

Conversely, there are situations where the stepper motor is more suitable. As the closed loop control of a servomotor relies on error feedback, the motor will not move unless given an error input. The presence of this error term causes an oscillation around the desired position, known as hunting. As the stepper motor employs an open-loop system, there is no 'seeking' and it can hold an accurate static position.

The use of a stepper motor with an encoder fixed to the shaft to provide shaft position feedback to the controller has been investigated. With this arrangement, the stepper motor can be controlled in both open loop and in closed loop. This arrangement combines the advantages of a stepper motor with some of those of a servomotor. This arrangement is discussed by Quick Silver Controls [4], where they consider using a stepper-motor as a servomotor. Methods of detecting the shaft angle *without* the use of a shaft encoder, known as *sensorless* detection have also been examined. Such methods are explained in section 2.2.3.

1.2 Applications of Stepper Motors

Stepper motors are used for many types of applications and both the stepper motor type and the method of control need to be optimised to suit the specific requirements as closely as possible. The range of possible applications includes;

- Volume displacement pumps for pharmaceutical and medical applications
- Hard disk and optical disk drives for computer systems
- Head positioning in printers, scanners and photocopiers
- Robotics and general mechatronics applications
- Space Exploration for control auxiliary equipment on satellites or planetary rover vehicles and also for rocket guidance control
- Computer Numerical Control (CNC) used in engineering manufacture. This often consists of two, three stepper motors working in two or three axes of motion
- Winding applications such as in the manufacture of inductive coils, transformers or motors.
- Steering of equipment including telescopes or weapons systems

The above list, although not comprehensive, illustrates a wide variety of uses of stepper motors, ranging from miniature types as found in disk drives, through to larger industrial types such as may be used in CNC machines or larger robotic applications.
The main focus of this project is on industrial types of motor and more specifically on hybrid stepper motors (see chapter 2).

The following sections examine the requirements of the project and the equipment needed to measure and analyse the cause and effect of motor resonance.

1.3 Industrial Requirements

The industrial partner SmartDrive Ltd, [5] manufacture a stepper motor driver, the "Taranis" [6] drive. This product combines stepper motor power electronics with a Texas Instruments 24xx series digital signal processor (DSP).

The performance of the Taranis drive is very good but the company are seeking further improvements. A number of issues are to be investigated, concerned with improving the smooth operation of stepper motors at a range of speeds. SmartDrive consider that the operation through most of the speed range is smooth but are looking for improvements in the high speed range.

The Taranis micro-step controller utilizes sensorless closed loop control. This involves detecting characteristics of the motor current that are affected by the rotary motion of the motor and using the data to modify the control of the motor. Their control algorithm is designed to optimise the torque angle and to minimise problems of vibration and oscillation. It is believed that remaining problems with vibration and oscillation occur because of inaccuracy in sensing the position of the rotor. Because the rotor position is determined indirectly, an investigation is needed. This requires the use of instrumentation to compare the pulse width modulation (PWM) output of the motor with shaft angle information obtained from a high bandwidth digital shaft encoder. The company also wish to utilize *sensorless* closed loop for the purpose of detecting if the motor has slipped out of step.

Investigations to analyse the performance of the Taranis are required but ultimately using the Taranis drive as a centre of the research has limitations. Some of the signal functions required for research (such as the phase voltages) are not available as outputs from the Taranis. The company need an instrumentation platform not only for continued improvements to the Taranis but also for the development of new drivers.

There is a need to integrate the instrumentation control and the stepper motor drive control onto a common platform. An effective development system needs not just a ready-built controller (the Taranis) but also a DSP development board and drive circuits so that the drive circuits can be monitored directly. The 24xx series DSP used in the Taranis is too limited in respect of its interfaces (e.g. number of analogue to digital converters) to adapt to this task. The 2812 DSP (from the same Texas Instruments 2000 range of DSPs) has been proposed for this role. The 2812 has the necessary additional interfaces and is also backward compatible with the 24xx series. The backward compatibility enables the Taranis software to be migrated onto the 2812 DSP. A fast data connection between the 2812 DSP and a PC is available through the XDS560 J Tag pod.

1.4 Instrumentation Requirements

As it is necessary to measure micro-step changes of the stepper motor against rotor angle it is necessary to measure the rotor angle of the motor very accurately. Therefore, a high resolution optical shaft encoder (with 5000 slots per channel) is the key element of the instrumentation hardware.

An instrumentation system that is under software control was constructed, the details of which are described in chapter 5. Much care was needed in the layout of the hardware to minimise electrical noise problems, and careful design was needed to interface all of the elements of the instrumentation. Techniques used in commercial instrumentation systems were evaluated (see chapter 3) as a reference to determining the instrumentation requirements. The signals to be measured and analysed are as follows;

(1) Eight channels of digital pulse width modulation (PWM) from the stepper motor driver as described in Appendix B.

(2) Three channels of digital shaft angle position information from the optical shaft encoder. Two channels have 5000 slots per channel per revolution aligned in quadrature with each other. The third channel has one slot per revolution.

(3) Two analogue differential phase winding currents. The use of the term differential means that there are actually four current signals (two for each phase winding of the motor) and each differential signal is the difference of one pair of signals.

(4) Two analogue phase winding voltage signals. Again, this is the difference of two pairs of signals, similar to that described in (3) above.

1.5 Aims and Objectives

1.5.1 Aims

The overall aim of this project is to develop improved high bandwidth instrumentation for the purpose of monitoring vibration and resonance occurring in hybrid stepper motors. Therefore the specific aims of the project are:

- To produce an appropriate instrumentation solution that will monitor the drive characteristics and provide high bandwidth angular position data. This will enable detailed analysis of the vibrations and resonances within the system.

- To utilise the instrumentation for detailed analysis of the performance of stepper motors controlled in micro-stepping mode.

1.5.2 Objectives

In order to achieve the aims, the following objectives need to be achieved:

- Review types of stepper motors.
- Survey of systems for instrumentation and control of stepper motors.
- Develop an experimental test rig with instrumentation.
- Collect and analyse current, voltage, angular position data and the driving (PWM) signals using the existing controller.
- Build motor drive circuits for interfacing with Digital Signal Processor (DSP) target system.
- Analyse disturbances of the motor current under a range of operating conditions.

1.6 Outline of Thesis

Chapter 2 describes in more detail the construction, operation and control of the various types of stepper motor but with emphasis on the hybrid stepper motor, which is the focus of this research. Factors related to stepper motor vibrations and other instabilities are also explained.

Chapter 3 is a review of commercially available instrumentation systems developed for stepper motor analysis. Some of the techniques used in commercial systems were incorporated into the hardware and software systems described in chapter five.

Chapter 4 describes the hardware and software used in this research, and details the capabilities of the hardware used. Careful consideration had to be given to elimination or reduction of electrical noise such that the data of interest was not masked by spurious signal. The techniques of how noise reduction was managed are described. The techniques used for synchronising collating and organising the data are explained.

Chapter 5 is a presentation and examination of the results and a comparison is made between the actual results and the theoretical expectations.

Chapter 6 is a discussion of the achievements of the project and how it could form the basis for future research.

Chapter 7 is a conclusion of the achievements of the work and its relevance to practical commercial/industrial application.

The appendices refer to;

Appendix A is a description of the various types of stepper motor windings (unipolar, bipolar, and bifilar) and their associated commutation techniques.

Appendix B is a description of the test rig hardware.

Appendix C describes the stepper motor driver with DSP interface. This was designed and constructed to facilitate an instrumentation system under the control of a Texas Instruments 2812 DSP.

Appendix D contains the schematic electrical circuits and printed circuit board design for the stepper motor driver/DSP interface.

Appendix E is an explanation of the power electronics circuits used to control the stepper motor.

Appendix F is the specification for the A/D converter used in the instrumentation system.

Appendix G is the specification for the Heidenhain Rotary Encoder

Chapter 2
Stepper Motor Theory

2 Stepper Motor Theory

This chapter does not cover the complete theory of stepper motor design but rather aims to present sufficient information to explain the control techniques of a stepper motor.

A review of stepper motor history in covered in section 2.1. The basics of stepper motor types and drive configurations are explained in section 2.2 and 2.3. The various phenomena of stepper motor oscillations and instability are covered in section 2.4.

The technical terms used in this chapter can be found in the glossary of terms. A basic explanation of what a stepper motor is, is covered in the introduction in chapter 1. A number of references are made to the terms rotor, stator and field winding in this chapter. The rotor is the rotating element of the motor that turns the drive shaft. The rotor of a stepper motor has no electrical windings. Stepper motors may have two, three or more phase windings; the motors used in this project all have two phases. Each phase winding is a separate electric circuit that consists of a wire coil wound onto the iron poles of the stator. The rotating magnetic flux (the lines of magnetic field strength) that causes the rotor to turn is produced in the poles of the stator by switching or commutating the current to the phases. The stator, as indicated by the name, is fixed, while the rotor is suspended concentrically inside the stator on bearings.

2.1 Stepper Motor History

Stepping type reluctance motors known as "electromagnetic engines" [7] were the electric motors in use in the mid-nineteenth century. However, it was not until the 1920s that stepping motors were used in practical positioning applications. Some of the earliest requirements for accurate position control of apparatus were in the military sphere, principally for the positioning of naval guns and torpedo tubes. Often selsyns (described in section 1.1) were applied to such tasks. However, unlike a stepper motor, a selsyn can only produce minimal torque; Thus, to enable the steering of a naval gun the slave selsyn would merely operate contacts to control a larger motor that performs the work of moving the payload. Even though the stepper motor produced usable torque, early designs were bulk in relation to their torque output and selsyns continued in military use into WWII for automatic synchronisation of batteries of searchlights. Kenjo et al [8] cite an issue of the JIEE published in 1927 that carried an article "The application of electricity in warships [9]". Part of this article describes a three-phase variable reluctance stepping motor used to control the direction indicator of torpedo tubes and guns in British warships. Figure 1.2 [6] illustrates the system, a mechanical rotary switch is used to switch the exciting current. One revolution of the handle produces six stepping pulses resulting in 90° of rotation. The rotor motion was geared down to achieve the required degree of accuracy.

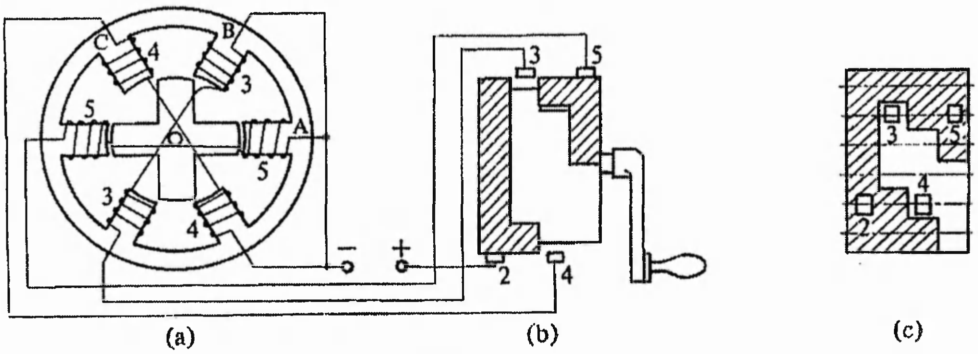

Figure 1.2 [6] Stepping motor used in British warships in the 1920s. (a) Motor; (b) rotary switch (c) section of rotary switch

The article also points out the machine should have a high ratio of torque to inertia to avoid missing a step; the time constant, the ratio of circuit inductance to resistance, should be small so as to attain a high speed of operation. These factors still affect modern stepper motors today and are explained in more detail later in this chapter. Two developments of 1919 and 1920 improved the practicality of stepper motors. Kenjo et al [8] refer to a patent taken out in 1919 "Tooth structure to minimise step angle" and a patent taken out in 1920 "Production of a large torque from a sandwich structure". The patent of 1919 served to provide smaller step angles; this principle is shown in section 2.2.3. The patent of 1920 [10] is for a type of motor construction where the rotor is sandwiched between two electromagnetic cores in an axial arrangement, instead of the more conventional arrangement of a rotor placed concentrically inside the stator poles in a radial arrangement. This can be seen in Figure 1.3 [6]. However, this design was not used until the 1970s, when a Japanese company manufactured a power stepping motor using the principle.

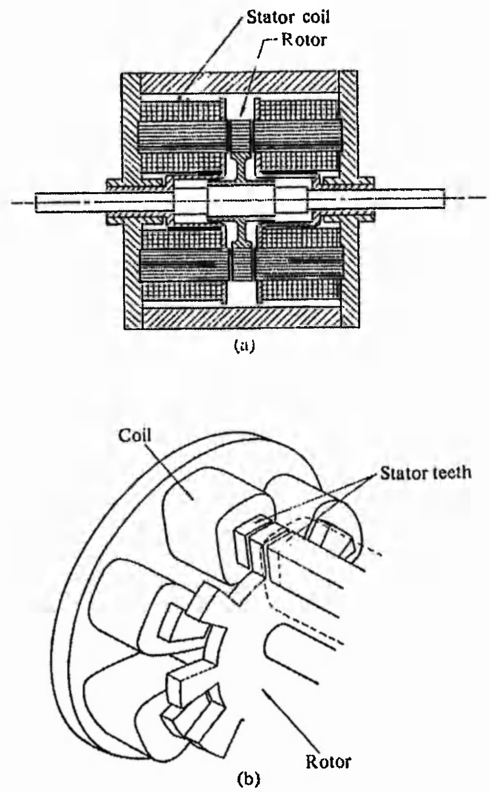

Figure 1.3 Construction of a High Torque Variable Reluctance Motor [8]

It was not until the end of the 1950s, when stepper motors were applied to numerical control (NC) that stepper motor control systems started to become more sophisticated. NC systems at that time would employ electronic switching of the stepper-motor field windings normally using thyratron gas filled thermionic valves. Development continued steadily in the 1970s up to the present day, with the improvement of solid state power electronic switches (thyristors, insulated gate bipolar transistors and mosfets), and the parallel development of electronic control devices, micro-processors and digital signal processors (DSPs).

2.2 Types of Stepper Motor

There are three principal types of stepper motors, namely: variable reluctance, permanent magnet and hybrid. The variable reluctance type has high resolution (small stepping angle) but low torque, the permanent magnet type has higher torque but low resolution and the hybrid type combines the advantages of the previous two. The hybrid stepper motor is more expensive than the other two types and would only be used in applications that require both high torque and high resolution. This research project is concerned with improving the function of high performance hybrid drives, however some of the findings may also be used to develop improvements to the other types of stepper motor. In order to understand the operation of the hybrid motor, it is useful to understand the operation of both the variable reluctance and the permanent magnet stepper motors. Other variations, not discussed here, include the disc magnet stepper motor, which is a sub genre of the permanent magnet stepper motor.

2.2.1 Variable Reluctance Motor

The only source of magnetic flux in a variable reluctance motor is from the current carrying windings on the stator of the motor. The windings of each phase are wound on a separate pairs of poles. A four phase variable reluctance motor is shown in Figure 2.1 [11]; it can be seen that the rotor has six teeth, whereas the stator has four pole pairs or eight pole faces, thus, at any instant in time only one pole pair can be fully aligned with a pair of rotor teeth. The flux (magnetic field) path is from one of the energised stator poles through the rotor to the other energised stator pole. The highest reluctance (magnetic resistance) section of the flux path is the air gap between the rotor pole face and the stator pole face; the magnetic force will always tend to minimise the reluctance of the flux path. Thus, referring to Figure 2.1, if current is passed through phase A-A', a turning force will act on the rotor tending to turn it counter clockwise, to align rotor teeth one and four with poles A-A'. Sequential switching of the phases causes the rotor rotation to continue.
The switching sequence is; A-A', D-D', C-C', B-B', A-A'. Note that the direction of switching proceeds clockwise around the stator but the rotor rotates in a counter clockwise direction.
The motor illustrated is a four phase motor at the first step in the sequence when 1-4 on the rotor aligns with A-A' on the stator. After four switching sequences (or steps), the first phase to be switched on or excited is once again

excited and again a pair of rotor poles or teeth (2-5) line up with this pair of stator teeth (A-A').The rotor will have moved one tooth pitch or 360/6 = 60° as there are six rotor teeth. Therefore, in four steps (as this is a four phase motor) the rotor has turned 60°. Taking the general case of an N phase motor with p rotor teeth:

$$StepAngle = \left(\frac{360}{Np}\right)^{\circ}$$

Note; this formula is only applicable to variable reluctance stepper motors.

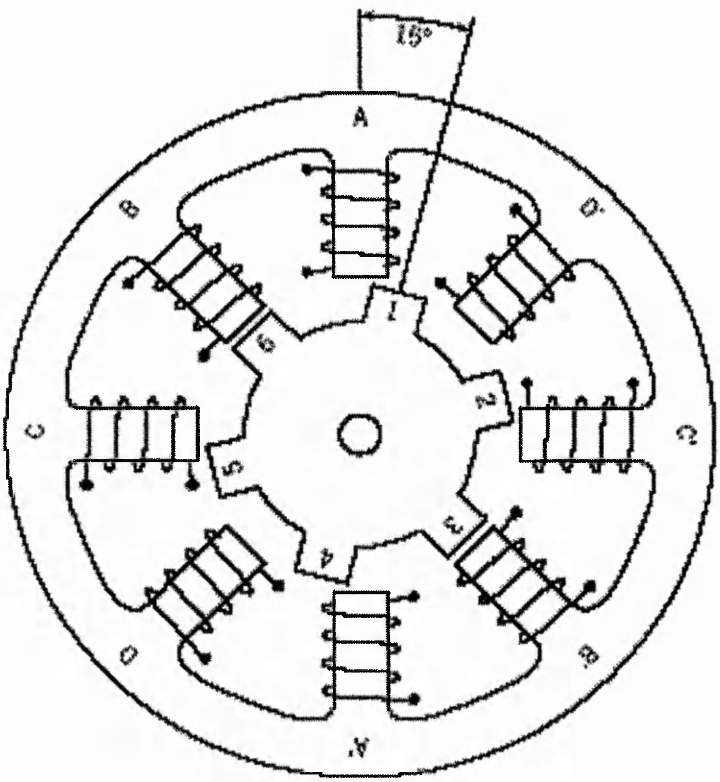

Figure 2.1 Variable Reluctance Stepper Motor [11]

2.2.2 Permanent Magnet Motor

The principle of operation of the permanent magnet stepper motor is explained by reference to Figure 2.2 [11]. Permanent magnets are used in the construction of the rotor. Unlike the variable reluctance motor, the rotor does not have teeth but is of cylindrical construction and has a north pole and a

south pole. The motor shown has two phases with one phase winding, on poles A and C and the other phase winding is on poles B and D.
Each stator pole pair (A and C are one pair, B and D the other) has a north and a south pole facing the rotor; the polarity of the poles is alternated by changing the polarity of the voltage applied to the stator phase windings. Alternative switching of the polarity causes the rotor to rotate. This type of motor provides greater torque than the variable reluctance stepper motor but with reduced resolution (the step angle is not as small). If the phase winding on pole pair A-C is referred to as X and the phase winding on pole pair B-D is referred to as Y, the single stepping sequence for clockwise rotation is Y+ X off / X+ Y off etc. This gives the stator magnetic pole sequence of B north – D south / A north –C south etc. Two other types of permanent magnet stepper motors exist, that have a rotor that consists of multiple North-South poles around the circumference of the rotor. These are the "tin-can" motor and the "disc-motor". Both provide greater resolution than a conventional permanent magnet motor. The rotor of the disc-motor has a very low moment of inertia; this is useful where high acceleration is required.

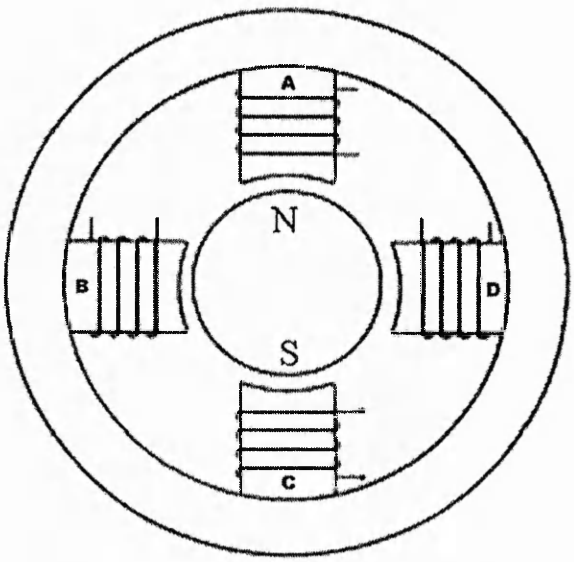

Figure 2.2 Permanent Magnet Stepper Motor [11]

2.2.3 Hybrid Motor

The hybrid stepper motor is a combination of the variable reluctance and the permanent magnet stepper motors and provides high resolution and greater torque than the permanent magnet stepper motor. The arrangement of a hybrid stepper motor is shown in Figure 2.3 [21]; the rotor is toothed in a similar manner to the variable reluctance rotor. The permanent magnet is contained within the rotor, runs axially and is positioned concentrically around the shaft.

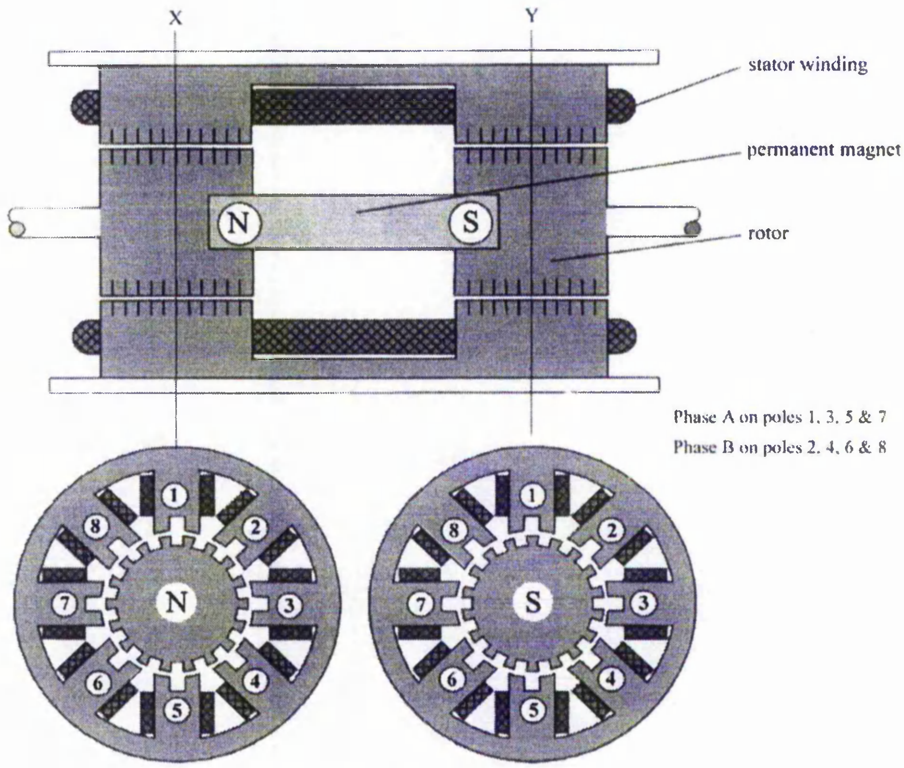

Figure 2.3 Hybrid Stepper Motor [21]

The rotor teeth at the north pole end of the rotor are displaced by one tooth pitch from those at the south pole of the rotor; this feature halves the stepping angle of the motor. The motor example shown has two phase windings, phase A and phase B. Phase A is wound onto poles 1,3,5 and 7, phase B is wound onto poles 2,4,6 and 8. The successive poles of each phase are wound in the opposite direction, that is, the windings on poles 1 and 5 are wound in the opposite direction to the windings on poles 3 and 7. Thus, when poles 1 and 5 are producing a magnetic flux that is in an outward radial direction, poles 3 and 7 will be producing a magnetic flux that is in an inward direction. The direction of the flux is reversed by reversing the polarity of the electrical connection to the phase winding. A switch sequence for clockwise rotation would be: A+, B+, A-, B-, A+ B+ or for counter-clockwise rotation: A+, B-, A-, B+, A+, B-.... Typical stepping angles for hybrid stepper motors are in the range of 3.6° to 0.9°. Four steps of movement result in a change of rotor position of one tooth pitch, that is, each step is ¼ of a rotor tooth pitch. Thus the step angle is related to the number of rotor teeth p and can be found from the equation:

$$StepLength = \left(\frac{90}{p}\right)^{\circ}$$

The path of greatest magnetic permeability is through the metal of the rotor and stator, so the flux is concentrated by the teeth of the rotor and stator. This increases the detent, holding and pull out torque characteristics of the rotor (the different torque characteristics are explained in the bibliography).

2.3 Stepper Motor Control

2.3.1 Single/Half Step Control

The following explanation can be applied to all types of stepper motors; however, as explained in 2.1.1, the direction of rotation of the rotor for the variable reluctance motor will be opposite to the direction of the rotating flux. In both the hybrid motor and the permanent magnet motor the direction of rotor rotation will be the same as the direction of rotation of the magnetic flux, as shown below by use of the conceptual motor model.

The basic form for stepper motor control is the single step drive; this can be in the form of wave drive or 'normal' single step drive. The wave drive system is achieved by applying a square wave voltage to each phase in turn. A conceptual stepper motor is shown in Figure 2.4. This represents a single step rotor motion with a step index point coincident with the pole face; the direction of the rotor is the same as the direction of the rotating field.

The conceptual motor diagram (Figure 2.4) depicts a motor with two phase windings and a step angle of 90°. When the windings are powered in a clockwise sequence, as shown for a wave drive in table 2.1, the rotor will be attracted to the positive energised pole and will index in a single step

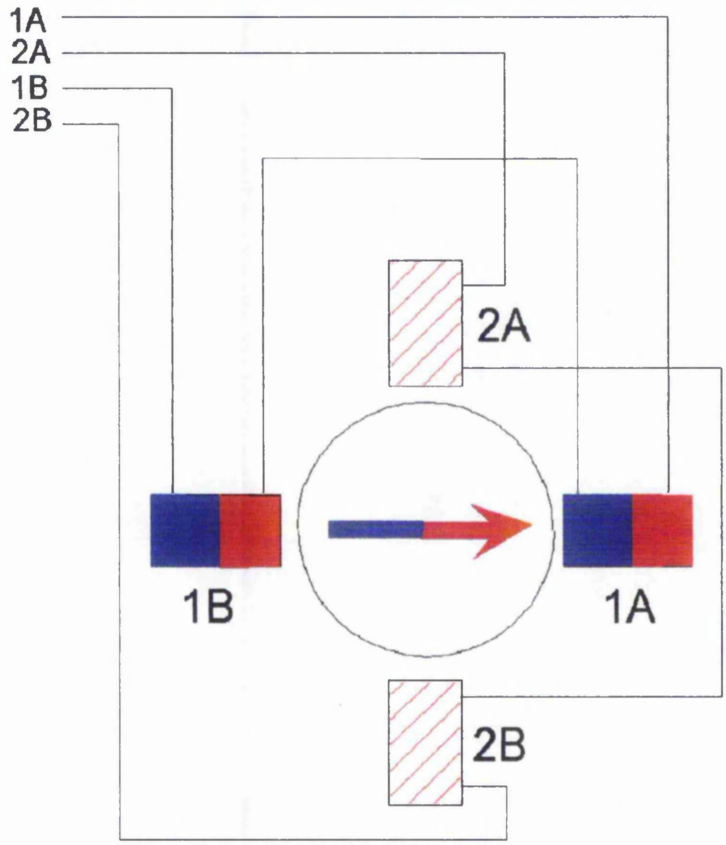

Figure 2.4 Conceptual Stepper Motor

fashion.

The single step section of table 2.1 indicates that the windings are energised as adjacent pairs in a clockwise direction around the motor. In this instance, the rotor will be attracted to the point of flux equilibrium, which is the mid point between the two energised poles. The rotor will index around the motor in single step mode but because two poles are energised, the torque produced will be the vector sum of the torque produced by the two poles and therefore greater than for the wave sequence.

The half step mode, as shown in table 2.1 is a combination of wave mode and single step mode, thus the rotor at each consecutive step of the cycle is alternately attracted to the energised pole position and subsequently to the next equilibrium point between two energised poles. Thus, the rotor will index around the motor in increments of half a pole pitch or half a step.

Step Mode	Field Sequence	Polarity	Remarks
(1) Single Step Wave	0001 0010 0100 1000	− − − + − − + − − + − − + − − −	•One winding energised per step •Low torque •Point of equilibrium in line with pole
(2) Single Step High Torque	0011 0110 1100 1001	− − + + − + + − + + − − + − − +	•Two windings energised per step •High torque •Point of equilibrium mid way between poles
(3) Half Step	0001 0011 0010 0110 0100 1100 1000 1001	− − − + − − + + − − + − − + + − − + − − + + − − + − − − + − − +	•Combines Wave and High Torque Single Step methods alternately to achieve half stepping. • Torque at two winding equilibrium point greater than a single winding equilibrium point by a factor of √2

Table 2.1 Stepping Sequence Commutation

2.3.2 Micro-Stepping Control

It has been shown in section 2.2.1 above, that if equal voltages are applied to two adjacent windings, then equal currents flow in these windings and therefore produce a point of equilibrium at the mid point between the two poles (see Table 2.1 item (2)). The torque produced by a half step controller fluctuates, as subsequent half steps use one winding energised followed by two windings energised. At the point where two windings are energised, the torque is increased by a factor of $\sqrt{2}$; this is the vector sum of the two equal lines of magnetic flux acting at right angle to each other. This fluctuation of torque contributes to rotor oscillation. Points of equilibrium at other positions between poles can

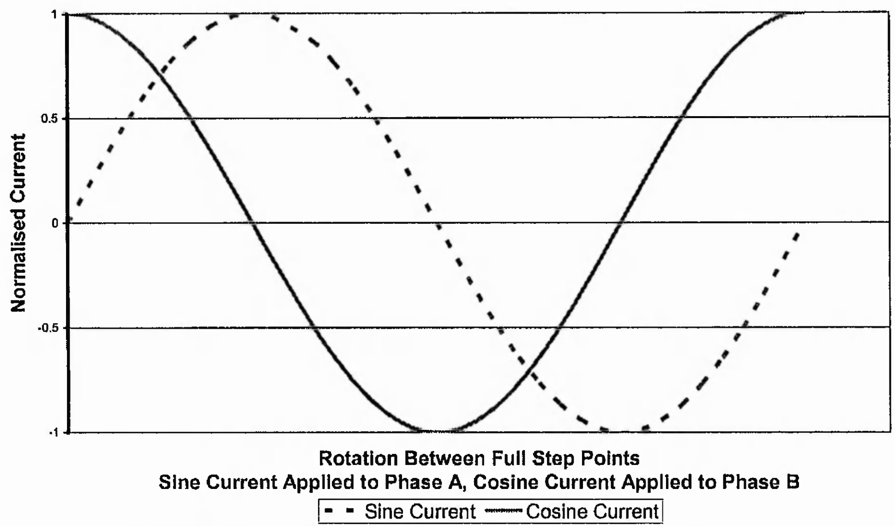

Figure 2.5 Current Applied to Two Phases for Micro-stepping

be generated by controlling the proportional voltage applied to adjacent windings. A micro stepping controller applies a sine wave to one winding and a cosine wave to the adjacent winding, as shown in Figure 2.5. The spacing and shape of the stator pole faces relative to the rotor teeth are designed to produce a natural torque for the motor that is as near as possible to being sinusoidal. As $\cos^2\theta + \sin^2\theta = 1$ the flux strength and therefore the torque distribution will be constant at all of micro-step positions as shown in the locus diagram of Figure 2.6. Note that Figure 2.6 shows only four micro-steps positions; modern micro-stepping drives generate 8 bit pulse width modulation (PWM), effectively 256 micro-steps per full step. As the windings effectively act as a low pass filter, such a drive is producing virtually continuous sinusoidal waves.

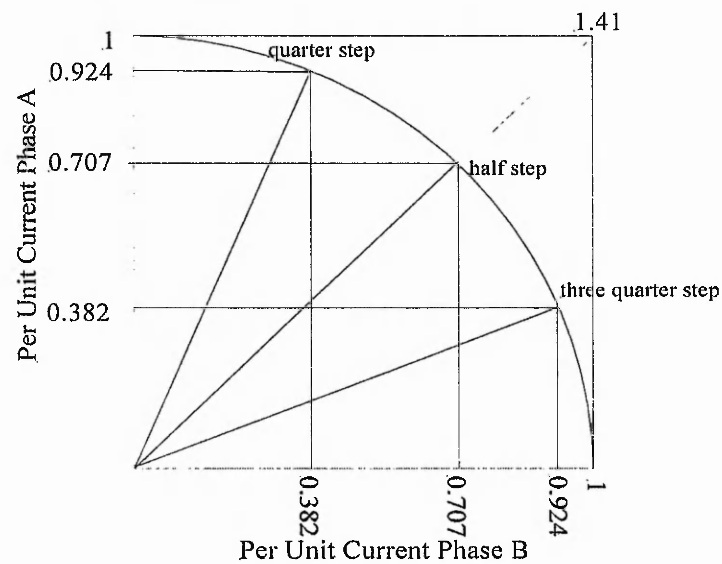

Figure 2.6 Locus Diagram of Current in a Two Phase Motor when Micro-Stepping

2.3.3 Closed Loop Control

A major disadvantage of a stepper motor used in the conventional open loop control (without motor shaft position feedback) occurs if the load torque exceeds the pull-out torque (the maximum torque that the motor can drive at a specific stepping speed without slipping out of step) of the motor. This will cause the motor to slip (or skip) out of synchronism, thus the position of the rotor no longer coincides with the position commanded by the driver control circuit. The motor may slip one full step or several steps or stall completely. The loss of step remains undetected. Closed loop control involves some form of motor position control, whereby errors in the tracking of the motor position are detected and the drive control is then corrected. If the rotor position tracking is of sufficiently high resolution then the rotor angular position can be compared with the stator flux position, the difference in position is the torque angle. As the load increases so does the torque angle. If either the torque or the stepping speed keeps increasing, the pull-out torque will eventually be exceeded and the rotor will be attracted to the previous step position, causing the motor to slip out of step. The characteristics of the load cannot be affected by the controller but the motor speed can be reduced (this will reduce the torque angle) to prevent the motor from slipping out of step. Given this level of closed loop control, the stepper motor will behave as a servo motor (the servo motor is described in sections 1 and 1.3) but it will still retain the advantages of a stepper motor.

A separate transducer such as an optical encoder can be used as the feedback element for closed loop control but the added expense and loss of convenience in ease of installation are a substantial disadvantage.

However, methods of positioning monitoring have been developed that do not use shaft encoders or any other type of hardware. Such methods are referred to as sensorless position monitoring systems. Two such methods are described in the next section. Research by Frus and Kuo reveals that many parameters influence the shape of motor waveforms [12], these include back EMF. The first system makes use of the motional voltage (back EMF) generated by the rotating motor; Figure 2.7 [21] is used to explain this method. The motional voltage affects the shape of the current waveform and a suitable feature is chosen to generate the rotor position signal [13].

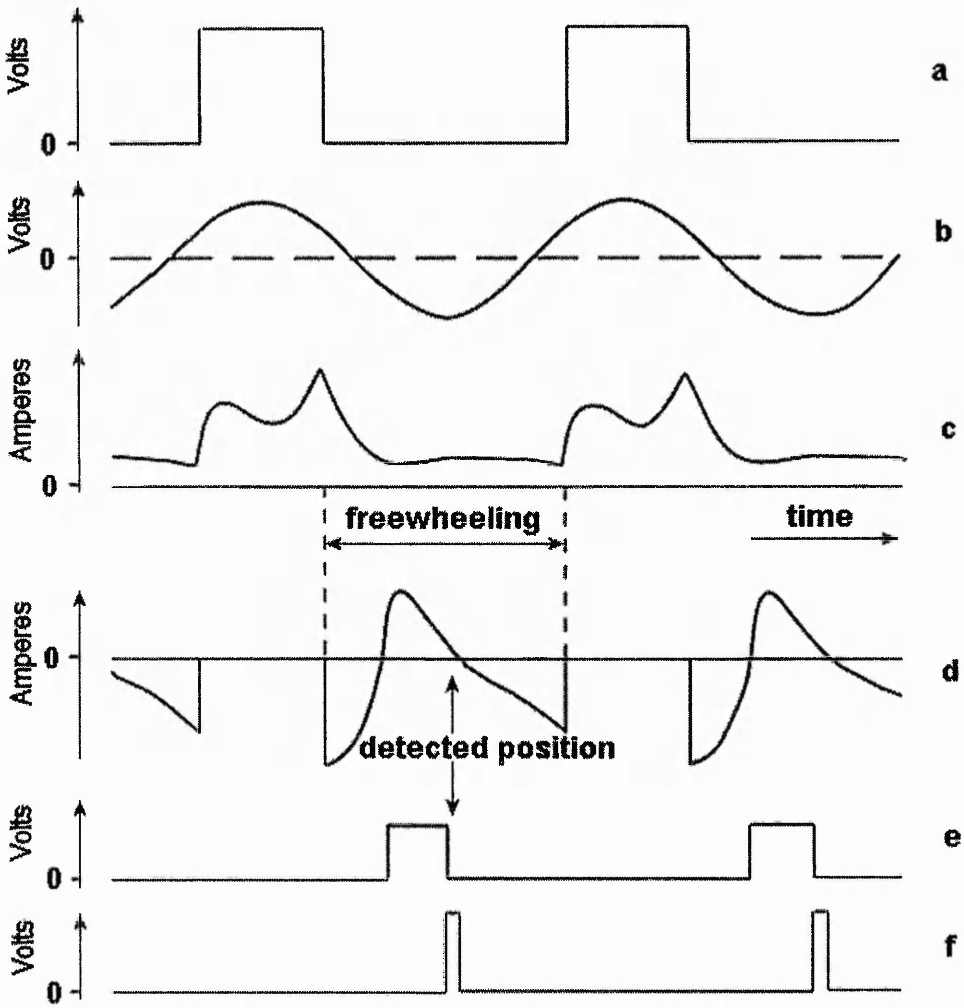

Figure 2.7 Motional Voltage Detection [21]

a) Applied phase voltage

b) Motional voltage waveform

c) Current waveform

d) Rate of change of freewheeling current

e) Comparator (zero crossing detector) output

f) Position detector pulses

The motional voltage reaches its maximum value during the period when a voltage is applied to the phase. At this time, the motional voltage opposes the phase current and may even cause decay in the phase voltage, while the square wave voltage is applied to the phase. When the applied voltage is removed from the phase, the phase current will decrease. The motional voltage moves to its negative half cycle and tends to increase or assist the current through the phase during the *freewheeling* period (the part of the cycle when the applied voltage to this phase is switched off) of the phase. Waveform d) is the derivative of waveform c), thus at the point during the freewheeling period where the phase current c) is at a minimum or maximum (zero rate of change), waveform d) passes through the zero voltage level. A comparator is used to detect the zero crossings and the comparator output produces waveform e). Waveform f) is a series of pulses produced by detection of the negative edges of waveform e) and can be used to control the commutation of the next phase. It has been demonstrated by Siefert and Lahr. [14] that the automatic commutation (switching) of the next phase ensures that the motor is driven at the maximum possible speed without slipping out of step.

This method is not suitable at very low speeds as the magnitude of the motional voltage is too small to be useable (Acarnley et al [15]).

The second method relies upon the constantly changing of phase inductance relative to the rotor angular position [16] [17]. This is due to the relative position of the rotor and stator teeth changing and varying the reluctance (resistance to the flow of magnetic flux) as the rotating magnetic flux changes the saturation level in the stator teeth.

As the current in a micro-stepping drive is limited by current chopping, the rise time of the individual chopped current segments are modified by the changing time constant of the circuit, as can be seen in Figure 2.8. The time constant is defined as resistance divided by inductance (R/L); the inductance L is dependent upon the path of the magnetic circuit. The magnetic path is through the iron of the stator and rotor (low inductance) and through the air gap between the rotor and the stator (high inductance). When the rotor is fully aligned with the stator in any given phase, the air gap will be at a minimum; therefore the time constant will be at a minimum. The air gap and therefore the time constant will be a maximum midway between the full step positions. Thus, at the beginning and end of a full step, the individual current segment rise times will be quick and will be proportionately slower the closer the rotor is to the midway point between steps. Detection of these rise times can give a continuous indication of the rotor position, throughout a wide speed range but most accurate at lower speeds.

A variation of this technique described by Petrović et al. [18] relies on PWM excitation transients. Other methods are reviewed by Husain [19].

Monitoring the mutual induced voltage in the inactive winding is also useful for estimation rotor position and is described by Husain and Ehsani [20].

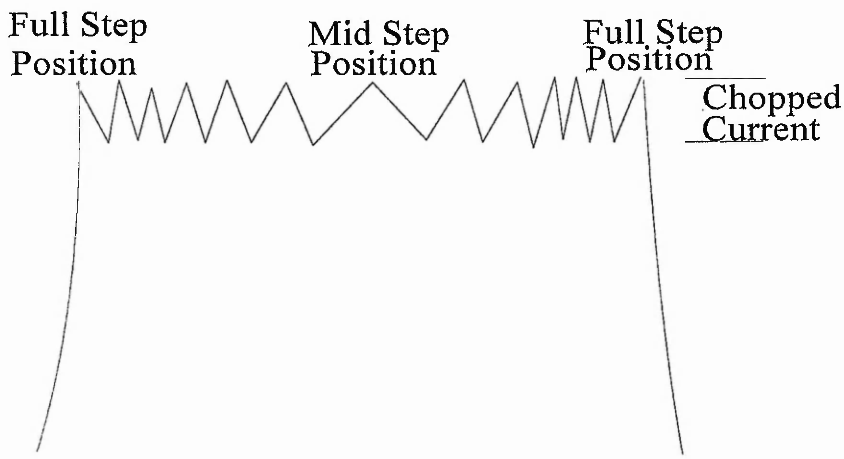

Figure 2.8 Current Chopping Ripple

2.4 Oscillation in Stepper Motors

2.4.1 Oscillations Associated with the Natural Frequency of the Motor

Because of inertia in the system, a single step motor will overshoot and oscillate about the step position. The effect on rotor position is shown in Figure 2.9; this is the natural frequency of the rotor (or of the combination of the rotor and the connected load). If the subsequent step is commutated during the period accelerating overshoot, the amplitude of the overshoot of the next step will be increased. This will be repeated at each step so long as the rotor is driven at this speed until the increasing instability drains torque from the system and the rotor will slip out of step. Acarnley [21] [22] demonstrates that the natural frequency of the rotor f_n is:

$$f_n = \frac{1}{2\pi}\sqrt{\frac{T}{J}}$$

where T is the holding torque and J is the motor/load inertia.

Thus if the stepping speed of the motor matches the natural frequency of the motor and load combination, then resonance will occur. Also if commutation occurs during any of the periods bounded by the dotted lines of Figure 2.9, resonance will occur. Therefore, if the motor is operated not only at the natural frequency of the motor/load but also at submultiples of this frequency, resonance will be manifested as described by Lawrenson and Kingham [23]. Thus, if the natural frequency is 100 Hz, stepping rates of 100, 50, 33 and 25 will result in resonance. The consequences of resonance may result in an increase of resonant amplitude that moves the rotor to a step position beyond the desired position or as a result of sinking energy will cause dips in the torque speed characteristic (see Figure 2.10) that may cause the rotor to pull out of step and lag behind the desired position.

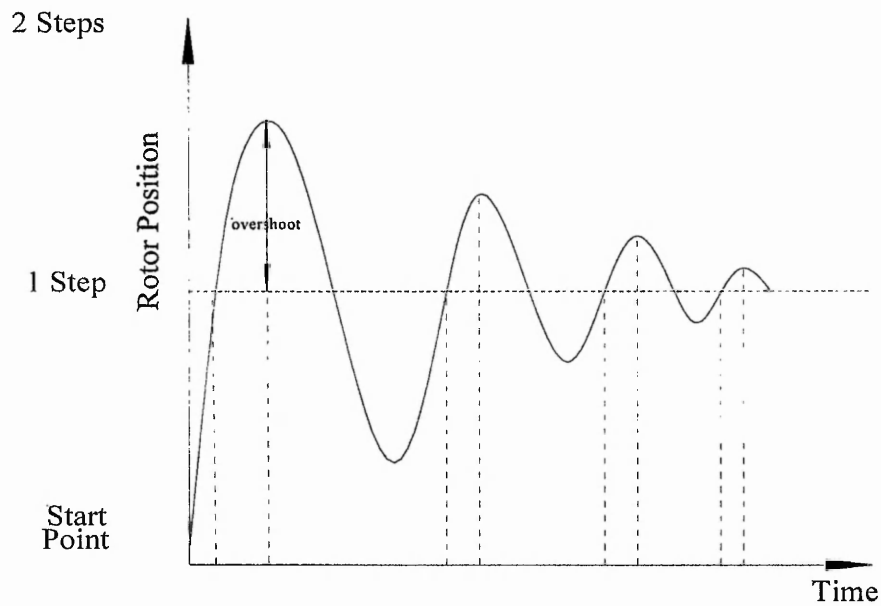

Figure 2.9 Single Step Response [21]

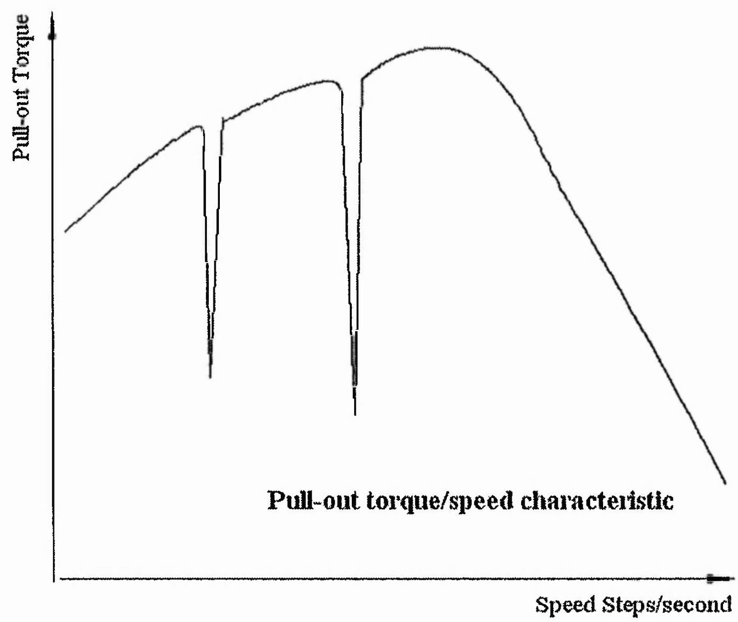

Figure 2.10 Resonance Effect on Pull-Out Torque [21]

The pull out torque is so named because, if the load exceeds the pull out torque, the rotor will slip out of synchronism or possibly stall completely. A typical pull out torque characteristic is shown in Figure 2.10, The two sharp dips in the curve occur due to energy being absorbed in resonance at the natural frequency and at the most significant sub multiple of the natural frequency (50%).

For clarity only two occurrences of the effect of resonance are shown above. There will in most cases be several more at lower speeds; these will be of decreasing severity. The drop outs in the pull out torque will limit the acceleration that can be maintained without pulling out of synchronism.

When a square wave voltage is applied to a phase winding, the resulting current through the winding is not an ideal square wave. Because of the inductive time constant of the windings, the rise time of the current is exponential and because of the stored energy in the winding, the fall time also decays exponentially (Figure 2.11). As the speed of the motor is increased, there is less time available for the current to rise to its maximum value, also at greater speed the back EMF (known as the motional voltage) generated by the motor opposes the flow of current in the windings. The combined effects reduce the pull-out torque of the motor as the speed increases. This causes the rotor to be more susceptible to resonance disturbances.

The current can be *forced* if a series resistor is used in series with the phase winding to improve the time constant of the winding and the voltage is increased to compensate for the voltage drop across the resistor. This is known as an L/R drive, however the efficiency is at best 25% [24], because of the losses in the resistor.

A high level control solution is to increase the applied voltage to a greater value than the rated voltage of the motor at high speeds, to force a faster rise time of the current. It is then necessary to limit the peak value of current. This is normally achieved by use of current chopping (rapid switching on and off of the applied voltage when the current is at the maximum value) or in the case of a micro stepping drive by control of the mark space ration of the PWM pulses. Chopper drives are much more efficient than L/R drives and are typically 75 to 90% [24].

Unfortunately, because of physical constraints of the motor, the natural single step torque of a motor will never be exactly sinusoidal. The torque may be a close representation of a sinusoid but the shape of rotor and stator pole faces

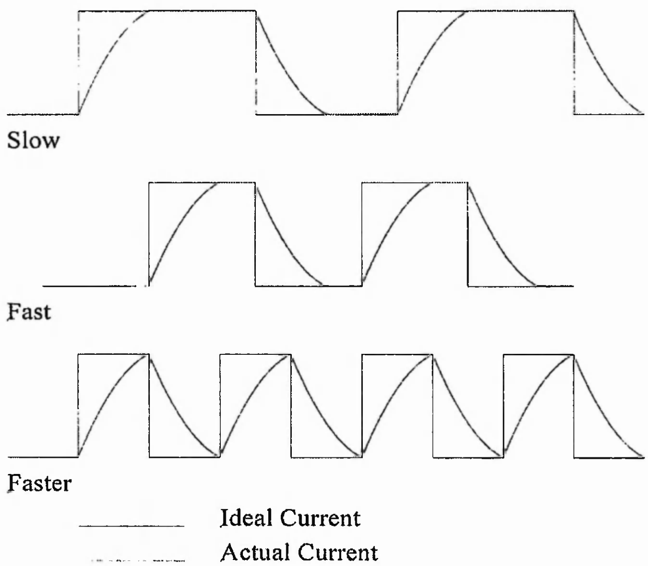

Figure 2.11 Effect of Stepping Rate on Current

cause deviations from the ideal.

It has been shown by Jones[25] that the resonant frequency of a permanent magnet or hybrid stepper motor is:

$$f = \sqrt{\frac{k}{J}} \times \frac{1}{2\pi}$$

where k is the spring constant of the system in Nm, J is the moment of inertia of the rotor and the coupled load, and k is a function of the holding torque. The holding torque for two winding single stepping is greater than that for single winding single stepping by a factor of $\sqrt{2}$ and Jones [25] also demonstrates that the relationship of resonant frequency for single winding stepping f_1 to two winding stepping f_2 is:

$$f_2 = \sqrt[4]{2} \times f_1$$

A useful method of avoiding the onset of resonance with a half stepping system is to step only with the single winding steps at the speed where resonance occurs when half stepping and reverting to half stepping after accelerating through this particular speed band.

If similar motors will have different loads coupled to them, the resonant frequency will not be the same. Indeed, the coupled load in a single system may be variable due to frictional changes. Thus, the natural frequency for any given system cannot be assumed and if resonance is to be avoided it must be detected at the onset or predicted immediately before the onset. If this is to be achieved, closed loop control is needed; either an encoder or alternately sensorless methods may be used.

The low and medium speed disturbances have been determined in terms of full stepping or half stepping. The effects of low speed disturbance are reduced by the use of micro-stepping because the comparatively small level of movement of each micro-step expends less energy. Thus, the level of overshoot at each micro-step is much lower than that produced when using a full or half step drive.

2.4.2 Other Instabilities

There are three ranges of instability discussed by Kenjo and Sugawara [8]: low frequency resonance as discussed earlier in section 2.3.1, mid-range instability and the higher range oscillation. The previously discussed low-frequency resonance occurs typically at stepping rates of below 200Hz or 200 full steps per second. Medium-range instability is usually within the range of 500 to 1500Hz with a period of 4 to 5 full-steps and Ward and Lawrenson [26] report that it has the following characteristics:

(i) The oscillations may have one or several frequency components. They are not simply related to the stepping rate, and are usually at a fairly low frequency, e.g. in the range 5-200Hz.

(ii) With constant operating conditions, although synchronism can be lost suddenly, there is normally a slow build up of oscillations, over a period of many seconds or even minutes before failure finally occurs.

(iii) The various characteristics of the instability depend in a complex way on the type of drive and on the mode of operation; e.g. full- or half-step mode.

(iv) The size of torque dip and capacity to run to high speed are very sensitive to the degree of mechanical damping. Often, with sufficient damping, dips can be 'smoothed out' or the speed range extended.

(v) Inertia is an important parameter; large inertias commonly exacerbate the problem.

Kenjo and Sugawaro [8] explain that it has been shown that drive circuit variations on bifilar (see appendix A) type drives have had the effect of shifting the stepping frequencies at which mid-range disturbance occurs. The circuit changes involve the use of additional passive components (capacitors). The text shows the results of the change of the disturbance characteristic but does not describe how the operation of the drive is modified. The added capacitor is in parallel with the winding and must have an effect on the time constant of the circuit. It is likely that, at some point within the speed range of the motor the stepping rate will coincide with the resonant frequency of the parallel LC circuit. This would cause the current drawn by the motor to fall to a very low or near zero value and the motor field would collapse. The text states that large amplitude instability appears at 1275Hz and synchronism fails. The system mechanical parameters of load and inertia, and also electrical parameters of the series resistor and the capacitors in circuit 2 are known to affect the speed at which mid-range disturbances occur, and that these effects are dissimilar for each of the to drive circuits. It would therefore appear to be possible to avoid the onset of disturbances by the use of high level control in the drive. The drive circuits are illustrated in Figure 2.13. It is observed that these circuits are not designed for micro-stepping due to the field forcing resistor in series with the phase windings.

2.4.3 Factors Limiting Resolution

Friction is the cause of a *dead zone* as described by Jones [25] as a combination of static and sliding friction that must be overcome by the motor before any useful torque is developed. The effect is illustrated in Figure 2.12; the dotted lines in part A of the diagram indicate the level of torque required to overcome the friction.

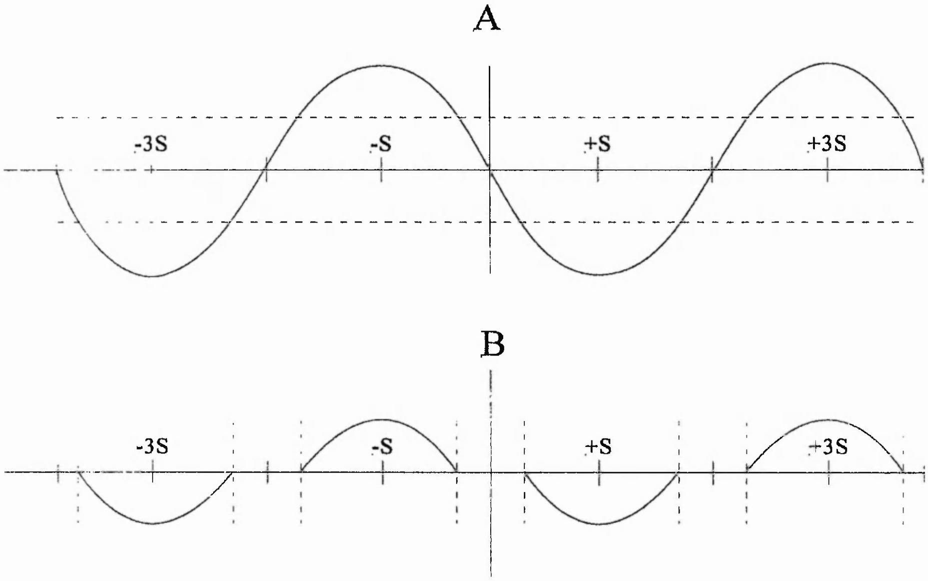

Figure 2.12 Dead Zone

Part B of the diagram indicates the available torque to drive the rotor and the width of the dead bands. Jones [25] shows that the angular width of the dead zone is:

$$d = 2\left(\frac{S}{\frac{\pi}{2}}\right)\sin^{-1}\left(\frac{f}{h}\right) = 4\left(\frac{S}{\pi}\right)\sin^{-1}\left(\frac{f}{h}\right)$$

Where:

d : width of dead zone, in radians

S : step angle, in radians

f: torque needed to overcome static friction

h : holding torque

Accurate positioning can be severely restricted in micro-stepping systems if the friction is significant. If the friction is so great that the dead zone angle is larger than the micro-stepping angle, it may not be possible to start the motor. The detent torque (the torque exerted by the magnetic poles without any voltage applied to the windings) is the cause of deviation of the rotor from the expected position during mid step transitions. The actual and expected positions will coincide at each full step detent.
Quantisation errors due to the d/a conversion of the PWM and hysteresis of the current control, cause a cyclic deviation from the expected position during the mid step transition.

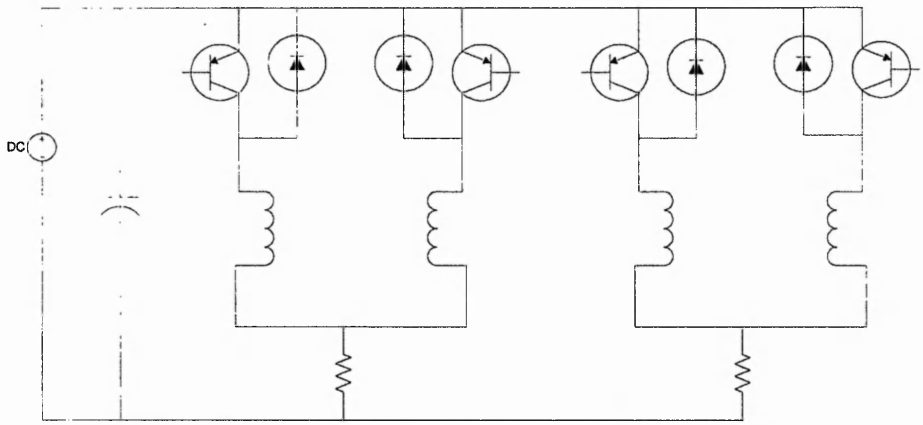

Circuit A

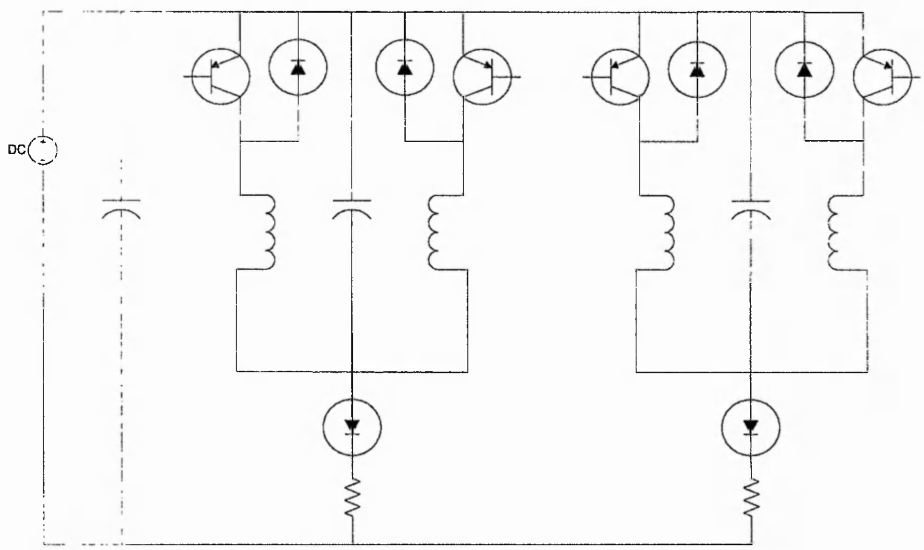

Circuit B

Figure 2.13 Alternative Circuit Arrangements for Forcing Resistor

The forcing resistor reduces the time constant of the phase windings enabling a faster rise time for the current in the winding and thus permitting faster motor speed. The applied voltage must be increased because of the voltage drop of the resistor. In a micro-stepping system, the applied voltage is increased to reduce the rise time and the current is limited by the PWM ratio, as previously described.

The third type of instability is higher range resonance occurring in the range 2500 to 4000Hz. Kenjo and Sugawaro [6] state that there are no reports which deal with this kind of oscillation.

Of the three ranges of disturbance described, little is known about high speed disturbance.

2.5 Stepper Motor Control Limitations

Sometimes servomotors are installed in systems where a stepper-motor would be the better choice. Often this is the result of concern over the possibility of stepper motors slipping steps, even if this is not an issue for the particular application. Sometimes this may be a result of manufacturers/vendors of servomotors exaggerating this particular stepper-motor problem. If the application is a duty where the load on the motor is consistent, there is no requirement for rapid acceleration and the correct size of stepper motor is selected, there should be no probability of the motor slipping. If the same application involves very low speeds, then it is likely that a stepper-motor would be the best choice.

Even so, one of the biggest disadvantages a stepper-motor has, when compared to a servomotor is the possible loss of position control due to the motor slipping out of step. If stepper-motors are to be more competitive then this particular disadvantage needs to be eliminated or minimised.

There are some applications where a stepper motor is clearly the best choice for the task and other applications where a servomotor is clearly the best choice. There are however many areas where both types of motors have attributes that could be favoured for the task in hand and the correct selection of motor type is not so obvious. The table below clearly compares the two types of motor.

Attribute	Stepper-Motor	Servo-motor
Low Cost	✓	
Can work in open loop (no feed-back required)	✓	
Good holding torque, no hunting, eliminates need for brakes	✓	
Good torque at low speeds (no gearbox required	✓	
Low maintenance	✓	
Rugged	✓	✓
Excellent for precise positioning	✓	
No loop tuning required	✓	
Position control maintained regardless of load or velocity		✓
High intermittent torque		✓
High torque to inertia ratio		✓
High torque at high speeds		✓
Good velocity control		✓
Wide range of motor sizes		✓
Quiet		✓
Readily Available	✓	✓

Table 1.1 Comparison of Stepper Motor to Servomotor [27]

A stepper motor can be endowed with some of the benefits of the servomotor without sacrificing the advantages specific to a stepper-motor. This can be done by providing a feedback to the controller without incurring the extra costs and more complex installation of using an encoder, i.e. *sensorless* feedback.

2.5.1 Control Methods

Stepper motor control methods can be broadly divided into the following categories:

1. Full Step Control. The motor construction defines the number of full steps in 360° of rotation or the step length in degrees. The step length for a hybrid motor is defined as follows. The switching sequence for full step motion is shown in the following paragraphs in table 2.1; it can be seen that

there are four switched states for a movement of one cycle of rotation. In the case of the conceptual motor in figure 2.4, one cycle of rotation is 360°. This is not representative of a motor with teeth on the rotor and the stator. If the hybrid stepper motor in figure 2.3 is considered, the four switched states will result in a movement of one tooth pitch of the rotor. So each state will produce a movement of ¼ of a tooth pitch. Therefore, one step of movement is ¼ of a tooth pitch. If p = the number of rotor teeth, the length of a step is defined as: ***step angle = (90/p)°***.

2. Half Step Control. This is achieved by alternatively energising one phase at a time and two phases at a time to create additional points of magnetic equilibrium midway between full step positions. This is fully defined in 2.2.
3. Micro-step control. Just as exciting two phases simultaneously can create a point of equilibrium midway between two step positions, additional points of equilibrium can be created by controlling the ratio of current through each of the two phases. This is explained in detail in 2.3.2.

There are different methods of switching the power to a stepper motor and the method used is dependent upon the type of stepper motor and upon the manner in which the motor phases are wound. The principal methods are explained in Appendix A.

2.5.2 Motor Resonance

Low speed resonance in stepper motors is a significant problem, being the cause of rough running and noise at low speeds. Resonance also has a detrimental effect on the pull-out torque of the motor, as energy that is required for driving the motor is used to produce the resonant oscillations in the rotor. This is explained in detail in section 2.3.1.

The natural frequency of a motor is dependant upon not only the inertia of its own rotor but also the inertia of the load that is coupled to it. If T = torque, J = inertia of the rotor plus load and f_n = natural frequency then:

$$f_n = \frac{1}{2\pi}\sqrt{\frac{T}{J}}$$

If the motor runs at the natural frequency or at a sub-multiple of the natural frequency the rotor will oscillate and the motor may slip out of step. This phenomenon is explained in detail in 2.3.

Oscillations due to the natural frequency of the motor may be reduced by either mechanical or electromagnetic damping. Research by Pickup and Russell [28] investigates frequency modulation of the PWM waveform may be controlled to induce electromagnetic damping effect.

Ripple torque is a phenomenon that affects the smooth motion of permanent magnet motors including stepper motors. Hung and Ding [29] have modelled current optimisation technique for the reduction of ripple torque and describe the causes of ripple torque as:

- Interaction between the permanent magnet field and the currents in the phase windings.
- The effect of dentent torque.
- Self-inductance variations of the motor winding that are a function of rotor position.

Further research by Cho et al. [30] demonstrates that torque harmonics are a function of the back EMF. They propose that by predicting the back EMF and the armature current, torque harmonics can be compensated by the addition of high order harmonics to the armature current. Torque ripple reduction methods are also reviewed by Husain and Ehsani [31].

2.6 Summary

Sensorless position detection provides an opportunity for improving the performance of stepper motor drives by reducing oscillations and optimising the motor speed, when compared to stepper motors operating in open-loop control. Operation in open loop requires maintaining a margin of safety with regard to the motor load, speed or acceleration, so the motor is under utilised as stated by Vraets et al [32]. Methods of control based upon motional voltage waveform and on the variation of phase inductance relative to rotor position have been discussed in section 2.3.3. The motional voltage method of position monitoring is not suitable for low speed operation; however variation of inductance with rotor position is valid over a wide speed range. Stout [33] states that closed loop control has only been used with limited success to reduce rotor oscillations as even with feedback the controller can only damp resonance within the limits of the controller. Therefore, different methods of utilising the change of inductance have been chosen for further investigation.

Available torque is reduced at high speeds because of the time constant of the phase windings restricting the build up of current in the windings. This is compensated for by increasing the voltage applied to the phases and using some method of limiting the current. The torque can be maintained at high speed, even if the current is reduced, by increasing the torque angle (the angle that the rotor lags the stepping sequence) [34]. The angle must be varied with motor speed and requires accurate feedback from a shaft encoder.

Chapter 3 Instrumentation

3 Instrumentation

3.1 Requirements for Stepping Motor Instrumentation

A reliable instrumentation system integrated and controlled by software is a requirement for the acquisition of meaningful results that will assist the achievement of the three basic objectives of this project; to detect when a motor slips out of step, to count how many full step are slipped and to determine the mid step position of the rotor. The investigation of commercially available instrumentation systems has provided an insight into what is currently used for researching stepper-motors and drivers. This chapter examines commercially produced stepper motor instrumentation systems in order to assess the benefits they provide and then to conclude if a commercial system is viable for use within this project or if it is necessary to build a custom instrumentation system. Requirements of the instrumentation package for this project include:

(i) Single Step Accuracy The capability to accurately resolve and record the rotational angle of the rotor for each full step of the stepper motor. This is necessary if the first objective of the project, the detection of the motor slipping of synchronism by one step, is to be investigated.

(ii) Micro Step Accuracy The capability to accurately resolve and record the rotation angle of the rotor to an angle of less than that moved in one micro-step. Note that, if the resolution of the instrumentation satisfies this requirement, then it must also fulfil the requirement of point (i).

(iii) Step Response (Damping) The capability to record the overshoot of the commanded step position, the subsequent resonance about the step position and the time to settle to the correct position.

(iv) Motor Step Slip The capability to show if at any stage the motor has failed to move to a commanded step position and to record this phenomena. The ability to do this is one of the stated objectives of the project.

(v) Motor Current To monitor and record the current in each phase of the motor and to resolve changes in the current value during the period of each individual micro-step of the motor.

(vi) Motor Voltage To monitor and record the voltage across each phase of the motor and to resolve changes in the current value during the period of each individual micro-step of the motor.

(vii) Resonance The presence of resonance should be identified by oscillatory fluctuations of the actual position of the rotor from the position of the magnetic flux. The instrumentation system should display this by comparison of the resultant current of both phases (in a two phase motor) with the position indicated by the shaft encoder. Note that there will be a difference between the position of the rotating flux and the actual position due to the load torque (the rotor will lag behind the flux); this is not due to resonance.

(viii) Resonance v Velocity The capability to record the changing level of resonance in the system, as the motor is accelerated through a range of speeds.

(ix) Pulse Width Modulation (PWM) To record the PWM pulses for each phase, produced by the stepper motor driver.

(x) Synchronisation of the Data To synchronise the measurements of individual time stamped datum (motor voltage, motor current and PWM pulses) with the rotational angle of the rotor and also relevant to a single fixed point on the circumference of the rotor.

(xi) Post Process Running of the Experiment. To record all of the data and any relevant notes for each experiment in a coherent form that can be examined at any time after the experiment.

A survey of commercial stepper motor instrumentation systems used for industrial research revealed some of the methods in current use for stepper motor development. There are a number of commercially made instrumentation packages designed for the sole purpose of investigating and evaluating stepper motor drive performance. A sample of these are detailed in the following subsections:

3.2 Ono Sokki Stepping Motor Station

The PV-7300 system of the Ono Sokki company [35] is a single system that can measure all seven of the characteristics important in a stepping motor. These seven characteristics are:

a. Static torque characteristics (θ-T, holding torque, detent torque). These features are mainly concerned with defining the characteristics of the motor rather than analysing control techniques.
b. Dynamic torque characteristics (pull-in torque, pull-out torque). This is related to motor step slip as defined in (iv) above.
c. Angular characteristics (damping characteristics and angular accuracy). These characteristics are defined in (i), (ii) and (iii) above.

Of the above, the static characteristics are relevant to the evaluation of motor parameters and are of secondary interest for this research. The remaining characteristics are relevant, in particular the angular characteristics, comprising the angular accuracy and the step response.

The "torque detector" (Ono Sokki terminology, this device is not only a detector but includes a motor/generator for driving or loading the stepper motor under test) enable a variable braking load to be applied to the motor or the ability to drive motor [24].

3.3 Euclid Research Motion Scope

Euclid Research manufacture an instrument for analysis of mechanical motion and related parameters [36]. This comprises an internal card for a PC connecting via the PCI bus plus software. The card provides an interface for digital inputs from a shaft encoder or from a motor driver as well as analogue inputs for voltage and current signals. The data capture can be plotted against absolute time, or against time relative to a pulse into one of the system's trigger inputs. A once per revolution pulse from the shaft encoder coupled to the shaft of the stepper motor could be the event connected to the trigger input (see section 4.2.2). The data is synchronised against a time-base and capture can be manually started or triggered from an external device such as the shaft encoder.

The Euclid features include capture and analysis capabilities for:

1. Single step and micro-step accuracy. Can be defined from requirements (i) and (ii) in section 3.1.
2. Magnetic errors induced by driver current errors. This is defined by requirement (v) above.
3. Resonance against velocity. This is defined by (viii) above.
4. Step response. This is defined by item (iii) above.
5. Dynamic position error. Euclid's definition of this is resonance v velocity this is derived from item (viii) above.
6. Motor drive current. This is defined in item (v) above.
7. Motor step slip. This is defined in, item (iv) above.

All of the above capabilities are of potential use for this research. Of particular interest are the micro-stepping accuracy (refer to item (ii) above) and the dynamic position accuracy (see figure 3.2 [36]). The micro-stepping accuracy is indicated below in figures 3.1(A) and 3.1(B) [36] and is the data capture from a 1.8° and eight bit PWM micro-stepping, that is $2^8 = 256$ micro-steps per 1.8° full step of the motor. Figure 3.1(A) [36] shows the ideal rotor position against the actual rotor position and also a trace of the difference between the ideal and actual rotor positions. Figure 3.1(B) [36] shows the magnetic error induced by current errors. The PWM drive is unable to maintain a perfect sinusoidal form near to the zero cross-over position as can be seen in the current trace. A trace of the current deviation from the ideal sinusoid (as flux is directly proportional to current, this represents the magnetic error) is also present on the same graph.

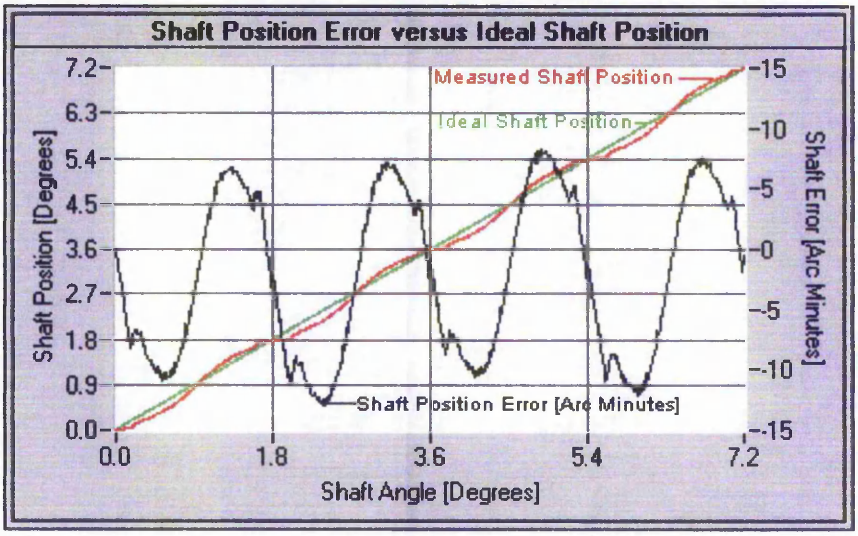

Figure 3.1(A) Euclid Dynamic Error Graph [36] Reproduced by kind permission of Euclid research

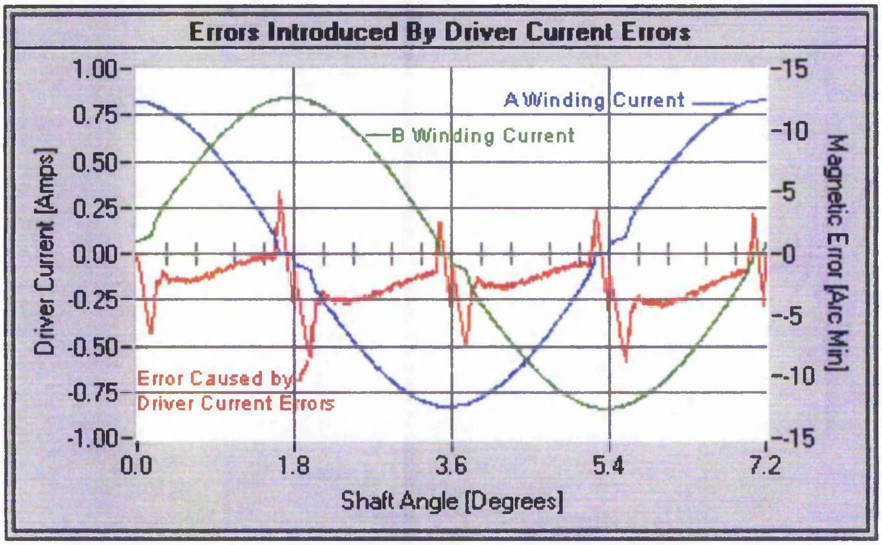

Figure 3.1(B) Euclid Magnetic Error Graph [36] Reproduced by kind permission of Euclid Research

The graph in figure 3.1 (A) [36] shows 4 full steps or one electrical cycle of measured shaft position against ideal shaft position, with the shaft position error superimposed at a larger y axis scale. The graph in figure 3.1(B) [36] shows the error of the generated magnetic flux caused by inaccuracies of the current waveform. Distortion can be seen in the current waveforms near the zero crossing point. The H bridge drive cannot generate a clean sinusoidal wave in this region; the errors are caused because the rate of change of current is at a maximum at the zero crossing and the drive is unable to fully discharge the stored energy in the non active winding in the time available.

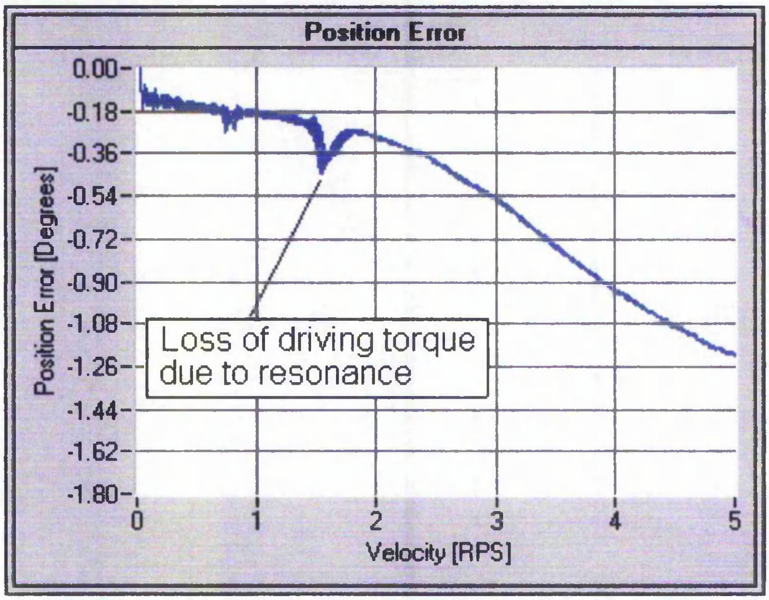

Figure 3.2 Euclid Dynamic Position Error [36] Reproduced by kind permission of Euclid research

3.4 Summary

It has been found that the two systems described above provide facilities that are of use to this research but are not flexible enough to fulfil all of the requirements. Neither of the systems provides a facility for comparing the phase relationship of the motor terminal voltage and current. An alternative method to obtain feedback of the angular position of the rotor is based on the variation of phase inductance with rotor position (see section 2.3.3). A useful feature of the Ono Sokki system is the torque detector (see section 4.2), which under software control can provide a braking effect to the motor or can drive the motor. The ability to drive the stepper-motor with another motor coupled to its shaft can be useful for examining motional voltage in isolation from the other signals that are present when rotating under its own power. The Euclid system provides a versatile method for capturing and synchronising analogue and digital signals and for the storage of the data, so that it can be analysed at a later time.

It was decided to design and build a system specifically for this research, because of the lack of flexibility of the commercial systems. Also, the financial constraints of the project precluded the expenditure for the acquisition of a 'ready built' instrumentation package; the Ono Sokki system was $8000.00 from a supplier of surplus equipment.

Chapter 4
Test Methods and Equipment

4 Test Methods, Equipment

4.1 Instrumentation Hardware

4.1.1 Digital Signal Processors

Digital Signal Processors (DSPs) have opened up possibilities for economically implementing complex control algorithms that operate in real time at very high speeds. DSPs are to be found in embedded systems in applications such as communications, video processing and motion control. Bolognani et al [37] use a DSP based solution for implementation of a Kalman filter to estimate the speed and position of the rotor in a permanent magnet (PM) synchronous motor. Although the core of a DSP is a microprocessor, the DSP unlike a conventional microprocessor does not rely solely upon ever faster clock speeds for improvements in performance but instead it gains processing power from the integration of hardware multipliers and other hardware sections for the rapid solution of mathematical functions including fast Fourier transforms (FFTs).

A number of other features distinguish a DSP from a conventional microprocessor such as parallel operations and pipelining. This permits several floating point operations to be processed simultaneously with each operation at a different stage in the pipeline (analogous to an assembly line). Vector operations allow a floating point operation to be executed in parallel with a load or store operation.

One measure of the performance is the number of MACs per second (Multiply and Accumulate operations it can perform per second). The ability to perform complex mathematical operations at speeds very much faster than a microprocessor has enabled these devices to be used for the implementation of digital filters that have frequency cut off points that are very much sharper than can be achieved with analogue filters. It is because of this capability that the devices are called digital signal processors, however the application of DSPs encompass much more than digital filtering.

Different families of DSPs are designed for use in particular types of application such as communications, video processing or motor control. Specific features of a DSP needed for motor control would be PWM (pulse width modulation) channels to control stepper motor drivers, ADCs (analogue to digital converters) to monitor motor current and voltage levels and a number of independent timers. The SmartDrive Taranis unit is based on a Texas Instruments (TI) 24xx series DSP and it was decided that further development should continue using a TI TMX320F2812PGFA. The 28xx series is faster than the 24xx series with a clock speed of up to 150MHz for the 28xx series and up to 40MHz for the 24xx series. Other benefits of the 28xx series include a 12 bit analogue to digital converter (ADC) as opposed to a 10 bit ADC, more onboard memory and more buffered serial ports. The 2812 therefore offers higher performance needed for the application of sensorless feedback techniques and to integrate the research instrumentation onto the DSP. The 2812 is also compatible with code already used by SmartDrive.

4.1.2 Incremental Modular Rotary Encoder

The positional resolution of the Taranis micro-step motor driver is 51200 steps per revolution or (360/51200)° = 0.007°. In order to be able to compare the control signals (PWM pulses) to the shaft position, a very high resolution encoder was required. The Heidenhain ERO 1324 incremental modular rotary encoder with 5000 slots per channel was selected (specification in Appendix G). This is an optical encoder that consists of a glass disc that mounts directly onto the motor shaft. The encoder is shown in Figure 4.1 [38] the glass disc is item B, the photo-detector and signal conditioning circuits are on item A. The encoder does not have any integral bearings to locate the correct mounting position of the disc within the photo-detector thus each time the encoder is attached to a different motor great care must be taken to ensure accurate alignment of the two components. Another consideration when the encoder is attached to a stepper-motor is the calibration of the position of the once per revolution slot relative to the motor full step positions. Detail of how this was achieved is discussed in section-5.1.1.

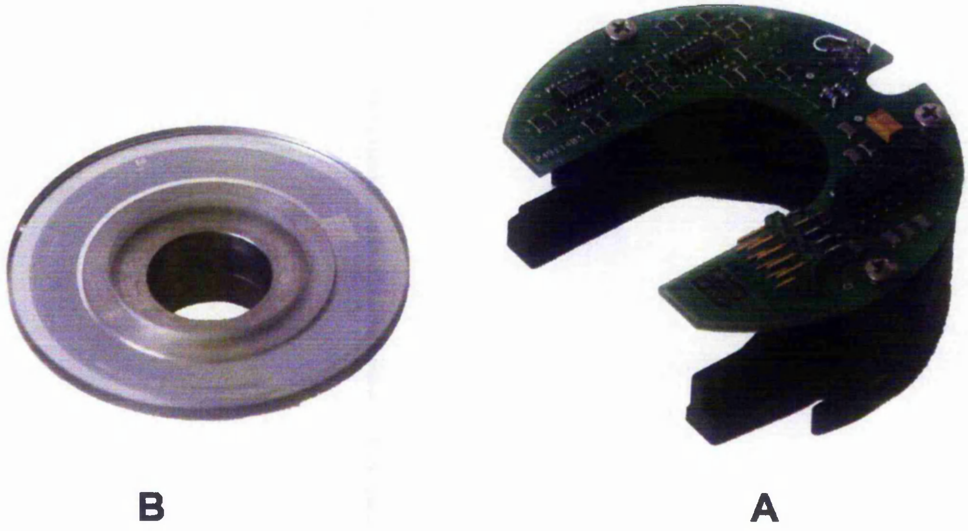

Figure 4.1 Heidenhain Rotary Encoder[38]

The disc has three concentric circular channels of slots engraved into it. The slot positions are counted optically; the optical detector is a LED-Photodiode pair. The outer channel has one slot to give a once per revolution count. The two inner channels each consist of 5,000 slots with an accuracy of ± 3.5 seconds of arc; the slots have quadrature displacement with respect to each other, that is the slots of one channel half overlap the slots of the other channel. As each slot has two edges, the absolute resolution of the encoder is 20,000 slot edges in each channel. The quadrature displacement of the channels is shown in Figure 4.2. The quadrature displacement of channels A and B is to enable automatic detection of the direction of rotation of the encoder. The sequence $\overline{A}.\overline{B} \rightarrow A.\overline{B} \rightarrow A.B \rightarrow \overline{A}.B \rightarrow \overline{A}.\overline{B}$ indicates counter-clockwise rotation and $\overline{A}.\overline{B} \rightarrow \overline{A}.B \rightarrow A.B \rightarrow A.\overline{B} \rightarrow \overline{A}.\overline{B}$ indicates clockwise rotation. This sequence can be detected either with hardware or with software.

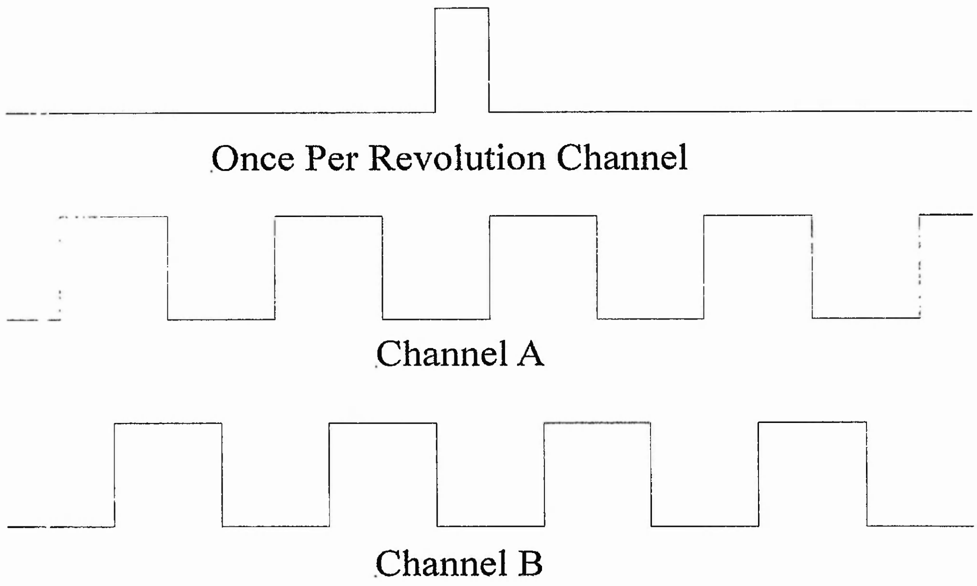

Figure 4.2 Relative Positions of Encoder Channels

4.2 Software and Hardware for Data Capture

- The instrumentation is comprised of an integrated hardware and software system. The framework of the instrumentation is described in sections 4.2.1 and 4.2.2.
- The hardware assembly is described in section 4.2.3.
- The software is described in sections 4.2.4 and 4.2.5.

4.2.1 Combined Instrumentation

The preliminary test rig was constructed to enable data capture of the following digital and analogue signals. Digital signals are from the rotary encoder and PWM signals from the motor driver control electronics circuit. The Analogue current signals are from the motor driver power electronics circuit.

Experience from the preliminary test rig revealed problems both in the signal quality of the data and difficulty in synchronisation of multiple mixed digital and analogue signals from a plurality of sources.

Signal quality was severely impaired by the presence of electrical noise at both low frequency and high frequency, from the mains supply and from electronic equipment. For the data to be useful and reliable, it was essential to increase the signal to noise ratio of all of the signals. The approach with digital signals is to use buffers at or as close as possible to the signal source. The buffers act as a repeater of the signal, the signal is strengthened and the source of the signal is not drained by excessive load.

Digital signals are relatively immune to the constantly varying electrical noise that disrupts analogue signals but are prone to contamination from "electrical spikes". Spikes are very short period pulses that may be periodic or random and can appear as a false digital pulse. By using buffers close to the source of the signal, the signal strength is boosted before the point of connection to signal cables and at this stage should be free of noise. Noise that is subsequently picked up by the cable should be of a lower energy level than the actual signal. Thus, the signal to noise ratio (S/N) is improved. The digital signals are captured with a logic analyser; the threshold level of the logic analyser should reject the noise if the S/N ratio is good. The threshold level of the buffers will also reject low amplitude spikes at the input terminals of the buffer.

The primary method with the analogue data is to eliminate 'common mode' noise by designing and constructing suitable differential amplifiers. The differential amplifiers are connected between the source of the analogue signals and the inputs of the analogue to digital converter. The concept of common mode noise rejection is explained as follows: A signal that is read by measuring the voltage amplitude between the source of the signal and electrical ground is called a single ended signal. Electromagnetic sources of noise are superimposed onto the signal when the signal voltage is measured with reference to ground; the result is a composite of the signal and the noise. A signal that is measured as a voltage between two conductors connected to the signal transducer terminals, with both conductors isolated from ground, is called a differential signal. As both conductors are isolated from ground, any electromagnetic noise is induced as an identical noise pattern into both conductors and is said to be common to both conductors and the term common mode noise is used. The two signal conductors are connected to the input terminals of a differential amplifier. This amplifier outputs an amplification of the voltage difference of the two signal conductors, thus rejecting the noise.

The term that defines the amplifiers effectiveness in rejecting the noise is the "common mode rejection ration CMRR".

The test bed layout (Figure 4.3) is designed to allow all signal cables to be as short as possible; screened cables are used and the screens are connected to ground at the source end. Short cables are less likely to pick up extraneous noise than long cables and because they are shorter, loss of signal strength is reduced. The earthed screens on the cables shield the signals from extraneous noise. All equipment is firmly secured to a common ground bed plate made from thick aluminium plate.

4.2.2 Time stamping of data

To enable meaningful data analysis, it is essential that all of the data is synchronised to a common time base. There are four differential channels of analogue data and twelve channels of digital data. The start of data capture is signalled by the once per revolution pulse from the encoder, triggering the logic analyser capture. A trigger pulse from the logic analyser starts the analogue capture.

Even at very low motor speeds the rate of the digitised analogue voltage and current signal captured from the drive terminals is very high, therefore to maintain the file size of captured data to manageable proportions it is necessary to store the incremental values of the signals rather than the absolute values. Therefore all of the digitised data must be time stamped at a regular interval to enable all of the channels to be accurately matched.

The time stamping is also necessary to enable velocity and acceleration of the signals to be calculated and displayed.

4.2.3 Hardware Assembly

Key to the feasibility of understanding the nature of rotor disturbances is very high integrity instrumentation. Incremental Encoder (IME) techniques developed within the Intelligent Machines Group [39] [33] [40] are pivotal to exploration of stepper motor phenomena. The principal transducer used is a

Heidenhain incremental rotary encoder, model ERO 1324, as described in section 4.1.2

Most of the test procedures have been oriented around the Taranis stepper motor drive, supplied and manufactured by the industrial partner to the research, SmartDrive. This drive is based on a TI 2000 family DSP, controlling power to the stepper motor through a dual mosfet H bridge (described in section 1.22 and Figure 1.3). Control parameters are uploaded from a PC to the Taranis drive using a SmartDrive high level program called Nimbus. The parameters are stored in non-volatile erasable memory of the DSP in the Taranis.

A number of two phase hybrid stepper motors are available from SmartDrive, and a method of applying differing inertial loads has been devised using a range of pulleys as flywheel and a taper locking system to facilitate ease of changing the load. A load attached to the motor shaft changes the natural frequency of the system; the additional inertia also damps oscillations in the motor. Additional load on the motor also reduces the rate of acceleration that can be attained without causing the motor to slip out of step.

Digital data of the system comprises three channels from the Heidenhain rotary encoder, eight PWM channels derived from the H bridge control of the motor driver (4 from each limb of the two H bridges) and the sampling clock pulse from the A/D converter. Digital acquisition is achieved with a PC based logic analyser (GoLogic) with bandwidth of 500MHz; data is buffered in the logic analyser and transferred to the PC via a USB2 link.

Analogue data acquisition is via a PowerDAQ 16 bit A/D PCI card, with a maximum sample rate of 333K sample per second. The card is provided with 4 single ended channels or 4 differential channels. The analogue signals of interest are 4 current monitoring points (two from each H Bridge) and the voltages from the two motor windings. The current signals are required as the differential of two pairs and also the voltage is required as the differential of the voltage across each phase. There are a total of eight analogue single ended signals; these are connected in pairs to separate differential amplifiers, the four outputs of which are connected to the A/D card as single ended inputs.

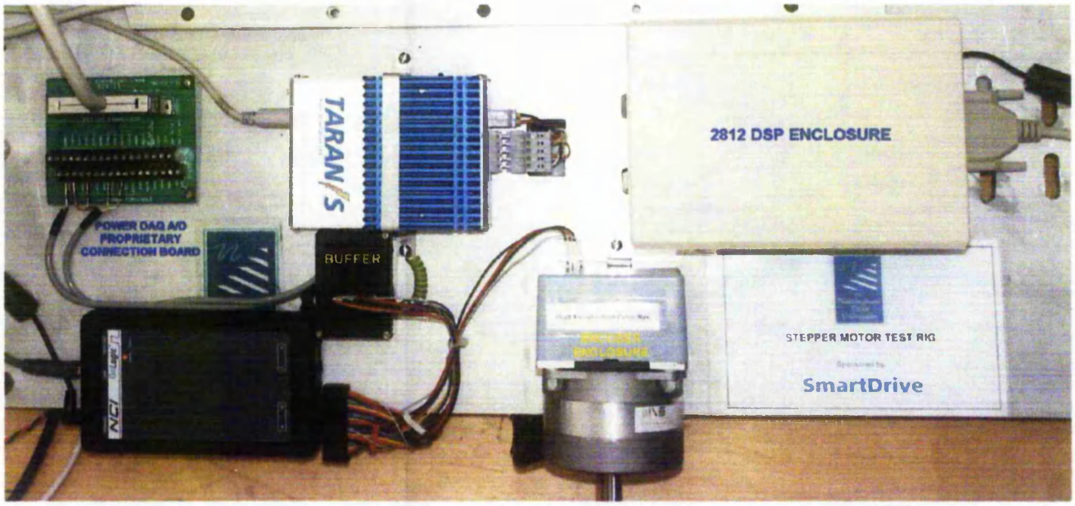

Figure 4.3 Stepper Motor Test Bed

Noise reduction is a priority in the layout design and the use of differential amplifiers, as close as possible to the point of processing that virtually eliminates all common mode noise (described in section 4.2.1) from the signals. The arrangement for acquiring the voltage signals is shown in Figure 4.4. The potential divider circuit at the amplifier inputs is necessary to shift the voltage levels to a range suitable for the amplifiers.

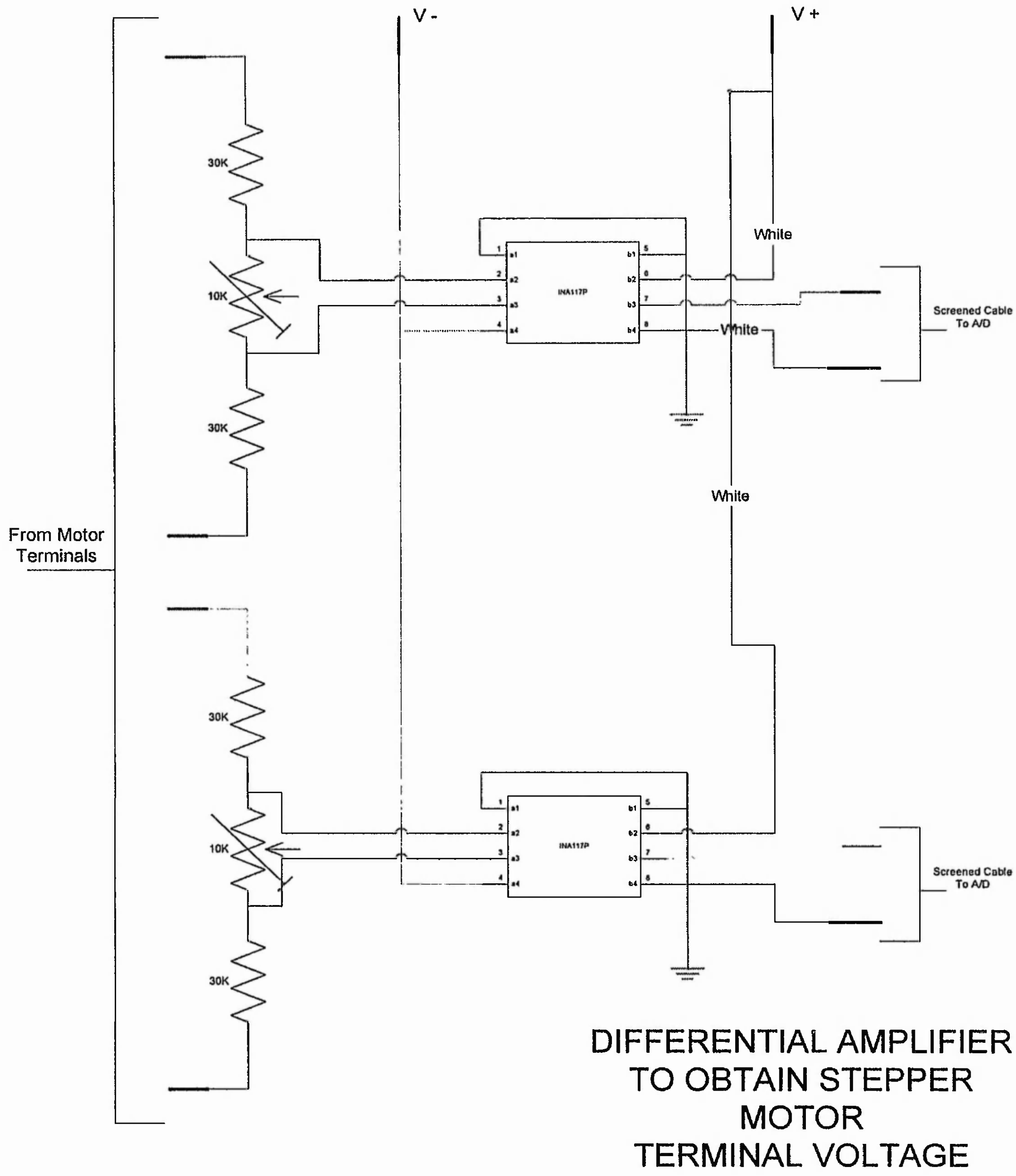

Figure 4.4 Differential Amplifier

Further methods to eliminate noise are the use of buffers at the source of digital signals and the use of screened data cable. The buffers also serve the purpose of matching differing voltage levels of the various parts of the system.

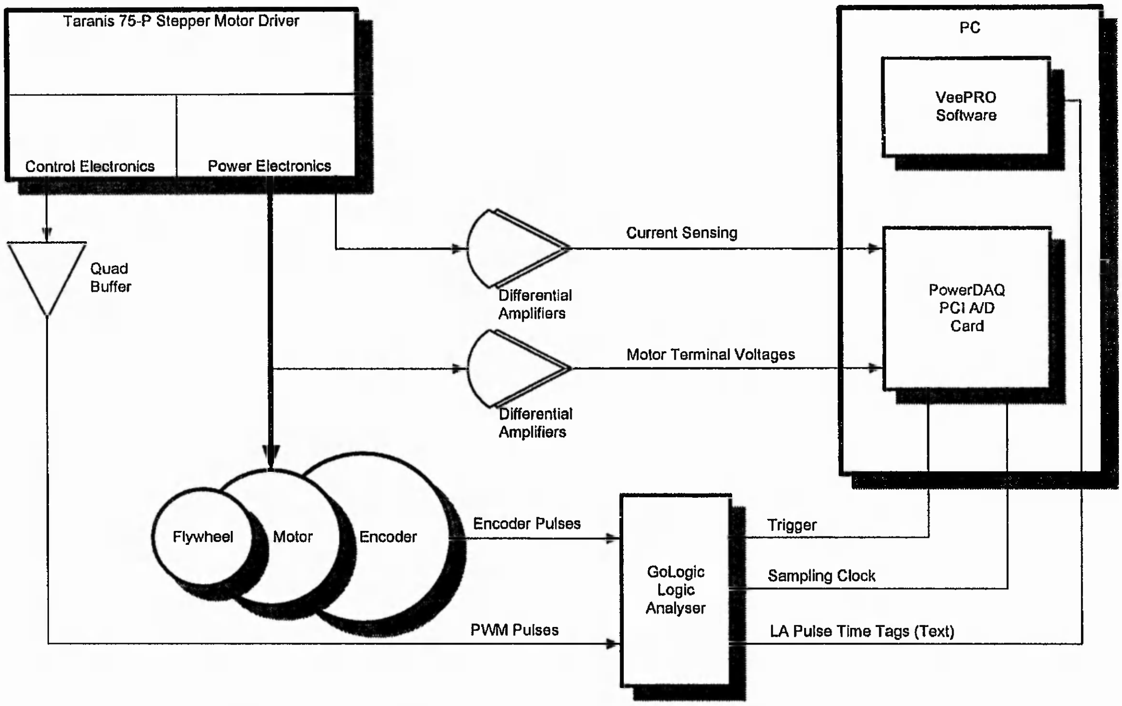

Figure 4.5 Stepper Motor Instrumentation Block Diagram

To achieve synchronisation of data capture the logic analyser is triggered by the once per revolution pulse of the rotary encoder, subsequently the logic analyser generates a synchronisation pulse to trigger the A/D capture. The A/D card clock pulse is fed back to the logic analyser as an additional calibration check. The instrumentation block diagram is shown in Figure 4.5.

4.2.4 Software Description

A robust and secure system of acquiring and processing the experimental data was a clear requirement. Further to this it is also a requirement to have a framework for filing the experimental results together with all of the experimental parameters such as load inertia, motor speed, a record of the Nimbus software, time and date etc. This has been achieved by creating such a secure experimental system using HP VEE Pro.

This software provides user interface to allow the input of the experiment parameters i.e.

- Channel name
- Type of signal (single ended or differential)

- Amplitude range of the signal

After the data has been captured another user interface allows further details to be added as required.

- encoder details
- motor details
- load inertia details
- motor speed
- motor direction
- analogue channel details
- the time and date of the experiment

Once all the details have been entered and accepted, an output file is created. The details of this HP Vee Pro system are described in section 4.2.5.

The output file is processed by another system developed using HP Vee Pro, for processing the results. The interfaces for this are shown in the section 5.2.

4.2.5 HP Vee Pro Data Processing

An overview of the HP Vee Pro data processing structure is shown in Figure 4.6. There are three main user functions:

1) **Analogue phase current with timing tags**. The logic analyser data was not sampled at regular instants, the sampling was done on level transitions i.e. a change in level of any of the channels would be a sampling instant in time. In order to combine data from both the analogue and digital sources, it is necessary to resample all of the data at regular intervals. This involves interpolation and spline curve fitting to create the regular time base. The detail of this user function is shown in Figure 4.7.

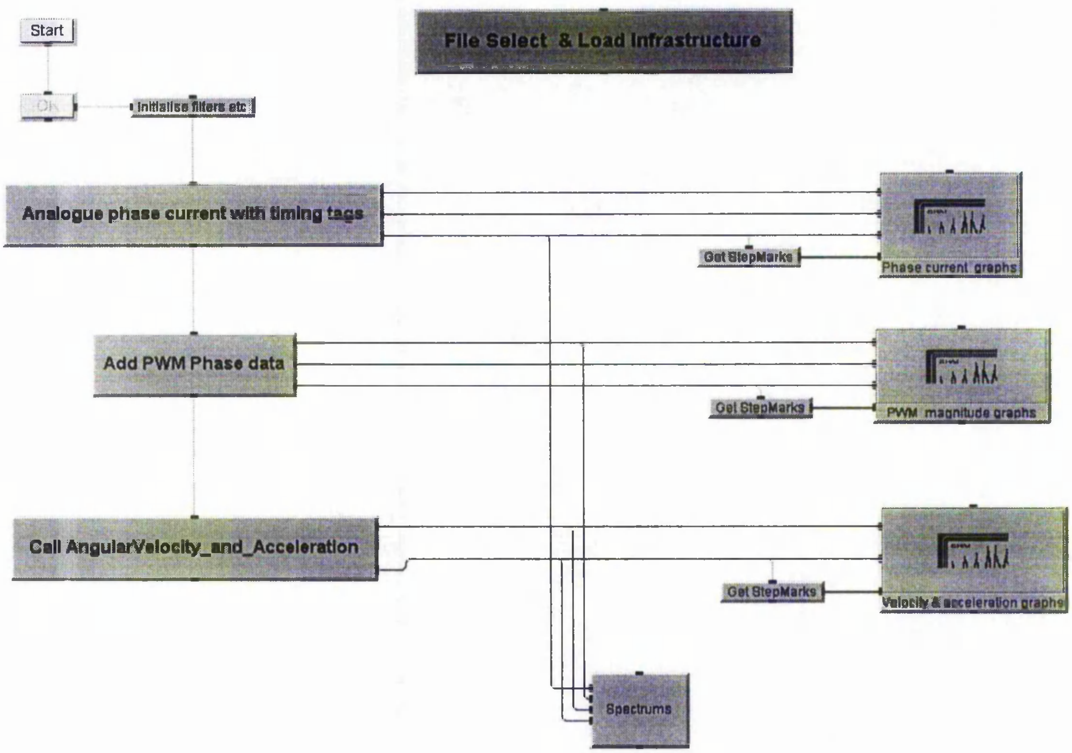

Figure 4.6 Data Processing Overview

2) **Add PWM Phase Data.** Performs the function of subtracting (adding the complement) of the PWM switching applied to each end of each motor phase to construct the equivalent alternating waveform of the phase. These alternating waveforms are also summed to produce the resultant waveform of the two phases of the motor. The detail of this user function is shown in Figure 4.8.

The call ‘make phase’ performs the subtraction to make the waveform for each phase. The ‘add phases’ function makes the resultant waveform. The data is then low pass filtered with an elliptical filter and finally the data is normalised.

3) **Angular Velocity and Acceleration:** This user function differentiates the data from the digital rotary shaft encoder to calculate the velocity and performs a second differentiation to calculate the acceleration (figure 4.9).

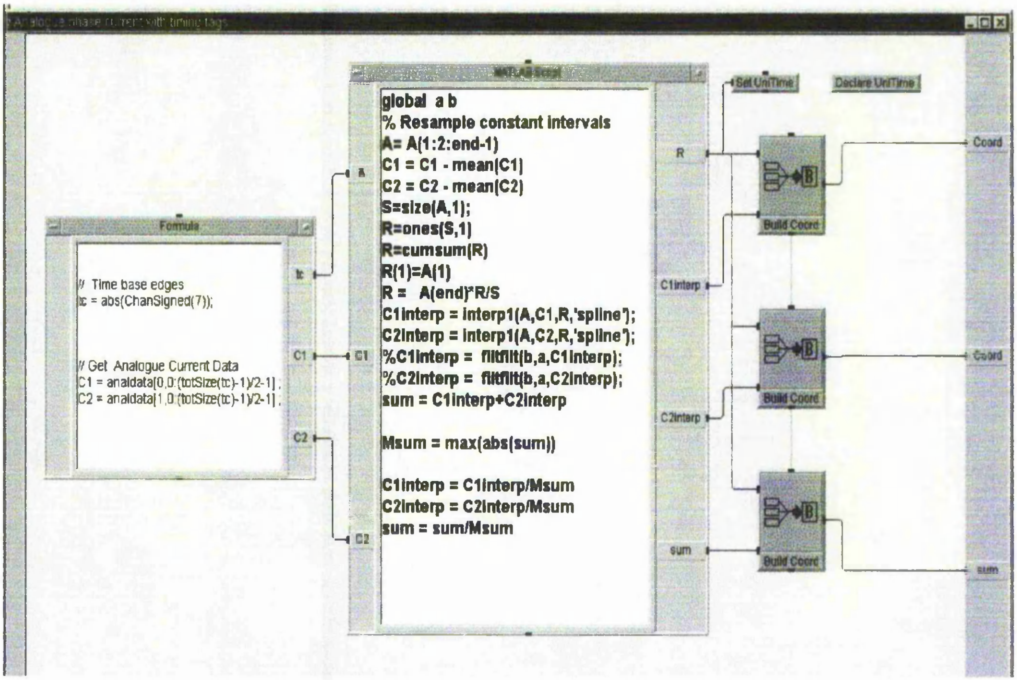

Figure 4.7 Analogue Phase Current with Timing Tags

The Matlab script in Figure 4.7 selects the rising edges of the ADC clock (rejecting the falling edges). The length of the time base array is calculated and divided into equal timing intervals. This builds a universal time base (Uni-Time). Uni-Time is the time base and is also used by the Add PWM Phase data and the Angular Velocity and Acceleration Functions.

The time intervals of the analogue data are spline interpolated by the interp function. The analogue data is normalised about zero by subtracting the mean value of the array from the array.

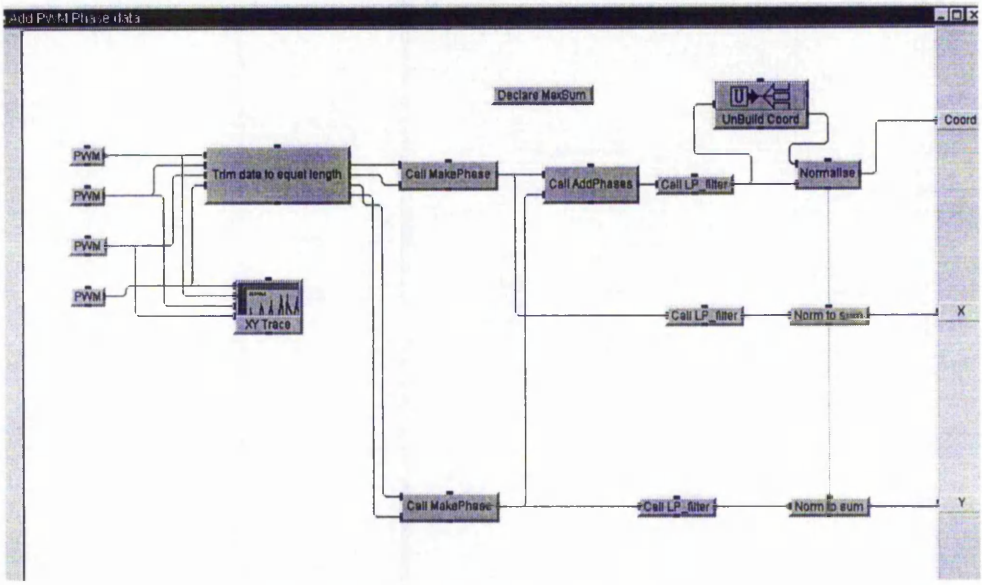

Figure 4.8 Add PWM Phase Data

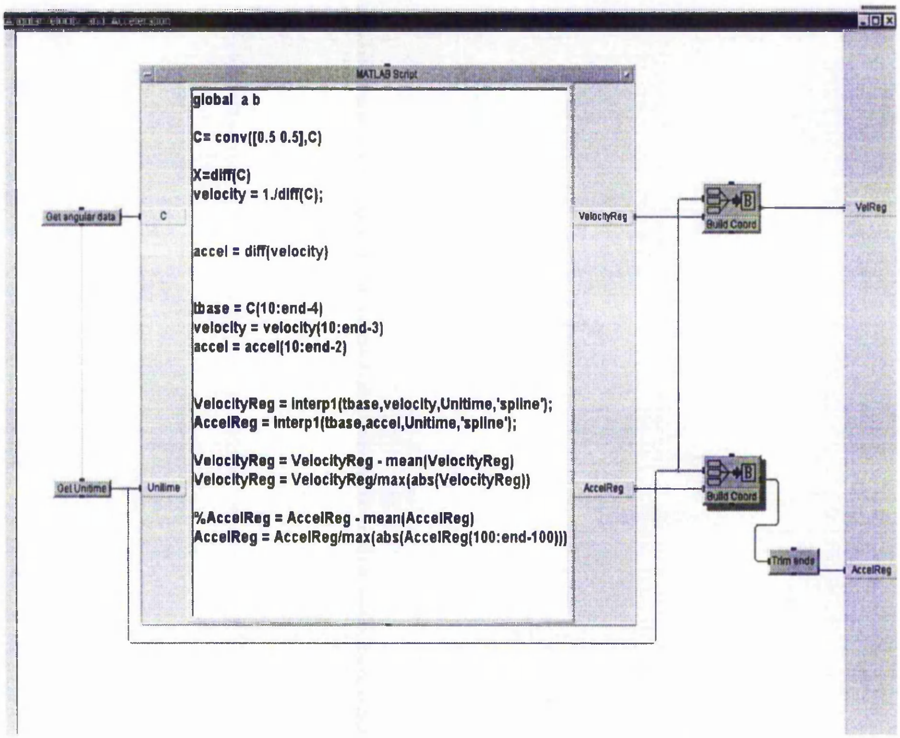

Figure 4.9 Angular Velocity and Acceleration

4.3 Development of DSP Centred Instrumentation

To implement changes in the control algorithm it is necessary to drive the stepper motor from a DSP development board. A stepper motor driver module has been designed and constructed to interface between a Ti 2812 EzDSP board and a stepper motor. The details of this system are shown in appendix C.

4.4 Summary

The large amount of small signal data that must be collected is very susceptible to electrical noise from external sources and from cross-talk. The construction of the test-bed combined with the electrical techniques used has reduced the effects of noise to negligible levels. Some noise must still exist however, such as shot noise and noise from alpha particles in semiconductors [41]. An efficient and secure system for marshalling and logging the data has been developed using HP Vee Pro. An electronic interface for combining the micro-stepping control of the motor with the research instrumentation has been developed.

Chapter 5
Results

5 Results

5.1 Raw Digital Data

5.1.1 Shaft Encoder Logic Analyser Channels

The starting point for synchronising the results is the angular location of the once per revolution pulse of the Heidenhain encoder relative to the detent position of the motor (see section 4.1.2). The motor was rotated in a micro-stepping mode at a very low speed for one full step followed by a pause and then repeated for as many times as required. The logic analyser is set to trigger on the once per revolution pulse and to show a 25% pre-fill (25% of the entire trace that is captured occurred before the trigger). This ensures that the trace shows encoder data before the position of the once per revolution pulse. The stepper motor used in this test has 200 steps. The encoder has two channels spaced in quadrature to each other and each of these channels has 5000 slots. Therefore the number of slots per step is 5000/200 = 25. By counting the number of quadrature encoder pulses that occur before the position of the once per revolution pulse the relationship of the latter to a detent position of the motor can be established. The result illustrated in figure 5.1 shows the logic analyser trace, A00 is the once per revolution channel, A01 and A02 are the quadrature channels. The once per revolution pulse occurs after 16 slots of one of the quadrature channels has been counted. Thus as one step = (360/200)° = 1.8° the once per revolution pulse is $\left(\frac{16}{25}\right)\times 1.8° = 1.152°$ from the detent position.

The test is also repeated in the reverse direction, which provides the complimentary position, that is 25 – 16 = 9 pulses. This gives an angle of;

$$\left(\frac{9}{25}\right)\times 1.8° = 0.648°.$$

The change in speed on rotation through the one step movement can be seen form the change in length of the pulses; the deceleration appears to be more abrupt than the acceleration. There is a continuation of pulses after the end of the one step of motion. Close examination of Figure 5.1 shows that after the 25th pulse the phase relationship of the quadrature channels A01 and A02

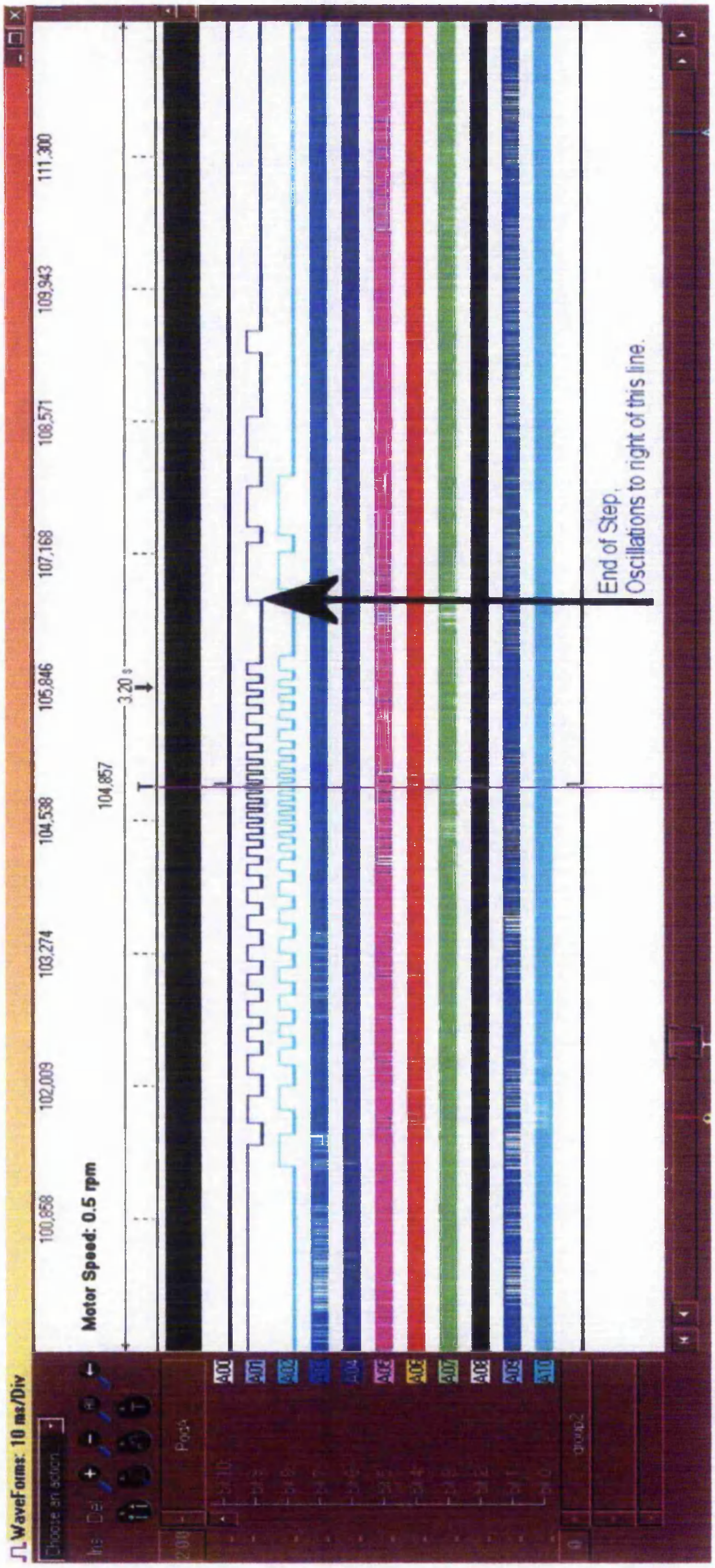

Figure 5.1 Section of Logic Analyser Trace Forward Direction

repeatedly inverts. This indicates repeated changing of direction of the motor or oscillatory movement; this is an indicator of the single step response of the motor. This calibration test must be done every time the encoder is fitted to a motor.

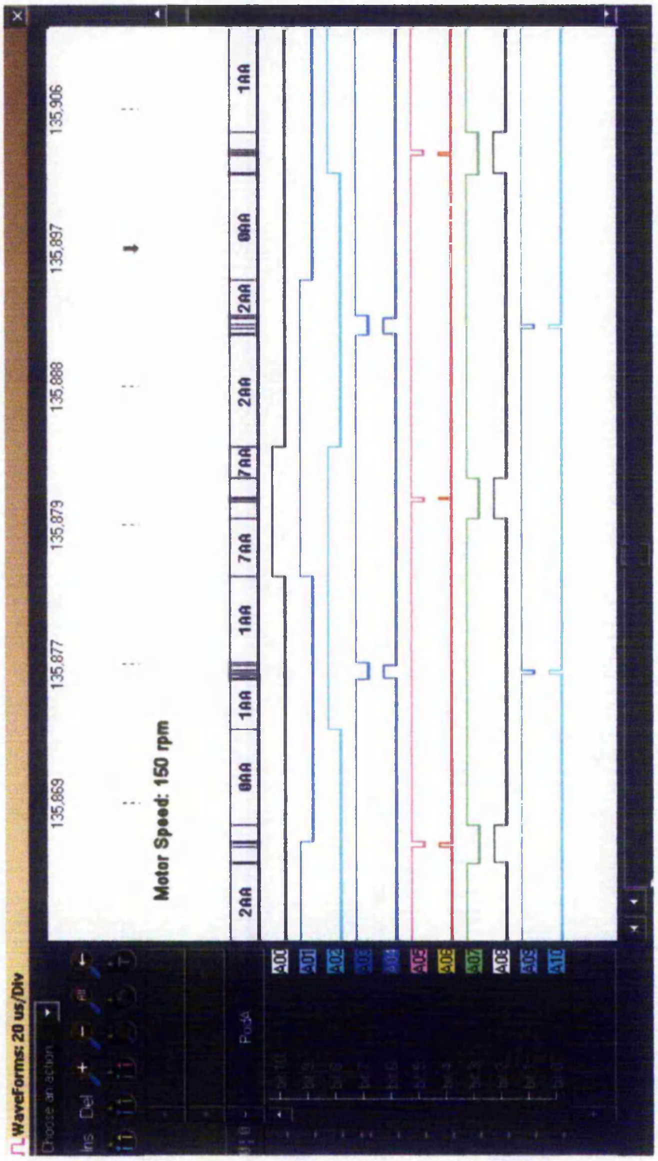

Figure 5.2 Logic Analyser Trace, Motor 150 rpm

5.1.2 Pulse Width Modulation Logic Analyser Channels

The other channels in Figure 5.1, A03 to A10, are the pulse width modulation (PWM) pulses from the Taranis drive. Because of the very low speed of the motor the display view of the logic analyser is zoomed out to enable the section of interest of the encoder pulses, thus the detail of the PWM channel cannot be clearly seen.

An example of the logic analyser data for a motor running at 150 rpm with a flywheel fixed to the motor shaft is shown in Figure 5.2. Both the PWM pulse detail and the encoder pulse detail can be seen. As before, traces A00 to A02 show the encoder channels. Traces A03 to A10 show the PWM pulses.

There are four pairs of traces, two pairs associated with each phase of the motor.

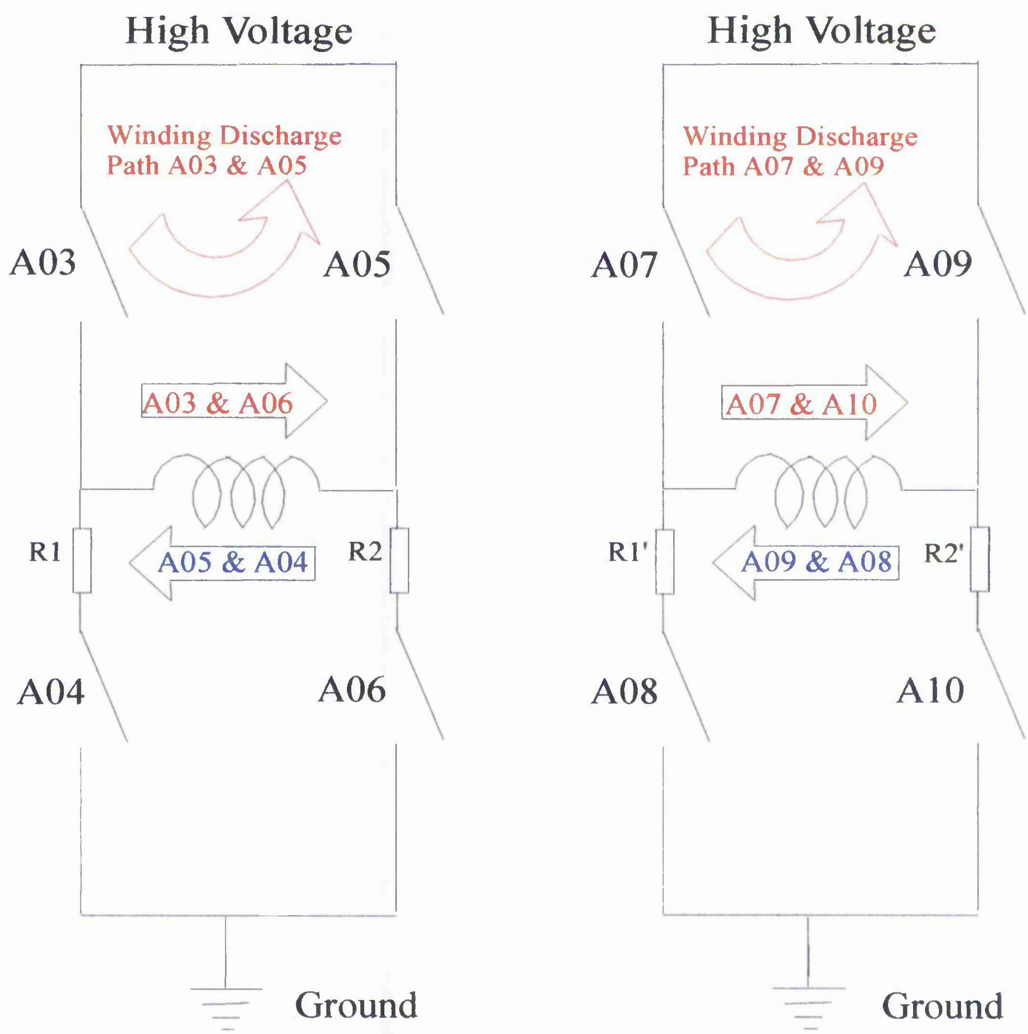

Figure 5.3 Simplified H Bridge Circuit

The explanation that follows refers to phase A, the procedures for phase B are similar.

For a more detailed explanation of the H Bridge see Appendix E, In the simplified circuit, the mosfet power transistors are represented by switches; each switch is labelled to correspond with a trace on the logic analyser output of Figure 5.2. When a trace is 'high', the corresponding switch is on (closed), to cause current to flow from left to right in phase A; traces A03 and A06 are high, causing the corresponding switches to close. The switches are switched on and off at timed intervals to generate a sinusoidal waveform for the positive half cycle. Current reversal is achieved by switching A05 and A04 on. The negative sinusoidal half cycle is generated by timed on/off intervals of A05 and A04. A similar process is used for phase B. Inspection of Figure 5.2 shows that the rapid switching to form the wave shape is always done with the either switch A04 or A06. These are referred to as the low side switches and there is less electrical stress on these switches than on A03 and A05, known as the high side switches. The term high side is used because of their position in the circuit between the phase winding and the high voltage supply.

It can also be seen that for much of the time A03 and A05 are both closed, this is to provide a path to discharge the stored energy in the phase winding. The discharge path is indicated by the curved arrow in Figure 5.3. Switches A03 and A04 are never on simultaneously and likewise for switches A05 and A06. The simultaneous switching on of either of these pairs of switches would short-circuit the supply and destroy the mosfet transistors (represented by the switches in Figure 5.3). However, this introduces a *dead band* causing disruption to the PWM waveform, this effect is considered by Dodson et al.[42] .It may appear in Figure 5.2 that these pairs of switches do close simultaneously, but careful scrutiny of the original logic analyser trace always reveals that this is not the case.

5.1.3 Raw Analogue Data

The analogue to digital converter (ADC) used is a PowerDaq with 4 analogue input channels (other relevant data is shown in appendix F). Initially current data was captured as single ended signals. Noise immunity of the circuit of the circuit was subsequently improved by using differential signals (as described in section 4.2.1). This also enabled two of the available channels to be used for analogue to digital conversion of the phase voltage.

The current signals are derived from current sensing resistors in the H Bridge. These resistors are shown in the H Bridge diagram in Figure 5.3 and are indicated as R1 and R2. They are situated at each side of the connections to the motor phase winding. Considering Phase A, if switches A03 and A06 are on, the current measuring point is the top of R2. When the current direction through the winding is reversed by A03 and A06 switching off and A05 and A04 switching on, the current measurement point is the top of R1. The current measured at each point is a unidirectional value but with opposite signs (+ or -) or opposite direction of current flow. The difference between the current measured at the two points (R1-R2) is the alternating current in the phase winding. The same principle is applied to phase B. The individual currents measured at R1, R2, R1' and R2' are shown in Figure 5.4. The differential current R1-R2 is shown in Figure 5.5.

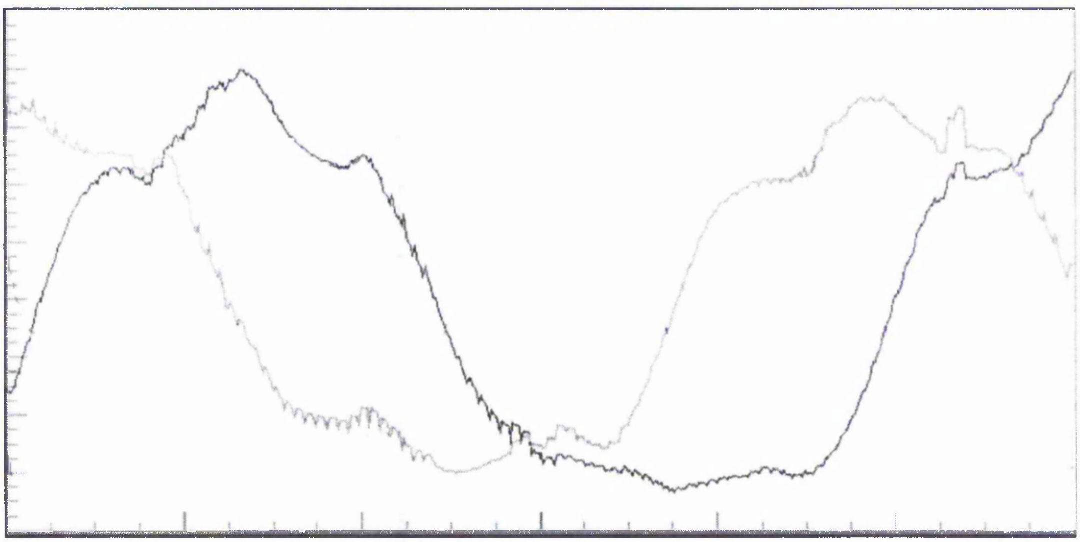

Figure 5.4 Unidirectional Currents Measured at R1 and R2

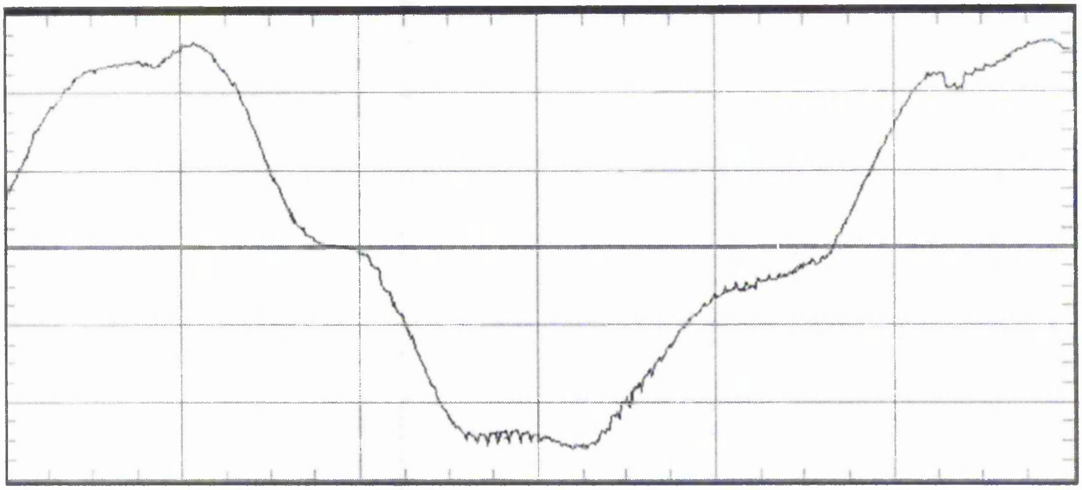

Figure 5.5 Alternating Currents Through Phase A (R1-R2)

The inductive time constant of the motor winding acts as a high pass filter which converts the digital PWM pulses into an analogue waveform. In the traces of figure 5.4, the regular small crests that appear on the wave are remnants of high frequency noise removed by filtering; the overall shape of the waveform is also fairly ragged. The difference of the two traces is shown in Figure 5.5. The resulting wave is smoother but still shows the effects of noise. The waveforms were captured as two single ended signals and converted to a difference signal by post processing the data. The current signals that are seen in the following section were capture as differential signals and therefore have much greater immunity to noise, as explained in section 4.2.1. The waveforms shown in 5.4 and 5.5 are both filtered; before filtering the signal contained inherent noise (not extraneous noise) that is a valid part of the captured signal. The presence of this inherent noise is considered in the following section. One phase of the unfiltered raw current waveform is shown in Figure 5.6.

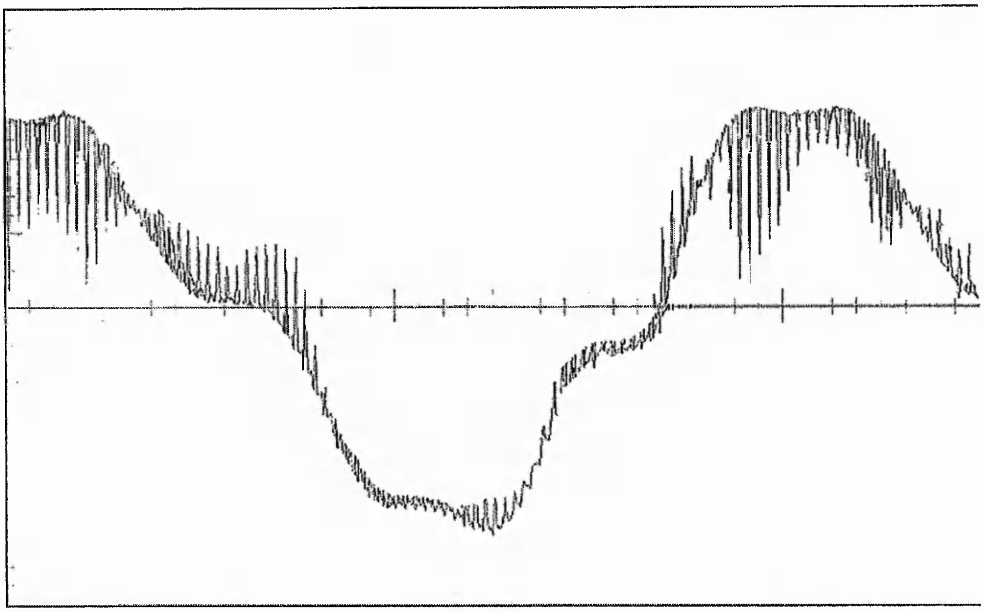

Figure 5.6 Unfiltered Differential Current (one phase)

5.2 Processed Combined Data

The scope for logical analysis of the data in its raw form is severely limited. The data presented below is the result of precise synchronisation of the multiple digital and analogue signals. Post processing of the signals reveals the correlation between the quality of the generated PWM waveforms, the current through the phase windings and the performance of the stepper-motor in response to the generated PWM.

Before post processing, the data is synchronised and collated as described in chapter 4. The current waveforms and PWM waveforms in Figure 5.8(A) have been "cleaned up" by application of an elliptical filter. As well as the two current waveforms (one from each phase), the sum of the two currents is also plotted. The torque produced by the motor is directly proportional to the current, thus the sum of the two currents is a direct representation of the resultant torque in the stepper motor (see section 2.2.2).

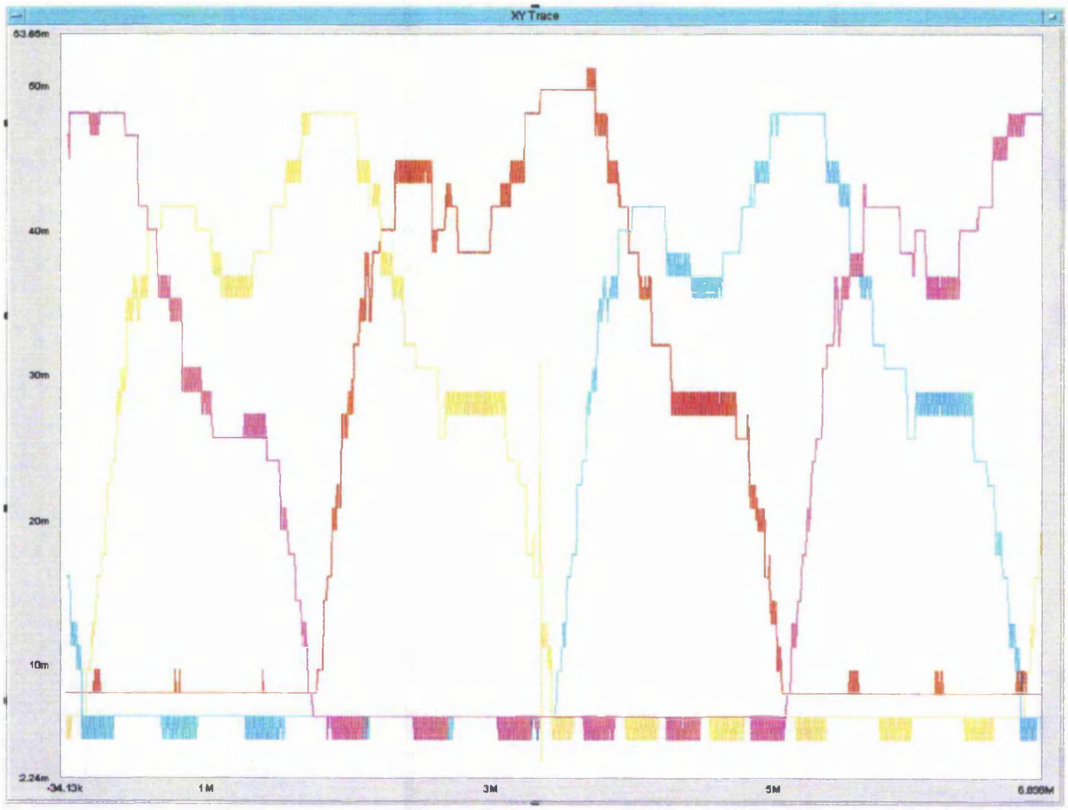

Figure 5.7 PWM Applied to Each Side of the Phase Windings

The PWM data is reconstructed by multiplying the mark-space ratio of each of the PWM pulses by one and are shown in Figure 5.7. The PWM data in Figures 5.9B and 5.10B are obtained by subtracting phase A2 from A1 and B2 from B1.

The filtered data is shown in Figure 5.8; this consists of part A - the currents through the phase windings, part B - the reconstructed PWM voltage generated waveforms and part C - the motor velocity and acceleration constructed from the shaft encoder digital data.

The shape and phase of the measured currents in the windings differ from the reconstructed PWM waveform. The reconstructed PWM waveform is the voltage applied to the phase-winding. The phase of the measured resulting current in the winding lags behind the applied PWM voltage because of the time-constant of the inductive windings. Current passing through the inductive phase windings generates a voltage as;

$$V = L\frac{di}{dt}$$

where (V) is voltage, (L) is inductance and (i) is instantaneous current.

The voltage V is the back EMF or motional voltage (see section 2.2.3) and this opposes the PWM voltage that is applied to the phase windings. This has the effect of modifying the shape of the current waveform. The shape of the current waveform will also be affected by the inductance varying as the rotor turns; this alters the degree that the current waveform lags the voltage waveform. Thus the current waveform differs in shape from the applied PWM voltage waveform.

Graph C indicates that the velocity varies in a cyclic manner about a mean level at the stepping frequency of the motor. Comparing graph C with graph A, the relationship of speed with velocity is complex. The velocity is below the mean level for the duration of one half step, in the subsequent half step the velocity is above the mean level. Thus the motor is oscillating about the mean speed at the stepping frequency of the motor. This indicates that the motor is running at or close to a sub multiple of the natural frequency of the motor. Another possible cause is the imbalance between the phases of the motor and may be due to the imperfection of the construction of the motor. The graph of the acceleration is very ragged, indicating that rotor oscillation is at a higher frequency than can be seen from the examination of the velocity graph. This high frequency disturbance is analysed further with the amplitude frequency spectra illustrated by figure 5.11.

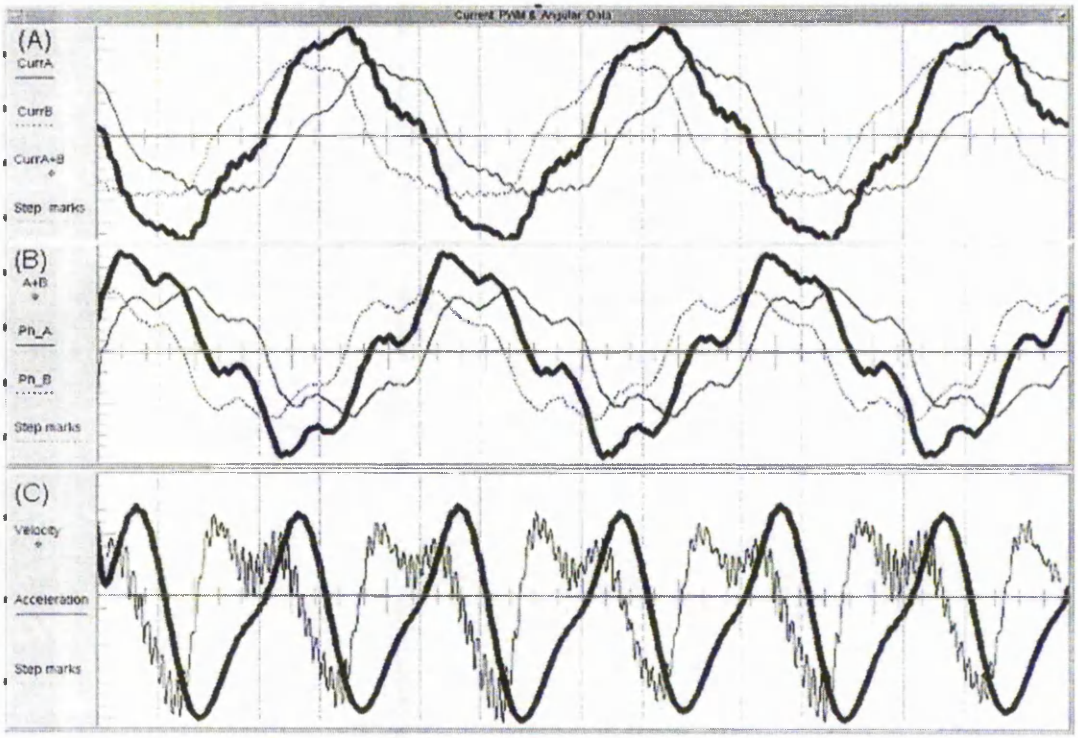

Figure 5.8 Filtered Data

The unfiltered graphs of current and PWM applied voltage are shown in Figure 5.9. The current waveform in diagram A is similar to the raw data shown in Figure 5.6 where the effect on the current of a single phase can be seen. Comparing 5.8 A and 5.8 B reveals that the raggedness of the current waveform is not reflected directly from the PWM waveform. The PWM switching is produced by the mosfet switches on the low side of the H Bridge.

Figure 5.2 shows the four pulses that control the high-side switches of the H Bridge. These are A03, A05, A07 and A09 in Figure 5.3. These four pulses are approximately the logical NOT of the PWM pulses (which are generated by the low side switches) and therefore they are at logic high for most of the time, thus the high-side switches are on for most of the time. When these high-side switches are on, they connect both sides of the phase winding to the high voltage supply. This sets both ends of the phase winding to the same potential which provides a discharge path for the phase winding. This is to ensure that at the time instants between PWM pulses the applied voltage is returned to zero; if this was not done the PWM waveform would be distorted.

The motor phase windings act as a low pass filter and the PWM should be reconstructed to a 'smooth' sinusoid. In the system under test, it appears that the timing of the high-side switching is the cause of a ragged current waveform that may effect the smoothness of motion of the motor. This effect should be less apparent when the motor is running at a higher speed, when the H Bridge pulses are at a greater frequency. In such circumstances the time constant of the phase windings should be sufficient to filter the shorter off periods of the pulses.

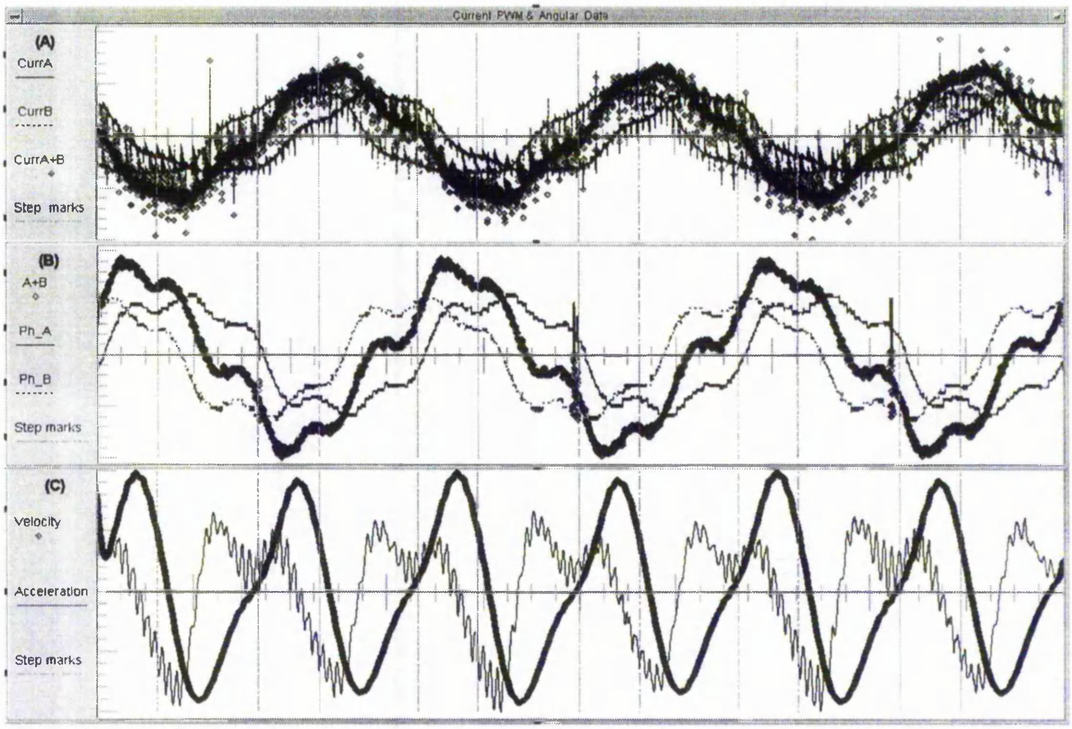

Figure 5.9 Unfiltered Current and PWM Spectra

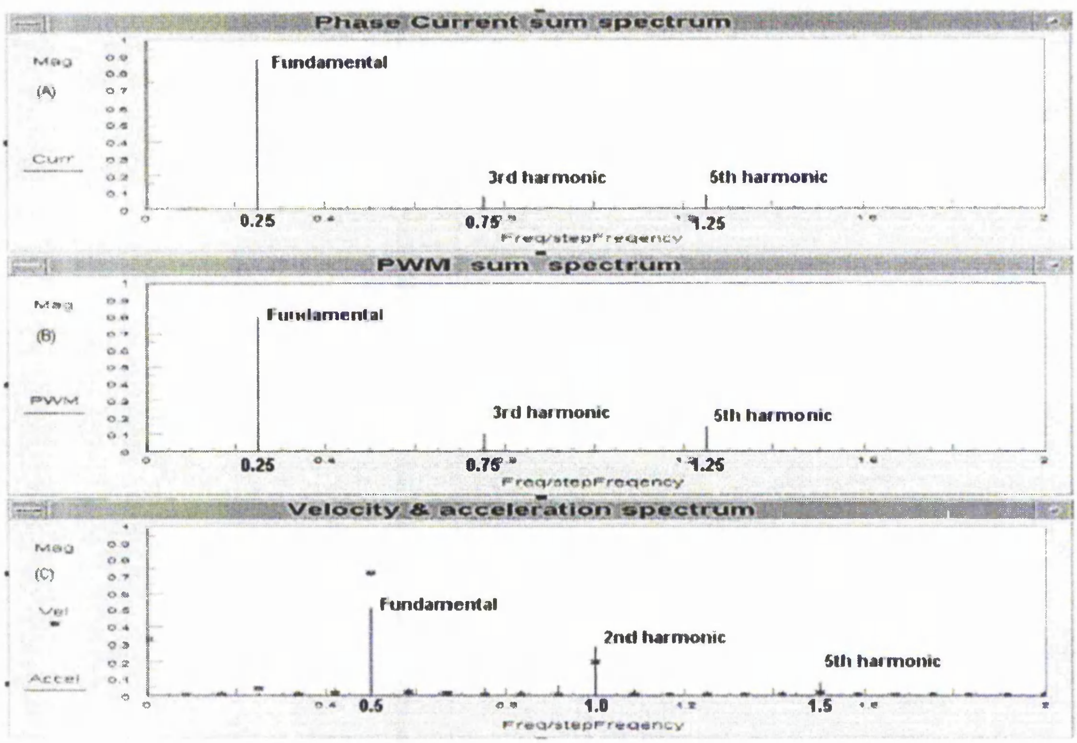

Figure 5.10 Fast Fourier Transform of Data

The normalised spectra of the phase current, the PWM voltage and the velocity/acceleration are shown in Figure 5.10 (A), (B) and (C) respectively. The frequency scales of Figures 5.10 and 5.11 indicate the number of times a particular frequency occurs in the duration of one full step of the motor. Thus, if the fundamental is scaled as 0.25 on the graph, then four steps of the rotor have elapsed for one cycle of the fundamental frequency. The same principle applies to the harmonic frequencies, e.g. if the fundamental is at 0.25 on the frequency scale and a harmonic is scaled at 0.75, then the harmonic is a third harmonic.

There is a close similarity between the transforms of the PWM and the phase current. The fundamental frequencies are of similar amplitude. Both signals contain a fifth and a tenth harmonic; both of these higher frequency harmonics are attenuated in the current signal. It is apparent that any potential disturbances on the PWM signal are reflected in the current signal.

The fundamental frequency of the velocity oscillations is double the frequency of the motor current signal, and likewise for the acceleration. The velocity/acceleration transforms contain fifth and tenth harmonics as do the current and PWM signals. However, the comparison of these harmonics shows that the amplitudes in the velocity/acceleration signal differ significantly.

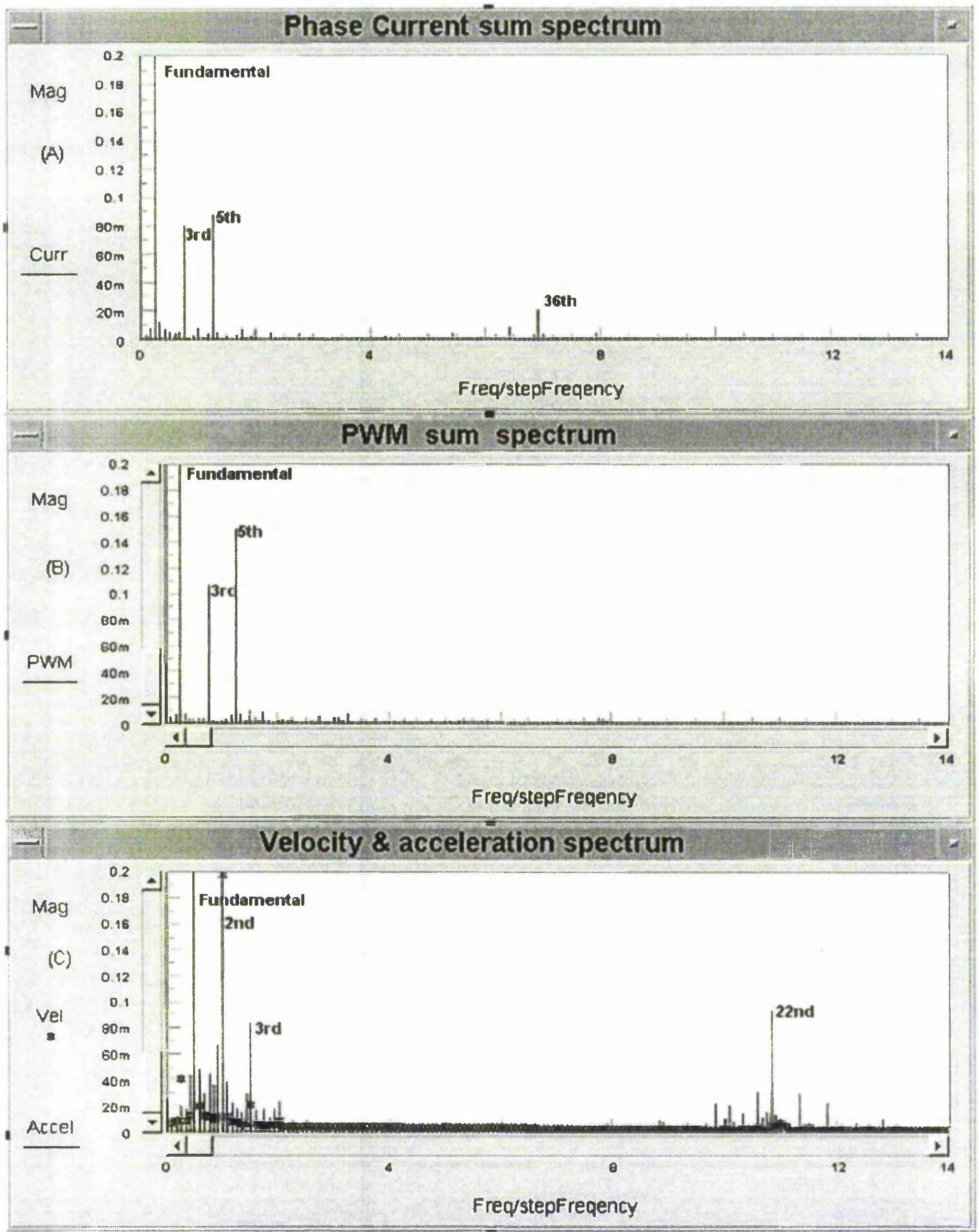

Figure 5.11 Zoomed Out Spectra

A zoomed out view of the frequency spectra are shown in Figure 5.11. This enables the higher frequency components to the acceleration spectrum to be seen.

However, this high frequency disturbance on the acceleration does not relate to spectra of the PWM or the current and does not look plausible. These high frequencies are probably due to aliasing of the signal. The slot count of the shaft encoder is 5,000 per revolution and both edges of the slots are used to construct the signal. This gives a resolution of 10,000 per revolution. SmartDrive literature [6] for the Taranis has stated that the micro step resolution with a 200 step motor is 51,200 micro steps per revolution. It is possible to double the resolution obtained with the Heidenhain shaft encoder used to 20,000 per revolution. This is still well below the Nyquist sampling rate needed to avoid aliasing. However, because of the damping effect from the inertia of the rotor, it is unlikely that such a fine resolution will actually be transmitted to the motor shaft; it is feasible that 20,000 steps per revolution may be good enough.

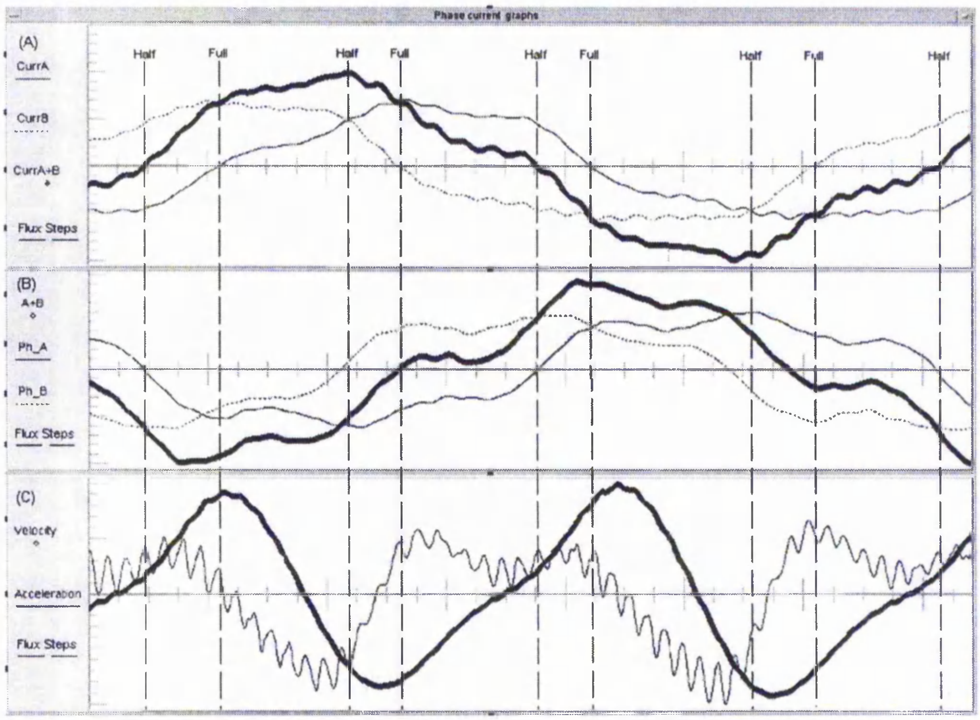

Figure 5.12 Waveforms Showing the Full and Half Step Position of the Rotating Flux

Figure 5.12 is a zoomed in view over one cycle of the summated currents. This shows the half step and full step incidents. The flux is coincident with the indicated step and half step positions, however, the velocity/acceleration is lagging the flux because of the inertia of the rotor. The degree of lag is the torque angle and this is proportional to the speed of the motor. If the torque angle exceeds the angle of one half step of the motor, the rotor will be attracted to the previous stator pole or tooth and will slip a step. The velocity is cycling through one oscillation during the period of two steps of the motor.

Figure 5.13 Ideal Currents and Step Positions

Figure 5.13 is shown for comparison with 5.12 (A), to clearly illustrate the full and half step incidents.

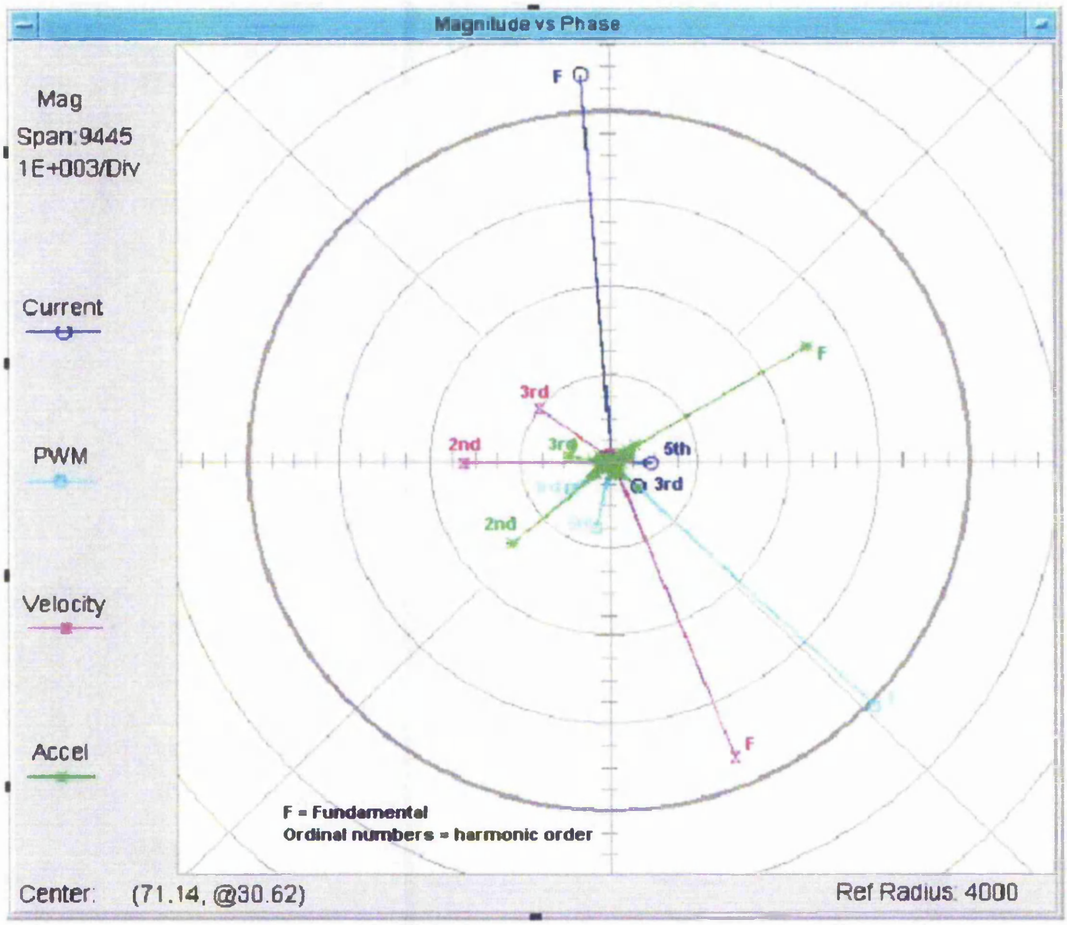

Figure 5.14

The amplitude and the relative phase displacement of the signals are shown in Figure 5.14. The phase displacements between the PWM and the current should be variable and change according to the rotor position (because of the variation in inductance as the rotor rotates). However, the phase displacement shown is constructed from the amplitude frequency spectra, obtained by performing a fast Fourier transform on several cycles of the data. The constantly varying inductance is one of the factors affecting the shape of the current waveform and at low speeds is the principal factor. Thus, if the motor is rotating at any given speed, the spectra will remain constant. However, if the motor slips the spectra of the current signal will change.

5.3 Analysis of the Processed Data

Stepper motors controlled by a micro step driver should be much less susceptible to oscillation associated with running at the natural frequency (or at sub multiples of the natural frequency), than a motor driven in full or half step mode. A very much smaller amount of energy is absorbed in moving the tiny increment of each micro step than in a motor that is incremented in full steps. Therefore, there is much less energy available to produce an unstable step response. However, the tests reveal a significant oscillation; this oscillation was also apparent by audible and tactile observation at the time of the test run.

The reconstructed pulse width modulation is not a close representation of a sinusoid. The waveform may be described as a quasi sinusoid that contains a number of plateaus (about four per cycle). This waveform is modified by the low pass filtering qualities of the phase windings but still contains four distinct plateaus. The waveform is further distorted by motional effects of the motor. The resultant flux waveform, which should be constructed from evenly spaced micro steps, is actually made up of a wave containing significant plateaus with a ripple superimposed on the waveform. The rotor is receiving a "kick" after each plateau, which imparts an energy surge to the rotor. Two plateaus per step can be seen in Figure 5.12. This results in two energy jumps per step. If the motor is at a critical resonant frequency, this energy is released in the step response of the motor and can lead to oscillation.

5.4 Summary

The instrumentation system is an efficient platform for capturing and post processing data. The hardware is robust and has very good immunity to electrical noise. The results demonstrate dynamic characteristics of the motor in an analytical format. The oscillation of the motor about the mean velocity is clearly demonstrated. This is probably due to the motor being operated at or close to a sub multiple of the natural frequency of the motor. The results have revealed characteristics of the flux waveform that probably contribute to motor resonance.

At slow speeds, the time constant of the phase windings is not effectively filtering the PWM pulses to reconstruct a smooth waveform.

The derivation of the motor acceleration exposed a problem with the resolution of the digital shaft encoder. The remedy for may be to use both channels on the existing encoder to give a resolution of 20,000 per revolution. If the encoder is still inadequate when using both channels then an encoder with a higher resolution will be required. A resolution of about 110,000 per revolution would enable sampling at the Nyquist rate. The need for such a high resolution assumes that all 51,200 micro steps are detectable at the shaft. In practise this is very unlikely due to damping effects from the inertia of the rotor and any load that may be connected to the motor.

Chapter 6
Discussion and Future Work

6 Discussion and Future Work

6.1 Discussion

This research has identified experimental techniques for analysis of stepper motors. The work has concentrated on analytical examination of hybrid stepper motors but the techniques can be adapted to other types of stepper motor.

A system was needed for the quantification of oscillations and vibrations that occur in stepper motors. It is necessary to be able to identify the profile of an oscillatory cycle and to relate it to the profile of the parameters affecting the motion of the motor i.e. the PWM applied to the phase windings and the current in the phase windings.

Paramount to achieving the objective of monitoring oscillations was the design of a comprehensive instrumentation system. The data needed for stepper motor investigation consists of both digital and analogue signals. There are high bandwidth digital signals originating from the motor driver and from the digital shaft encoder and analogue signals from the motor driver. It is essential that these signals are captured accurately and are not masked by extraneous electrical noise. Furthermore all of the signals, both digital and analogue, must be synchronised to a common time base so that they can be related to each other.

To prevent noise problems the design and construction of a test bed to ensure stability of the motor and other hardware was of prime importance. Investigations were concentrated on the performance of the SmartDrive Taranis stepper motor driver and this formed a central point of the test bed. The digital signals and the analogue signals were measured from the Taranis. The PWM signals are available via an external connector on the Taranis. Two analogue signals representing the phase currents of the motor were also available from the same connector. Care was required in connecting to these mixed signals that are in close physical proximity to each other. Experience from initial trial tests revealed that noise from external sources and also from cross-talk between the signals (because of the physical proximity of the signals) was at unacceptable levels. Noise reduction methods, as described in chapter 4 to improve the signal to noise (S/N) ratio and to reduce noise levels were implemented. Additional analogue data that was required from the Taranis drive but was not readily available was the stepper motor phase voltages. The voltage signals required are the differential voltages from each end of the two phase windings. Differential amplifier circuits were constructed as described in chapter 4. Commissioning of these amplifiers resulted in the failure of the Taranis drive power electronics section. This precluded the acquisition of further data using the Taranis drive. Consequently the results obtained do not include phase voltage data.

Following the loss of the Taranis drive a stepper motor driver was designed and constructed. This driver is designed to interface with a Texas Instruments 2812 digital signal processor as detailed in section 4.3. The driver was completed and tested successfully but the final stage of installing the Taranis software onto a 2812 processor was not completed.

The instrumentation has been designed to investigate the benefits and limitations of existing sensorless feedback control systems for stepper motors. The instrumentation helps to determine variations on the existing methods. Specific limitations to the existing methods have been documented by Acarnley [21], this documentation is reviewed in section 2.2.3. The two principal methods of sensorless feedback are:

1) Motional voltage method.

2) Variation of phase inductance method.

All types of motors generate a voltage if they are rotating. This phenomena is generally called the back Electro Motive Force (EMF_b). The EMF_b is a voltage that is proportional to the speed of the motor and opposes the voltage that is applied to the motor terminals. In stepper motors this voltage is called the motional voltage and the waveform of the motional voltage has identifiable characteristics that change in time with the steps of the motor. Like the EMF_b the magnitude of the motional voltage is proportional to the speed of the motor. Consequently at low speeds the motional voltage is too weak to be reliably used as a means of tracking the motor position. The variation of phase inductance method can be used through the full speed range of the motor but is more difficult to use accurately at higher speeds

The phase inductance method (2) relies on detection of the rise time of individual segments of the chopper current regulator and is described in section 2.3.3.

6.2 Observed Results

The results revealed a pattern of resonance in the motor that relates to the switching action of the high side mosfets in the H Bridge of the stepper motor driver (this is explained in section 5.2). It appears that at low motor speeds the period between PWM pulses (this is when the high side mosfets are both switched on) is too long. The low pass filtering effect of the phase winding is not fully removing the spaces between the PWM pulses. Therefore the current waveform has dips in it due to the gaps between the PWM pulses. This is the cause of the noise on the waveform as described in section 5.3. It is possible that shortening the period that both high side mosfets are switched on when the motor is running at low speeds may reduce the jagged edge on the current waveform.

The low speed phase current of the motor shown in Figure 6.1A (a duplicate of Figure 5.8 is reproduced here for convenience) was not a very good representation of a sinusoid. The current closely resembles the PWM voltage applied to the phase windings but is low pass filtered by the phase windings, this is shown in Figure 6.1B. There are definite plateaus in the waveform. When the motor stepping rate coincides with the natural resonance of the motor the plateaus on the waveform will exacerbate oscillations to a greater level than would be normally expected with a micro-stepping drive. As the motor velocity is increased the windings will filter the current waveform resulting in a smoother shape. There is scope for improvement to the shape of the waveform particularly at low motor speeds.

6.3 Future Work

There appears to be a high frequency harmonic present on the acceleration waveform of figure 6.1C (reproduced from section 5.2) but it is difficult to ascribe a cause to this. It may be that this apparent high frequency is a result of aliasing due to an inadequate sampling rate. The limitation of the sample rate is due to the encoder used. This has 5,000 slots or 10,000 edges per revolution, thus the sampling rate is 10,000 per revolution.

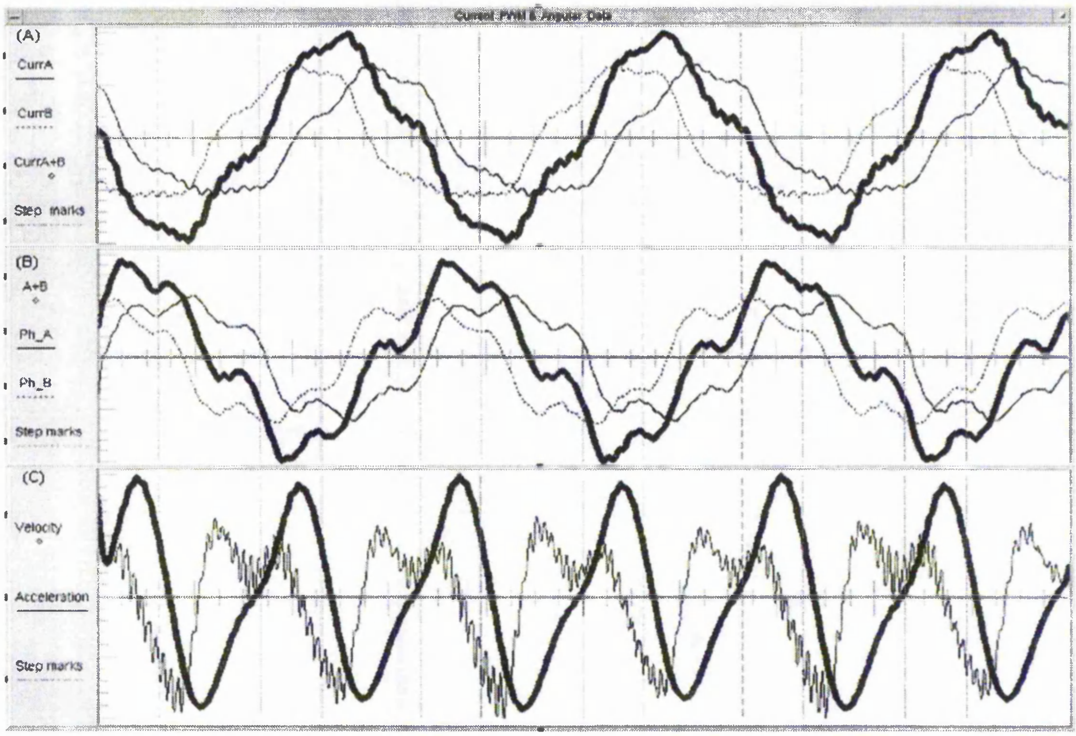

Figure 6.1 Filtered Data

Future work with the same encoder could lead to improvements by using both channels of 5,000 slots as the slots of each channel are phase shifted from one another by 180°. This would double the number of edges used for sampling from 10,000 to 20,000 per revolution.

There are a total of 51200 possible micro step positions per revolution with the driver/motor combination used [6]. To obtain a reliable indication of the acceleration the shaft position should be sampled at the Nyquist rate, at least double the 51,200 micro steps per revolution. An encoder with more than 102,400 edges is required, thus a 25,600 slot per channel encoder would suffice if both channels were utilised. However the inertia of the rotor will provide some damping to the motion and it is unlikely that all 51,200 micro-steps will be detectible. This means that it may be possible to use an encoder with fewer edges. Therefore, the resolution of 20,000 available from the existing encoder may be adequate.

With a suitable encoder sampling rate it will be possible to identify any relationship existing between the PWM voltage and the motor oscillations.

The conclusions drawn from the results so far are not effected by the line count of the shaft encoder; the resolution is suitable for relating the rotor angle and velocity to the other signals.

The voltage waveform produced by the PWM pulse (Figure 6.1B) appears to be quantised because of a low level of PWM levels produced by the Taranis. This can be seen more clearly from inspection of Figure 6.2 (a duplication of Figure 5.7).

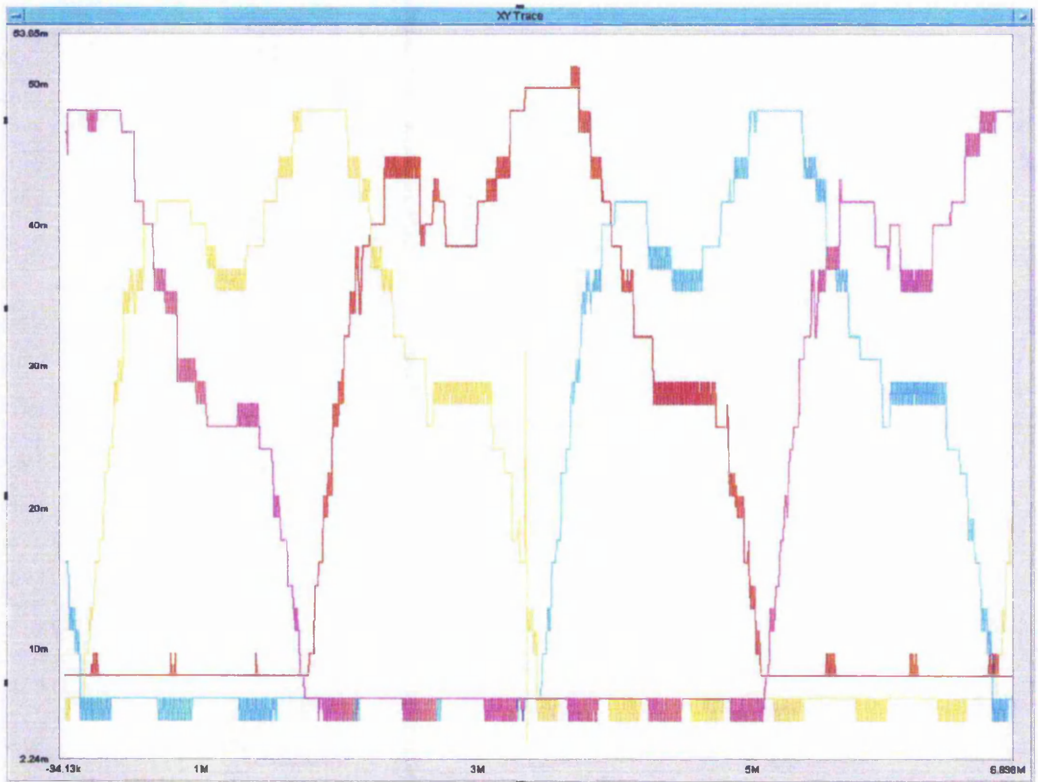

Figure 6.2 PWM Applied to Each Side of the Phase Windings

Sixteen levels (2^4) of PWM can be identified. The amount of processing by the DSP in the Taranis precludes the use of a higher level of PWM resolution.

However a method of reducing the number of calculations required to generate PWM in real time is demonstrated by Bowes and Lai [43].

6.3.1 Improvement of Motional Voltage Analysis

An improved method for the analysis of motional voltage is proposed; this requires the facility to rotate a stepper motor without applying any voltage to the phase windings. A second motor (this must be another stepper motor with identical characteristics) would be used to rotate the shaft of the motor under test.

The driven motor has identical characteristics to the driving motor and is rotating at the same speed. There is no voltage applied to the driven motor therefore the induced voltage from the driven motor will be identical to the motional voltage of the driving motor. However the voltage induced by the driven motor is not obscured by power applied to its phase windings.

6.3.2 Improved Integration of Instrumentation

The design and construction of the stepper motor driver/DSP interface detailed in section 4.3 provides a system for fully integrating the stepper motor control and research instrumentation onto a common platform. It is proposed that the drive software should be integrated together with the instrumentation management onto the 2812 DSP. This will remove four of the intermediate steps of the instrumentation. These are;

1) The pulse width modulation signals are available eliminating the need for an external interface.

2) The phase winding currents are available on the same electronics circuit board. This improves immunity to noise.

3) The phase voltages are available directly from the driver circuits of this board. This improves immunity to noise and simplifies capture of the voltage signal.

4) On board analogue to digital converters (ADCs) on the DSP remove the requirement for a separate ADC board.

Further research can be developed more efficiently with this board and with reduced probability of equipment failure. Because of the modular construction of the driver/interface any component failures can be speedily and more economically rectified.

6.4 Summary

The theories and existing knowledge of stepper motor control and sensorless feedback system have been researched and examined. Improvements to researching factors that effect stepper motor stability have been postulated and a reliable instrumentation system has been designed and built for the development of this research. Theories have been proposed for determining the characteristics of motional voltage of the motor phases. Improved knowledge of these characteristics is fundamental to improving stepper motor control techniques. Further additions and improvements to the instrumentation are required to enable work to progress. These are an improved digital shaft encoder and the incorporation of analysis of phase voltage waveforms. A new stepper motor driver/DSP interface has been designed and constructed that incorporates the reliable capture of motor phase voltages. The new driver/interface will also further improve the integration of the multiple mixed signals and enhance future work.

Chapter 7
Conclusions

7 Conclusions

The initial aim of this research is to investigate problems with vibration and resonance occurring in sensorless closed loop stepper motor drive systems, which are thought to be due to the motor drive circuitry. This investigation requires an appropriate instrumentation solution that will monitor the drive characteristics and additionally provide high bandwidth angular position data to enable a detailed analysis of vibrations and resonances.

It was found that there were commercial systems available for the analysis of stepper motors and stepper motor drivers. A survey of commercially available integrated instrumentation systems for stepper motor drive analysis has been undertaken. The commercial systems did not fully meet the requirements of the research. The available systems were unable to provide a facility for comparing the phase relationship of the motor terminal voltage and current, a method of obtaining feedback of the angular position of the rotor based on the variation of phase inductance with rotor position. One of the systems incorporated a very useful feature comprising a motor/generator system. This provided a facility for imposing a variable load on the stepper motor under test. The same facility enables the motor under test to be rotated without applying a driving voltage to the motor under test. Unfortunately this system was prohibitively expensive.

Ultimately it was decided to design and build an instrumentation system tailored to the requirements of the research. This instrumentation system has been integrated with the test rig that has been designed and constructed to enable the safe and convenient running of experiments and to provide a low noise environment for the instrumentation. These integrated test rig and instrumentation systems have achieved the aim of providing a solution for monitoring the drive characteristics and to enable detailed analysis of vibration and resonance. The instrumentation system fulfils the requirements of enabling the detailed analysis of motor stability under a range of operating conditions, including, oscillatory phenomena that occur when the motor is stopped at its target position.

The causes of resonance in stepper motors have been investigated with material from both academic and industrial sources researched. This study included the various types of resonance that occur through different speed ranges. The established techniques for sensorless position detection have been investigated. Attention has been given to the priorities assigned by various manufactures of stepper motor control equipment.

Test results have been captured and analysed using the Taranis controller to drive the stepper motor. The synchronised signals of phase current, PWM pulses and motor shaft velocity/acceleration has revealed an oscillation pattern that was greater than expected from a micro stepped motor driven at a low speed.

It has been found that the most significant vibrations affecting stepper motors occur at low speeds, and are the result of the stepping frequency coinciding with the natural frequency or an integer sub-multiple of the natural frequency. The effects of this type of oscillation are most severe on motors that are being driven in single stepping mode. As the step angle is reduced, the amount of energy in the step movement also decreases. Thus, in theory, motors that are driven by a micro stepping drive with a very small step angle should not be subject to this type of oscillation at low speeds. Stepper motors do run more smoothly when using micro stepping but unfortunately oscillations due to the natural frequency of the motor still arise, because the PWM generated waveform in not very close to a sinusoid.

The instrumentation system has been designed to analyse oscillations of this type and the results have indicated problems with the drive performance contributing to the problem. As stated above, the reconstructed pulse width modulation is not very close to a sinusoid. The waveform may by described as a quasi sinusoid that contains a number of plateaus (about four per cycle, as shown in section 5.2). This waveform is modified by the low pass filtering qualities of the phase windings but still contains four distinct plateaus. The waveform is further distorted by motional effects of the motor. The resultant flux waveform, which should be constructed from evenly spaced micro steps, is actually made up of a wave containing significant plateaus with a ripple superimposed on the wave form. The ripple may be due to the inductance of the phase winding not being able to completely low pass filter the PWM pulses. This problem occurs because at low motor speeds the PWM frequency is also necessarily low.

The instrumentation system that has been produced meets the aim of implementing a solution that will monitor the drive characteristics and provide high bandwidth angular position data. This has enabled a detailed analysis of vibrations and resonances to provide the base for developing improved algorithms for micro-stepping control drivers.

The integrated experimental test rig and instrumentation has fulfilled the objective of providing a system that captures reliable data that is free from noise and spurious signals.

Angular position data, PWM signals from the existing stepper motor controller and electric current waveforms have been collected and processed. The data is presented in a comprehensible form that has enabled sustainable analysis of the characteristics of the stepper motor driver.

A stepper motor driver has been designed and built and successfully tested to interface between the TI 2812 DSP and the stepper motor. This provides for the complete integration of the driver software with the instrumentation on the same target DSP.

The instrumentation that has been implemented is a significantly improved system for the capture, processing and collating of multiple channels of mixed signal data. The application of this system has revealed stability problems associated with micro-stepping at low speeds. These were previously unsuspected by the manufacturer of the micro-stepping driver under test. The completion of the new driver interface has provided the platform for even greater improvements to the instrumentation already developed. This will enable further work on the analysis and development of micro-stepping control techniques.

[1] Hughes R. O., Dynamics of incremental motion devices associated with planetary exploration spacecraft, proc. fourth annual symposium on incremental motion control systems and devices, dept. of electrical engineering, University of Illinois, 1975.

[2] Remote gallbladder operation spans 3,800 miles, news item, foreign desk, New York Times, September 20 2001.

[3] Cepolina F., Development of micro tools for medical applications, PhD co-tutelle thesis, Universite' Pierre et Marie Courie, Geneva, and Laboratoire de Robotique, Paris, 2002.

[4] Stepper as a servo: A new type of servomotor, technical white paper: QCI-WP003, Quick Silver Controls Inc, 14 May 2001.

[5] SmartDrive Ltd. The Old School, 8 Colne Road, Earith, Huntingdon, Cambridgeshire, UK.

[6] Smart systems, stepper systems tools and resources compact disc, issue 2, May 2001, SmartDrive Ltd., 8 Colne Road, Earith, Huntingdon, Cambridgeshire, UK.

[7] Byrne, J. V. and Lacy, J.C. (1970. Characteristics of saturated stepper and reluctance motors, IEE conf. pub. 136 (Small Electrical Machines), pp.93-96

[8] Kenjo T.and Sugawara A., Stepping motors and their microprocessor controls, second edition, Oxford University Press 1994, reprinted 2000.

[9] McClelland W., The application of electricity in warships, JIEE-65, 829-71, 1927.

[10] Chicken C. B. and Thain J. H., Electrical signaling apparatus. US patent 1,353,025, 1928.

[11] Industrial circuits application note, stepper motor basics, The New Japan Radio Company, 3-10, Nihonbashi Yokoyama-cho, Chuo-ku, Tokyo 103-8456, Japan.

[12] Frus J. R. and Kuo B. C., Closed-loop control of step motors without feedback encoders, PP CCI-11, proc. 5th ann. symposium on incremental motion control systems and devices, May 1976.

[13] Kuo B.C. and Cassat A., On current detection in variable–reluctance step motors, proc. of the sixth annual symposium on incremental motion control systems and devices, University of Illinois, 1982.

[14] Siefert W. and Lahr B., Self-synchronisation of permanent magnet energised stepper motor with detection of position by evaluation of the BEMF, PCIM, November 1985.

[15] Acarnley, Hill and Hooper, Detection of rotor position in stepping and switched motors by monitoring of current waveforms, IEE transactions on industrial electronics, vol. 1E-32, no. 3, August 1985

[16] Amaratunga G., Kwan K-W. TSO and Crawley D., A single-chip CMOS IC for closed-loop control of step motors, IEEE transactions on industrial Electronics, 36(4), pp. 539-544, 1989.

[17] Cardoletti L., Cassat A. and Jufer M., Indirect position detection at standstill for brushless dc and step motors, proc. of the European power electronics conference, Aachen, pp. 1219-1222 1989.

[18] Petrović V., Stanković A. M. and Blaško V., Power estimation in salient PM synchronous motors based on PWM excitation transients, IEEE transactions on industry applications, vol. 39 no. 3, May/June 2003.

[19] Husain I., Indirect rotor-position estimation techniques for switched reluctance motors - a review, Electromotion, vol. 3, no. 2, pp. 94102 June 1996.

[20] Husain I. and Ehsani M., Rotor position sensing in switched reluctance motor drives by measuring mutually induced voltages, IEEE transactions on industry applications, vol.30, no.3, May/June 1994.

[21] Acarnley P. P., Stepping motors a guide to theory and practice, 4th edition, publisher the IEE, 2002.

[22] Acarnley P. P., Stepping motor technology for undergraduates, int. j. elect. engineering education, Vol. 20, pp. 227-228. Manchester U.P., 1983

[23] Lawrenson P. J. and Kingham E., Resonance effects in stepping motors, proc. the IEE, vol. 124, no. 5, May 1977.

[24] Hunt S., National Semiconductor application note 828, May 1993.

[25] Jones D. W., University of Iowa, department of computer science, control of stepping motors, a tutorial, 1995, major revision 1998.

[26] Ward P. A. and Lawrenson P. J., Backlash resonance and instability in stepping motors. proc. sixth annual symposium on incremental motion control systems and devices, department of electrical engineering, University of Illinois, pp. 73-83, 1997.

[27] National Instruments, Developer Zone, Motor Fundamentals, website

[28] Pickup I. E. D. and Russell A. P., Analysis of frequency and modulation in the stabilisation of permanent magnet synchronous/stepping motors, IEE proc.-b, vol. 139, no. 4, July 1992

[29] Hung J. V. and Ding Z., Design of currents to reduce torque ripple in brushless permanent magnet motors, IEE proc: b, vol. 140, No. 4, July 1993.

[30] Cho K. V., Bae J. D., Chung S. K. and Youn M. J., Torque harmonics minimisation in permanent magnet synchronous motor with back EMF estimation, IEE proc: electrical power applications., vol. 141, no. 6, November 1994.

[31] Husain I. and Ehsani M., Torque ripple minimisation in switched reluctance motor drives by PWM control, IEEE transactions on power electronics, vol. 11, no. 1, January 1996.

[32] Vraets J. W. and French D., Minor closed loop control of stepping motors for use in high speed positioning, 1981.

[33] Stout A., Instrumentation techniques and improved control of stepper Motor driven machinery, page 80, PhD thesis, The Nottingham Trent University, September 1999.

[34] Shimotani K. and Kataoka T., Characteristics of stepping motor driven by position feedback pulses, translation, Japanese institute of electrical engineers, 1973.

[35] Publication, Stepping-Motor Station PV-7300 System, Ono Sokki Co., Ltd. Yokohama, Japan. Printed in Japan 994 (SK) 3K

[36] Web Publication, MotionScope Overview, Euclid Research, "www.euclidres.com/motionScope/msSummary.html". Euclid Research 2 North Street, San Jose, California, USA.

[37] Bolognani S., Oboe R. and Zigliotto M., DSP-based Extended kalman filter estimation of speed and rotor position of a PM synchronous motor, proc. IEEE-IECON, 1994.

[38] Heidenhain J., Brochure: Position Encoders for Servo Drives, Traunreut, Germany.

[39] Poliakoff J. F., Thomas P. D., Orton P. A. & Sackfield A., The incremental motion encoder: A new approach high-speed monitoring of rotating shafts, Measurement and Control, volume 33, pp 49-51, March 2000

[40] Ayandokun K., The incremental motion encoder: A sensor for the integrated condition monitoring of rotating machinery, PhD Thesis, The Nottingham Trent University, December 1997.

[41] Whitaker J. C., IEEE press/technical press, Beaverton, Oregon, The electronics handbook pp. 30-39, 1st edition 1996.

[42] Dodson R. C., Evans P. D., Tabatabaei-Yazdi H.and Harley S. C., Compensating for dead time degradation of PWM inverter waveforms, IEE proc. vol. 137 pt. b, no. 2, March 1990.

[43] Bowes S. R.and Lai Y. S., Investigation into optimising high switching frequency regular sampled PWM control for drives and static power converters, IEE proc.-electrical power application, vol. 143, no. 4 Jul 1996.

Appendix A

Stepper Motor Windings and Switching Methods

The type of winding connection employed in the motors used in this research project is known as the ***bipolar*** type. Other arrangements are *unipolar* and *bifilar*. The three types are briefly explained below:

1) **Unipolar:** This type of motor winding is centre tapped as shown in Figure A.1 [25]. The arrangement of the connections enables the control switching to be simplified. The common centre tap connections indicated as (1) and (2) are connected to the negative terminal of the supply. The directions of flux in the motor poles are reversed by switching the positive electrical connection from (a) to (b) or vice versa. This can be accomplished with only two transistors per phase. The penalty for the

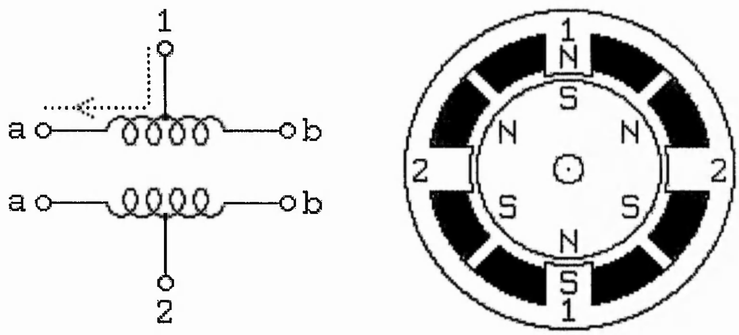

Figure A.1 Unipolar Motor Winding [25]

simplicity of this arrangement is only one half of the total winding per pole is in use at one time. This effectively reduces the maximum torque of the motor by 50%.

2) **Bipolar:** This design of motor utilizes all of the available winding to produce magnetic flux and there for maximises the torque that can be produced by the motor. In this case the penalty is a complicated switching circuit that requires four transistors per phase. The additional transistors are not the only problem however. Two of the transistors (usually power mosfets) are on the high voltage side of the phase winding whilst the other two are on the low voltage side of the winding. This requires careful circuit design as the gates of transistors on the high voltage side must be

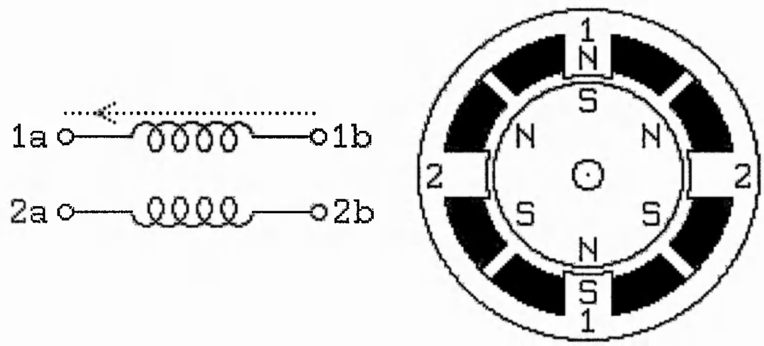

Figure A.2 Bipolar Motor Winding [25]

electrical isolated from the transistors on the low voltage side. Further more the gate voltage levels must be referenced to the drain voltage of the transistor. The electrical connections are terminals (1a) or (2a) are switched to the high voltage side with (1b) or 2(b) switched to the low voltage side, for one direction of magnetic flux. To reverse the flux (1a) or (2a) are connected to the low voltage with (1b) or (2b) connected to the high voltage. This arrangement is called an H Bridge and is explained in Appendix E.

3) **Bifilar:** A motor of this type has two windings covering the full length of the motor poles. The windings are interspaced but wound in opposite directions. This type of winding permits the use of either unipolar or bipolar connection. Winding one in Figure A.3 shows unipolar connection.

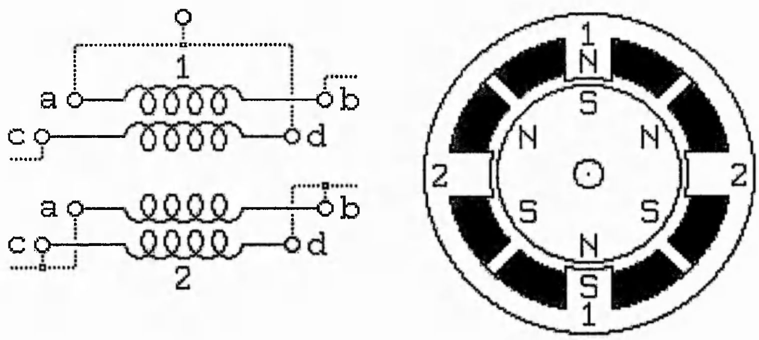

Figure A.3 Bifilar Motor Winding [25]

In this case because the two windings utilize the full length of the pole the motor torque is maximised. However the additional winding requires a greater winding volume and therefore a larger frame size is required for a given torque. The alternative connection for bipolar is shown in winding 2 and in this case the windings are connected in parallel. This is a low voltage high current configuration (high torque at low speeds). The windings may also be connected in series to give a high voltage low current configuration (high torque at high speeds).

Appendix B

Test Rig Notes

Acquisition of digital data is to a GoLogic logic analyser (LA); inputs to the LA were originally achieved by using insulation displacement ribbon cables from the Taranis ('D' socket) and from the encoder. Connection from the end of the ribbon cables to the LA was by means of laboratory test clips. It was decided that the optimum solution would be to connect the LA proprietary pod input cables as directly as possible to the equipment.

Analogue acquisition is via a PowerDaq A/D PCI card mounted inside the PC. Again the original connection of the Taranis was by means of ribbon cable from the Taranis 'D' socket to the propriety PowerDaq connection block. Improvement to this arrangement must rely on an improved cable connection from the Taranis 'D' socket.

Rotary Shaft Encoder

The power supply to the rotary encoder is achieved by use of a Heidenhain proprietary cable. To enable direct connection of the LA to the encoder an in line IDC test connector has been adapted. The inline test connector is inserted between the incoming power cable and the encoder socket. The LA pod cables are attached directly to the inline test connector. The in line test connector has been 'trimmed' to a suitable size for the task.

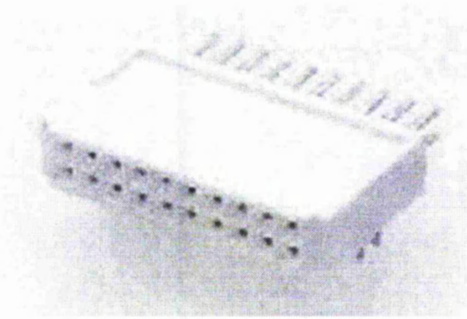

In Line Test Connector

To provide protection against the ingress of foreign bodies and also to ensure that the encoder is not affected by external UV light sources such as sunlight, the encoder has been fully enclosed.

Digital PWM Signals from the Taranis

To allow direct connection LA pod cables to the Taranis 'D' socket a right angle PCB 'D' connector is used. The original (available) right angle connector used was a filtered connector.

It soon became apparent that this connector was having a detrimental effect on the performance of the Taranis drive. A non-filtered right angle connector was obtained and this rectified the problem. However it was decided that because of the effect of the filtered connector that the PWM output of the Taranis should be buffered before connecting the LA. Therefore a 74LS244N buffer IC has been incorporated into the connection path.

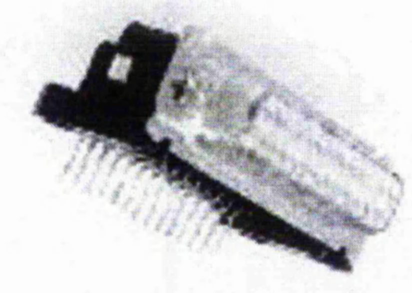

Right Angle PCB 'D' Connector

The buffer is totally enclosed and makes a push on connection to the Taranis 'D' connector. A row of pins from the buffer circuit board protrude through a slot in the top cover of the enclosure to provide the means of connection for the LA pod cables.

The buffer circuit board also provides the means of connection for the analogue cables.

Analogue Connections

The current sensing analogue data from the Taranis is achieved by use of a short four core individually screened cable from the buffer circuit board to the proprietary PowerDaq connection board. A proprietary PowerDaq cable links the connection board to the A/D PCI board. A second short four core individually screened cable is used for the analogue earth, all four cores are used for this connection. The screens of the two cables are connected to the case of the Taranis drive and to the aluminium base of the test rig via the buffer circuit board.

Test Rig Layout

The Taranis drive is securely fixed to the bedplate of the test rig by means of an aluminium strap screwed to the plate. The PowerDaq connection board is also secured to the bedplate but is insulated from it.

The 2812 DSP is also housed in a plastic enclosure and positioned on the bedplate. The layout is illustrated in the two pictures below:

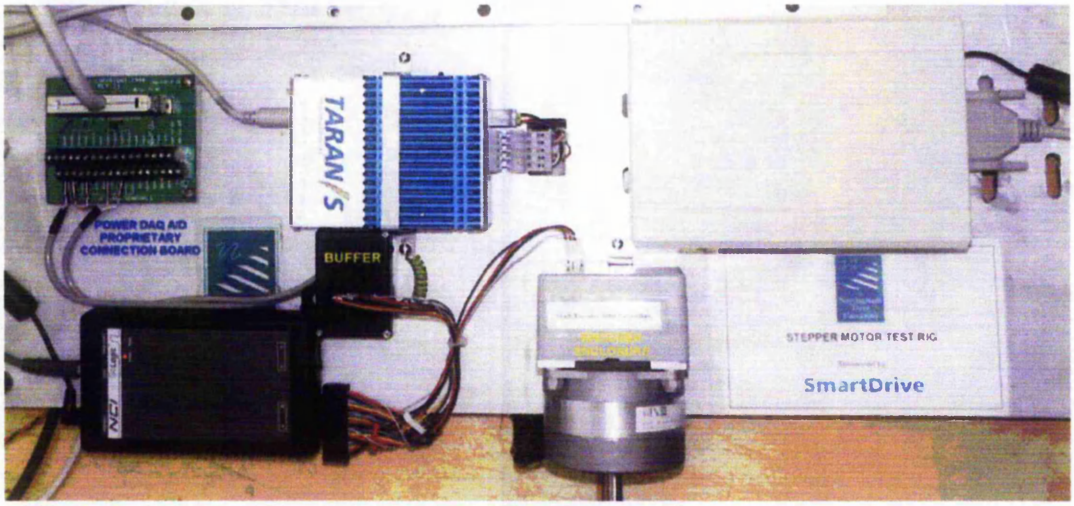

Test Rig View 1

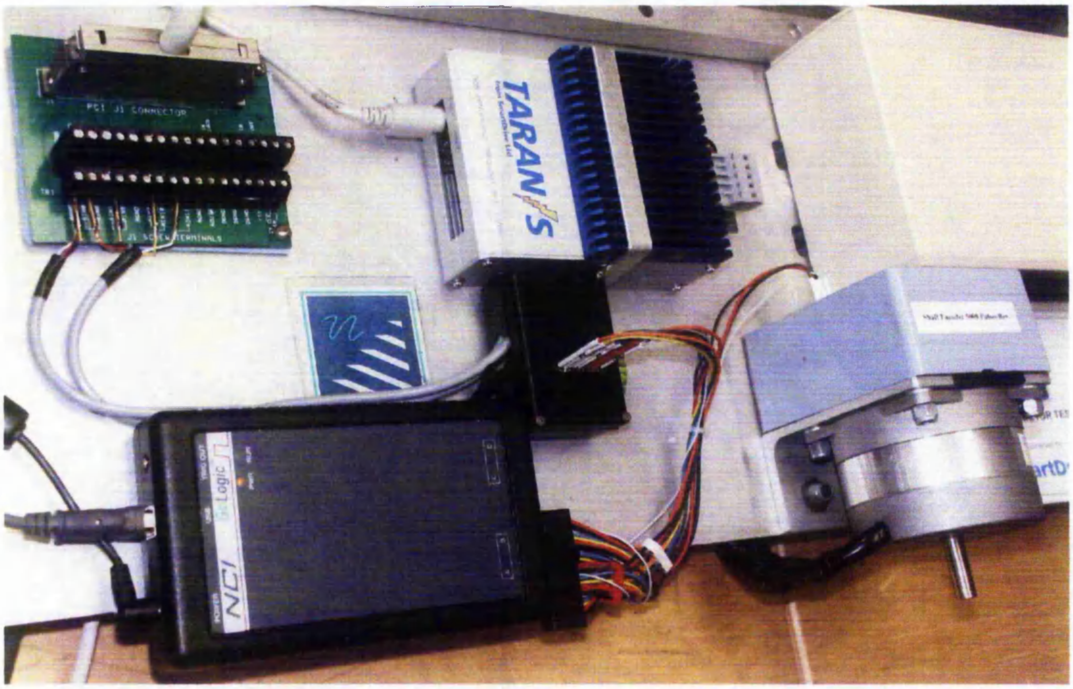

Test Rig View 2

Noise Reduction

The application of the above measures appears to have been successful as can be seen from the trace window of GoLogic. The GoLogic trace window shows from the top, the one per revolution encoder output, the two quadrature outputs of the encoder and the eight PWM outputs.

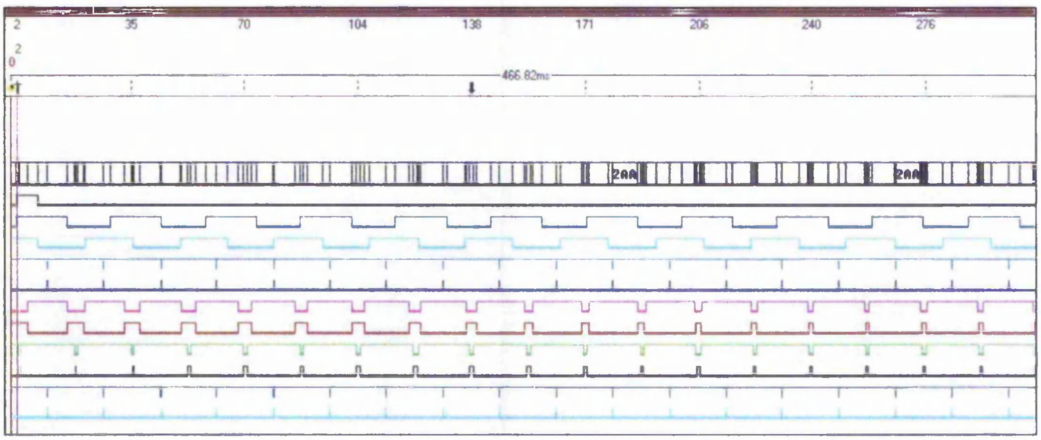

GoLogic Trace Window

Appendix C

Development of DSP Centred Instrumentation

To implement changes in the control algorithm it is necessary to drive stepper motor from a DSP development board. A stepper motor driver module has been designed and constructed to interface between a Ti 2812 EzDSP board and a stepper motor. The design is based upon the SmartDrive Taranis stepper motor driver, but is modular in construction and generally more versatile for use with laboratory experiments. The driver electronics board includes analogue outputs of motor phase currents and voltages scaled to a voltage range to connect directly to the analogue to digital converters (ADCs) on the DSP.

With the driver software mounted on the same DSP that is used for data capture and processing, the PWM pulses are inherently available to the instrumentation.

The modular construction of the driver electronics allows for ease of use with a range of motors and ease of repairs and maintenance in the event of a component failure. The Module which is shown in Figure C1 consists of four daughter boards each with a high side/low side driver circuit and two driver boards per H bridge. The mosfet drain of the high side of the H bridge is connected to the motor supply voltage which can be up to 85 volts; the source of the mosfet on the low side of the H bridge is connected to ground. Thus, the mosfet gate on the high side must be bootstrapped to the supply voltage (up to 85 volts). The input voltage to the gate of the high side mosfet is referenced to the high side voltage and is isolated from the system ground. The boot strap components are selected to reference the base input voltage to the drain of the mosfet which is connected to the high voltage supply. This arrangement is critical and component damage is a considerable risk. The plug in arrangement of four daughter boards into a common main board allow for easy changing of components. The main board is designed as a piggy-back plug in assembly onto the H bridge board. The H bridge board is mounted directly onto a large heat-sink. The circuit design and printed circuit board (PCB) design are shown in Appendix D.

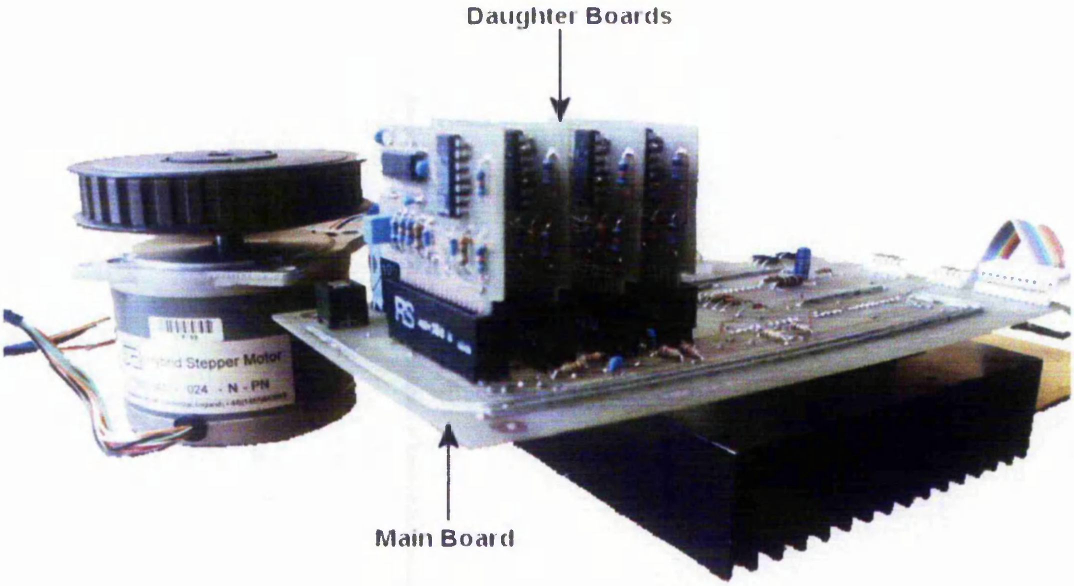

Figure C1 Stepper Motor Drive Electronics

With the instrumentation now tightly integrated with the control, the only external signals that are connected to the module are digital inputs from the rotary encoder. This has provided a method that is much more accessible for development purposes to analyse the reaction of experimental changes to the control algorithm.

Appendix D

DSP – Stepper Motor Driver Interface

Mother Board Schematic Circuits

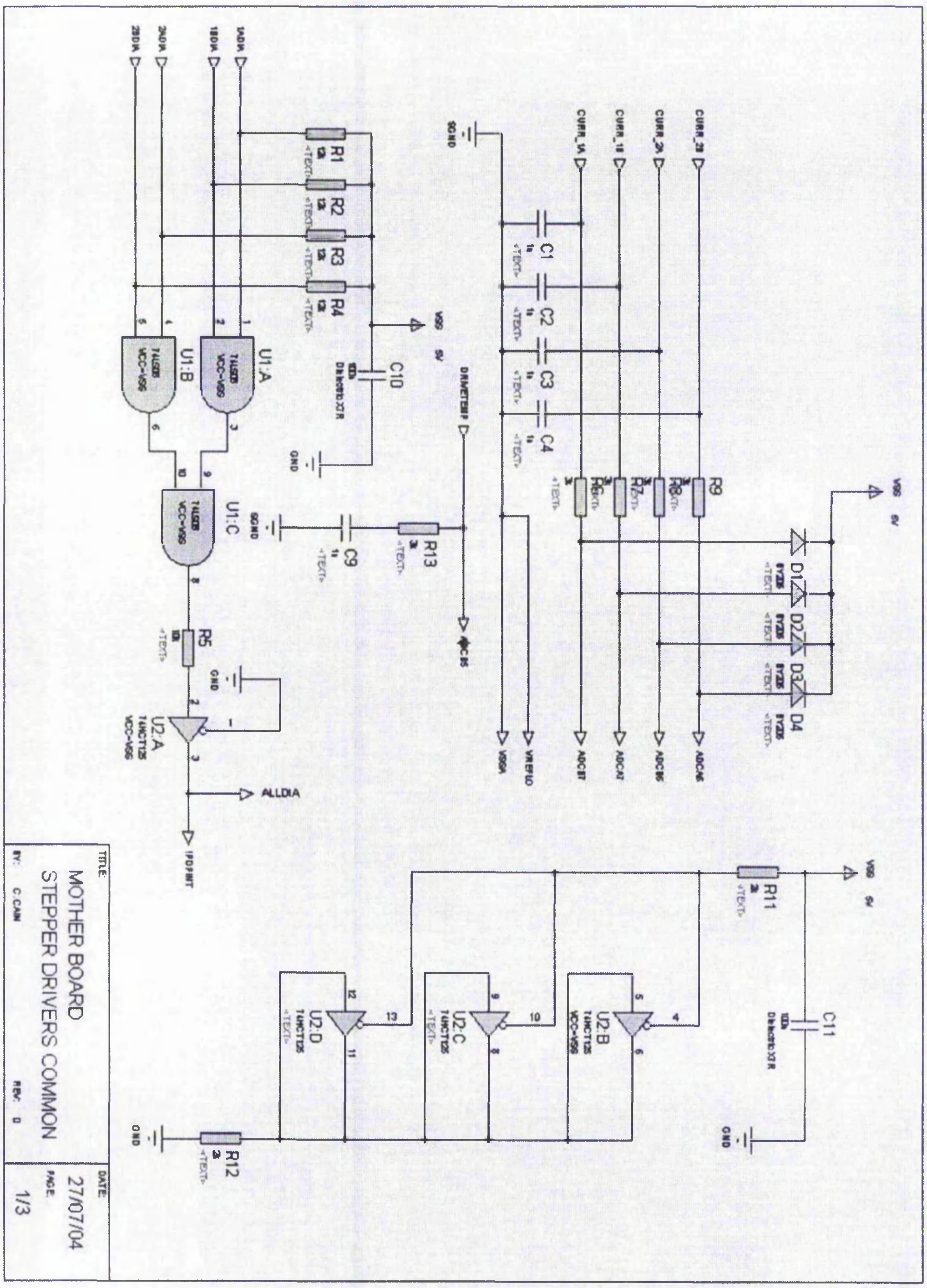

Figure D.1 Mother Board Sheet 1/3 Schematic Circuit

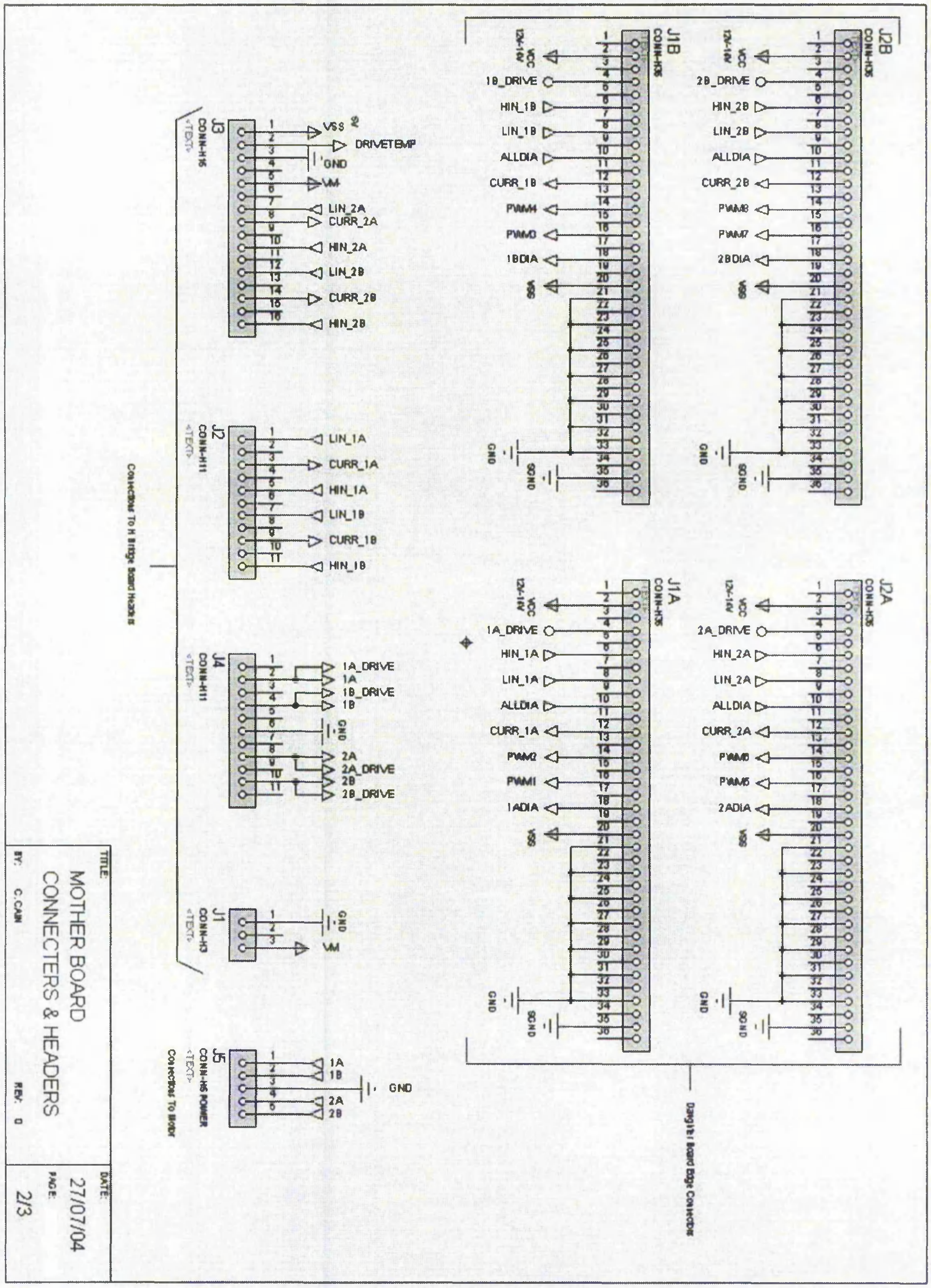

Figure D.2 Mother Board Sheet 2/3 Schematic Circuit

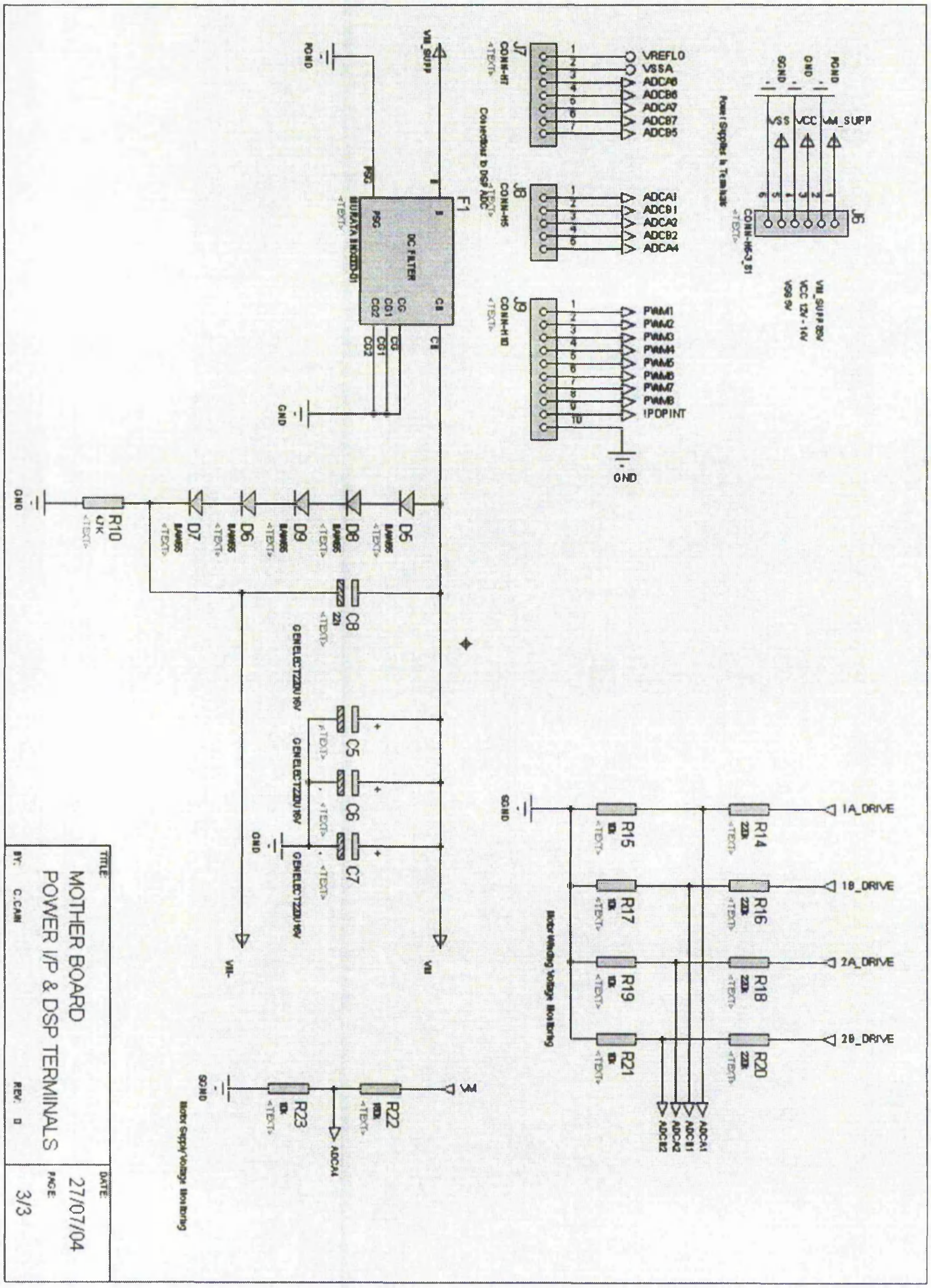

Figure D.3 Mother Board Sheet 3/3 Schematic Circuit

Mother Board Printed Circuit Board Layout

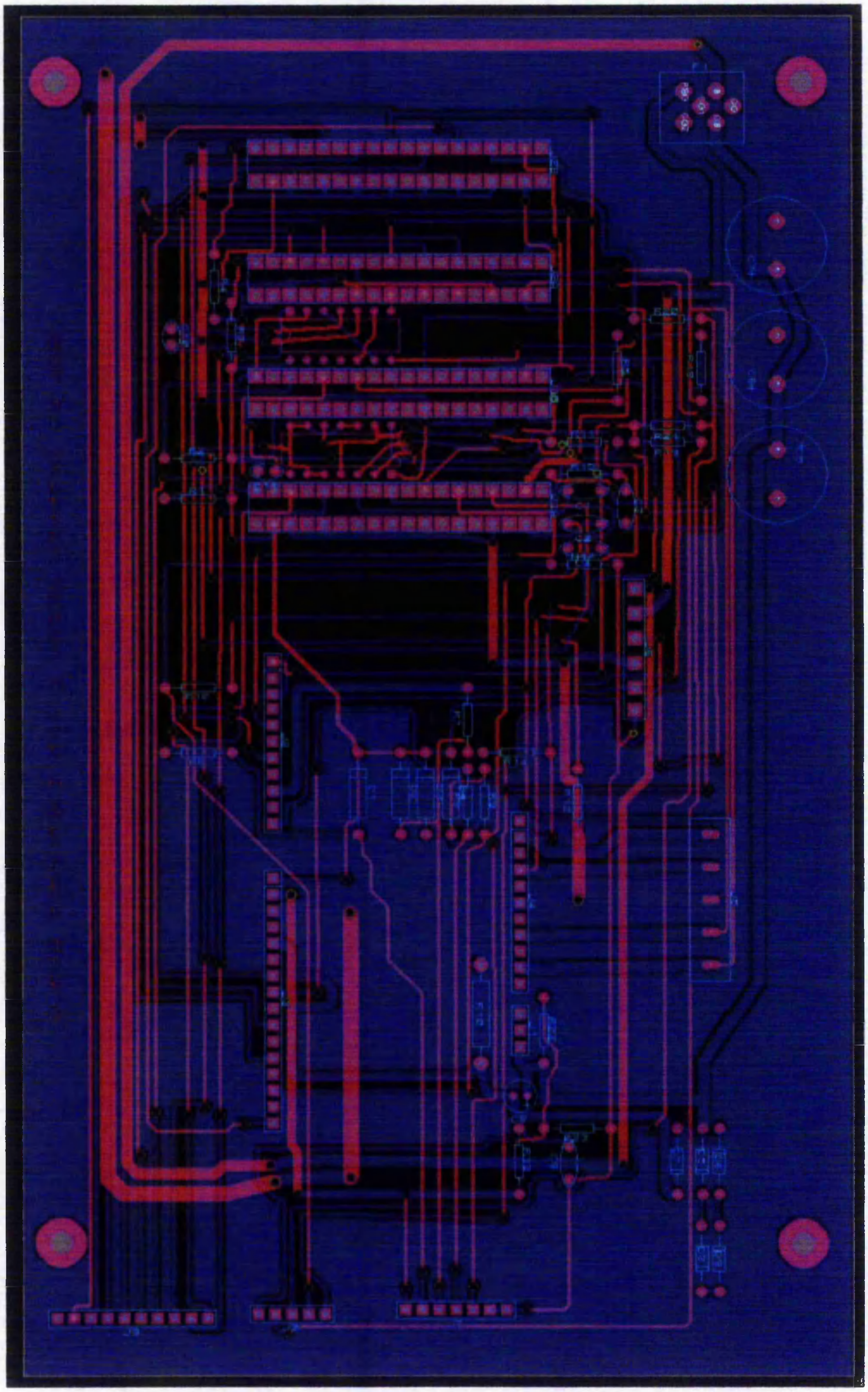

Figure D.4 Mother Board Printed Circuit Board Layout

Daughter Board Schematic Circuits

Four of Daughter Boards with Identical Circuits and PCBs.

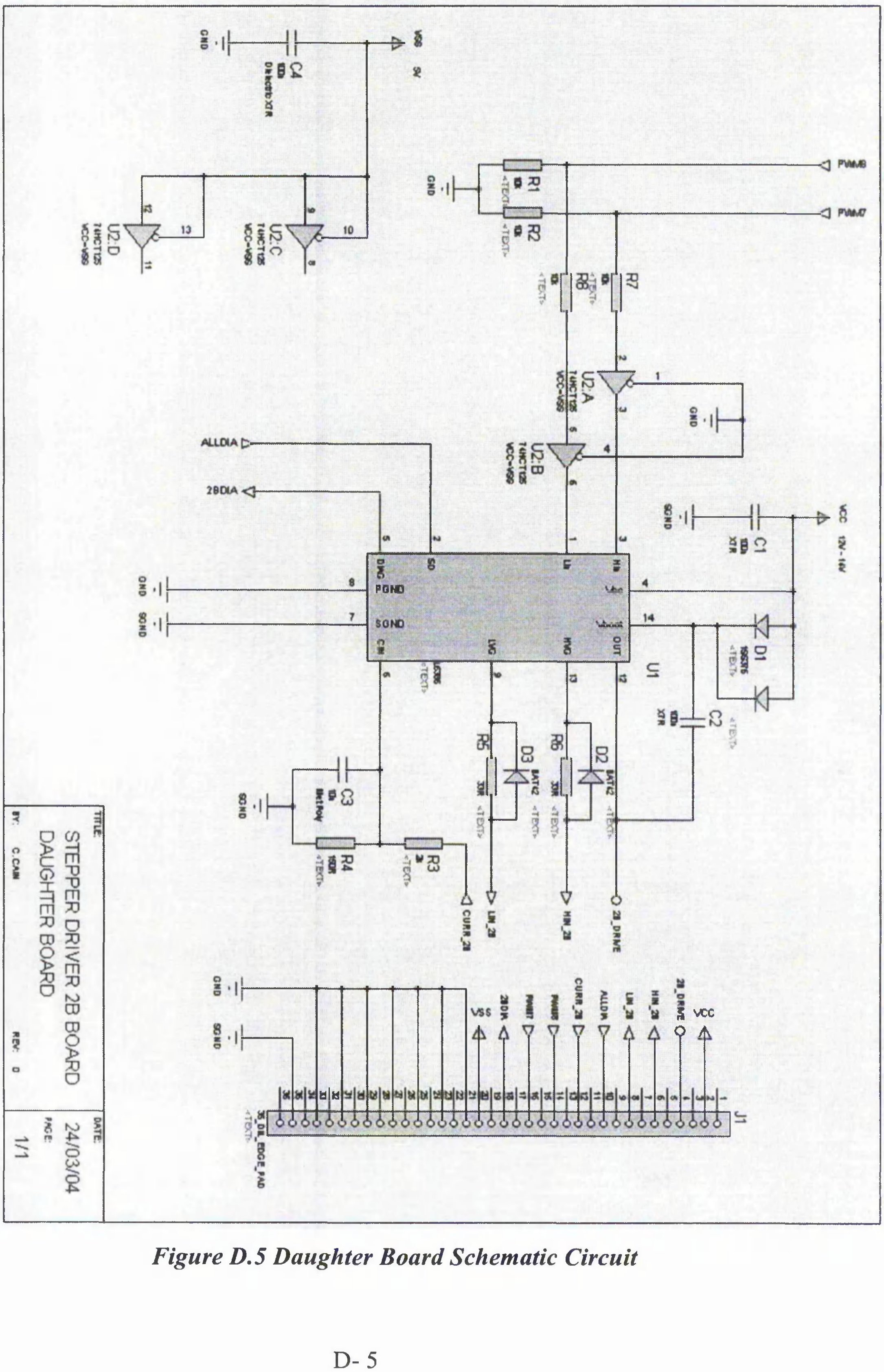

Figure D.5 Daughter Board Schematic Circuit

Daughter Board Printed Circuit Board Layout

Four Identical Daughter Board Printed Circuit Boards

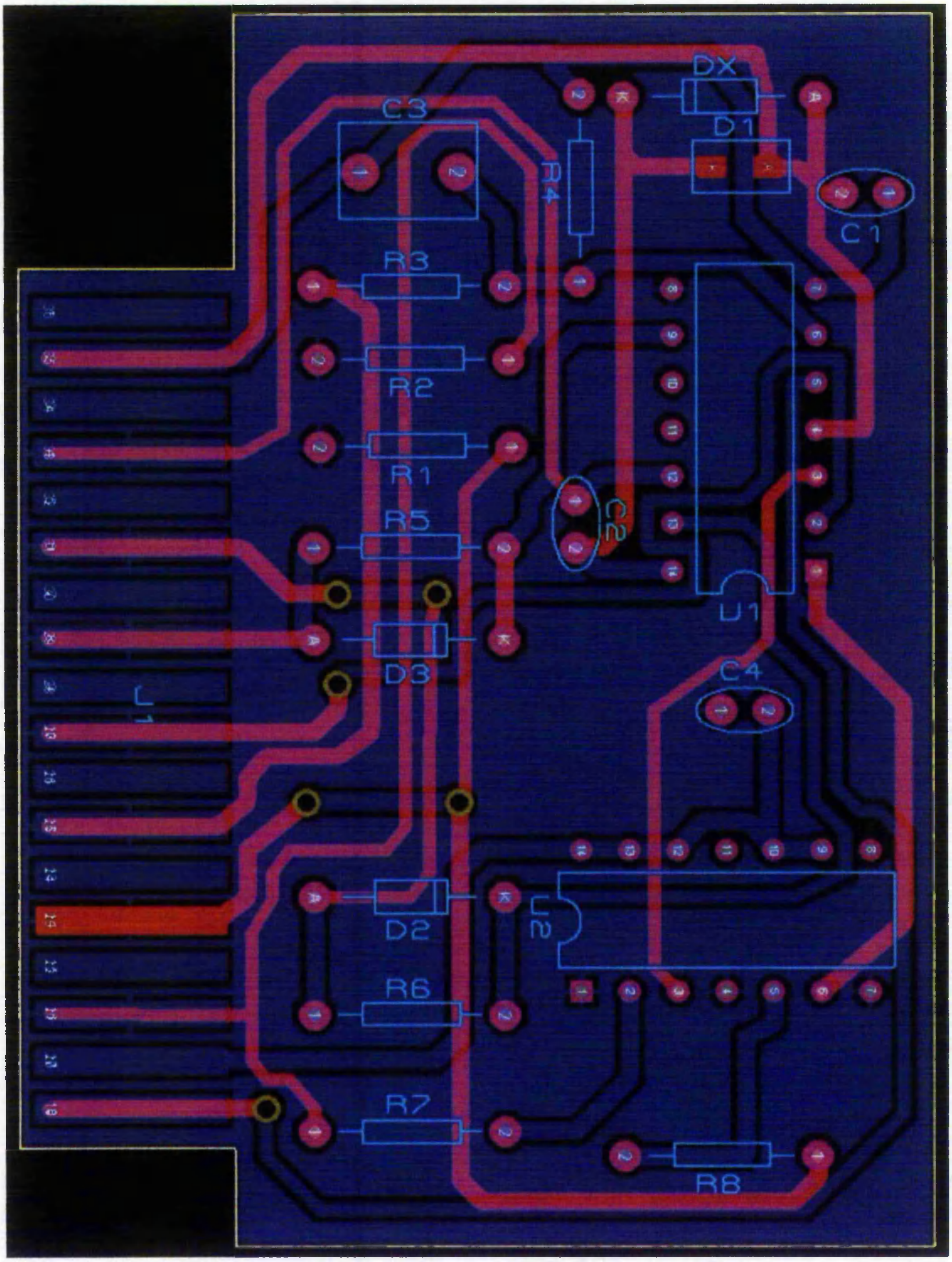

Figure D.6 Daughter Board Printed Circuit Board Layout

Appendix E

H Bridge Circuits for Controlling Stepper Motors

There are different methods of switching the power to a stepper motor and the method used is dependent upon the type of stepper motor and upon the manner in which the motor phases are wound.

The main types are the unipolar drive circuit which is normally used with a variable reluctance stepper motor. The bipolar drive circuit is used with both permanent magnet and with hybrid stepper motors. The bipolar drive needs double the number of switching transistors that are used in a unipolar drive; this is because in a permanent magnet or hybrid motor it is necessary to be able to reverse the magnetic polarity of the pole. Some hybrid motors have a special type of winding called a bifilar winding which has two windings on the same pole but the windings are wound in opposite directions. This means that unipolar switching can be applied to one winding or the other to reverse the polarity of the magnetic field. The disadvantage of a bifilar winding is that because of the additional windings the motor size must be increased to maintain the same torque as a machine with conventional phase windings. In this project we are only concerned with the bipolar drive which is explained by reference to figure E1

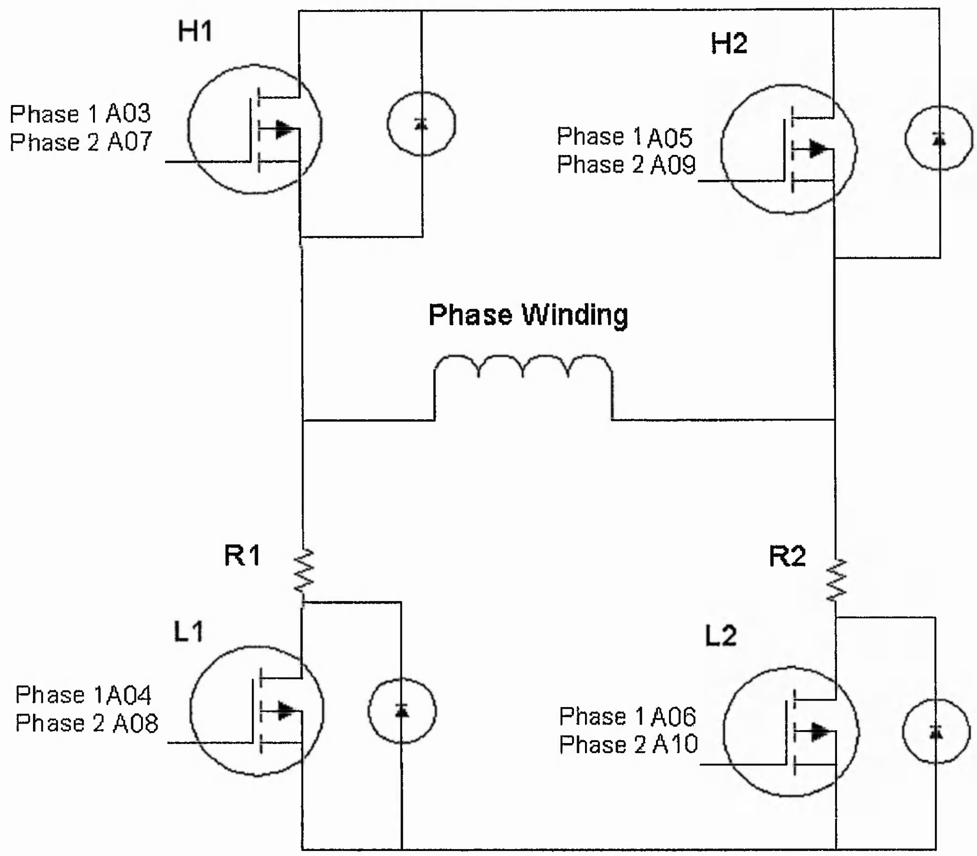

Figure E1 H Bridge Control of a Bipolar Switched Stepper Motor

The H Bridge control shown in figure E1 enables bipolar switching of one phase of a stepper motor. Thus the circuit is duplicated for each phase of the motor. The term bipolar refers to the function of reversing the current flow through the phase winding to change the polarity of flux through the poles that the phase winding is wound onto. The diagram is a simplification of the power electronics in the SmartDrive Taranis stepper motor controller and the pin numbers refer to connections on this unit and within the terms of this explanation may be disregarded. The direction of switching through the phase winding is controlled by turning on two diagonally opposite mosfets. For a current flow from left to right mosfets H1 and L2 will be switch on, to reverse the direction of current flow H1 and H2 will be switched off and H2 and L1 will be switched on. The terminology H refers to the high side (high voltage side) of the bridge and L refers to the low side (low voltage side of the bridge). It is essential that H1 and L1 are never switched on at the same time and likewise for H2 and L2 as this would cause a short circuit and would result in the destruction of the mosfets. Pulse Width Modulation (PWM) is used to regulate the level of current through the phase winding; this is a method of switching the power on and off for varying periods to generate the required waveform. During periods when both diagonally opposite mosfets are turned off the control system may be arranged to switch on H1 and H2 simultaneously, this is to provide a discharge or freewheeling path for the phase winding. This is to allow for a rapid collapse of the magnetic field.

Appendix F

Analogue to Digital Converter Specification and Features

PCI-PD2-MFS-4-300/16

The following manufactures specification are reproduced from the website of PowerDaq http://www.superlogics.com/pci-data-acquisition-boards/high-performance-high-speed-board/pci-pd2-mfs-4-300-16/16-644.htm

FEATURES

- 4 single-ended simultaneous sample/hold A/D channels
- 16-bit resolution, 300 kS/s sampling rate
- Gains: 1, 2, 5, 10
- Two 12-bit analogue outputs; 32 digital I/O lines; three 16-bit counter/timers
- Simultaneous operation of all subsystems
- Stream-to-disk capability
- Multiple boards operate in one PC Calibration certificate included
- PowerDAQ Software for Windows 9x/Me/NT/2000/XP and Linux/RTLinux
- Upgrade options
  - Upgrade 4SE to 4DI with gains (1, 2, 5, 10)
  - Upgrade 1K FIFO to 16K FIFO
  - Upgrade 1K FIFO to 32K FIFO
  - Upgrade 1K FIFO to 64K FIFO

FULL DESCRIPTION

The PCI-PD2-MFS Series data acquisition boards allow for simultaneous-sampling of several channels within a few nanoseconds. These boards are available with as many as 8 sample/hold amplifiers. The PCI-PD2-MFS Series boards have either 4 single ended / 4 differential analogue inputs or 8 single ended / 8 differential inputs. These inputs are multiplexed to a 12, 14 or 16 bit A/D converter with maximum throughputs ranging from 300 kHz to 2 MHz. The PCI-PD2-MFS Series data acquisition boards are PCI "Bus Masters" achieving optimum performance without the need for the computer's interrupts or DMA channels. The data acquisition boards also have 32 lines of TTL level digital I/O, 16 digital TTL inputs (8 can generate interrupts on change of state) and 16 digital TTL outputs. The PCI-PD2-MFS Series data acquisition boards also feature two 12-Bit Waveform Quality D/A voltage outputs with 2K FIFO support. Three 16-bit counter/timers are available to the user, while onboard pacer clocks perform both A/D and D/A functions. All subsystems run simultaneously under the control of a Motorola 66 MHz DSP chip. The board connections are terminated in a 100 pin connector at the rear of the PC. The boards' extensive software support includes drivers for Windows, Visual Basic, Visual C++, Delphi, Test Point, LabVIEW, WINview Series Software, DASYLab, MATLAB DAQ Toolbox...Plus support for Linux, RTLinux, QNX.

Appendix G

Heidenhain Rotary Encoder Details

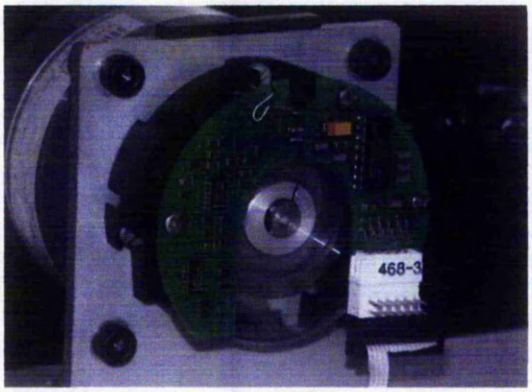

Figure G.1 Rotary encoder attached to stepper motor

The following specification for the Heidenhain Rotary Encoder ERO 1324 is reproduced from the Heidenhain data sheet:

Incremental signals	TTL
Line Count	5000
System accuracy/Accuracy of the graduation	5000 lines ± 72″/± 3.5″
Reference mark	One
Scanning frequency	Max. 400 kHz
Power supply	5V ± 10%
Current consumption (no load)	≦150 mA
Electrical connection	Via 12-pin PCB connector
Max. cable length	100 m (329 ft)
Shaft / Moment of inertia of rotor	Hollow through shaft ∅ 20 mm: $26 \cdot 10^{05}$ kgm^2
Mech. Permissible speed	≦16,000 rpm
Permissible axis motion of measured shaft	± 0.05 mm
Vibration (55 to 2000 Hz)	≦100 m/s^2 (IEC 60068-2-6)
Shock (6 ms)	≦1000 m/s^2 (IEC 60068-2-27)
Max. operating temperature	70 °C (158 °F)
Min. operating temperature	0 °C (32 °F)
Protection (IEC 60529)	IP 00
Weight	Approx. 0.2 kg